2023-05-11

Deficiency of DNAJC19 Leads to Upregulation of Cellular Stress Responses

Wachoski-Dark, Emily Mary Ann

UNIVERSITY OF CALGARY

Deficiency of DNAJC19 Leads to Upregulation of Cellular Stress Responses

by

Emily Mary Ann Wachoski-Dark

A THESIS

SUBMITTED TO THE FACULTY OF GRADUATE STUDIES

IN PARTIAL FULFILMENT OF THE REQUIREMENTS FOR THE

DEGREE OF MASTER OF SCIENCE

GRADUATE PROGRAM IN CARDIOVASCULAR AND RESPIRATORY SCIENCES

CALGARY, ALBERTA

MAY, 2023

Abstract

The dilated cardiomyopathy with ataxia syndrome (DCMA) is a rare autosomal recessive mitochondrial disease that results from mutations in the poorly characterized *DNAJC19* gene and is frequently associated with premature death in children. DNAJC19 is a component of the TIM23 complex which imports proteins into mitochondria but has also been implicated in cardiolipin maturation. Better understanding of the role of DNAJC19 will provide insight into the mechanism of disease. Since previous work did not identify abnormalities in cardiolipin content within patient cells, I hypothesized that deficiency of *DNAJC19* would negatively impact mitochondrial protein homeostasis.

To address my hypothesis, I quantified the impact of DNAJC19 deficiency on the proteome of DCMA patient dermal fibroblasts. I identified an increase in mitochondrial fission, confirming previous observations. Pathway analysis predicted an upregulation of eukaryotic translation initiation factor 2 (EIF2) signaling in patient cells, indicating increased cellular stress. I identified significant increases in gene expression for key genes involved in the integrated stress response (ISR) and the mitochondrial unfolded protein response (UPRmt). Activation of these stress responses was not accompanied by increases in apoptosis, potentially indicating that patient cells can mitigate the cellular stress they face. I then tested two potential therapeutics: SS-31, which reduces oxidative stress, and tauroursodeoxycholic acid (TUDCA), which refolds proteins in the cytosol. Both compounds prevented upregulation of the ISR and the UPRmt.

In conclusion, I have identified a novel upregulation of two key cellular stress response pathways in DCMA patient fibroblasts. This work also identified TUDCA as a potentially novel treatment for DCMA and supports the classification of DCMA as a disease of mitochondrial proteostasis.

Preface

This thesis is original, unpublished work. Patient fibroblasts were supplied by The Alberta Precision Laboratories' Genetics & Genomics facility at the Alberta Children's Hospital and the Coriell Institute for Medical Research. Cell culture, mitochondrial isolation, protein extraction, RNA extraction, cDNA synthesis, and LDH cytotoxicity assays were performed by the author, Emily Wachoski-Dark. Samples were submitted for proteome analysis to the Southern Alberta Mass Spectrometry Facility wherein 1D liquid chromatography with tandem mass spectrometry was performed by Laurent Brechenmacher. Real-time quantitative PCR was performed by the author, Emily Wachoski-Dark with contributions from Vladislav Degtiarev and Dr. Radha Singh. Western blotting was performed the author, Emily Wachoski-Dark with contributions from Laurie Lee-Glover. The TUNEL apoptosis assay was performed by the author, Emily Wachoski-Dark with assistance from Nazanin Vaziri.

Acknowledgements

I would like to thank my supervisor, Dr. Steven Greenway for providing me with unconditional support and mentorship. Despite unexpected challenges Dr. Greenway continued to encourage me to persevere and created a safe space for me to navigate the ups and downs of graduate studies. I also wish to extend thanks to my committee members: Dr. Tim Shutt and Dr. Janice Braun. They provided exceptional support, advice, and guidance during this project.

I would also like to give special thanks to Dr. Tim Shutt for allowing me to utilize the equipment in his lab and putting me in contact with Laurie Lee-Glover. With that said, I cannot thank Laurie enough for her support during the completion of this project.

Thank you to my fellow lab members for the sense of community that they provided me throughout my time as a graduate student. I extend a massive thank you to Vladislav Degtiarev and Nazanin Vaziri for their support and helping me when needed.

Lastly, I would like to thank my friends and family for encouraging me during difficult times and celebrating my successes.

Table of Contents

List of Figures

List of Tables

List of Abbreviations

3-MG – 3-methylglutaric acid

3-MGA – 3-methylglutaconic aciduria

3-MGC – 3-methylglutaconic acid

ASNS - Asparagine synthetase

ATF4 – Activating transcription factor 4

ATF5 – Activating transcription factor 5

BAX – Bcl-2-associated X protein

CHOP – C/EBP homologous protein

CL – Cardiolipin

CLPP - Caseinolytic mitochondrial matrix peptidase proteolytic subunit

DAF – Complement decay-accelerating factor

DAPI - 4’,6-diamindino-2-phenylindole

DCMA – Dilated cardiomyopathy with ataxia syndrome

DIC – Mitochondrial dicarboxylate carrier

DNAJC15 - DnaJ heat shock protein family member C15

DNAJC19 - DnaJ heat shock protein family member C19

Drp1 – Dynamin-related protein 1

DYN2 – Dynamin 2

eIF2α - Eukaryotic translation initiation factor 2 alpha

ETC – Electron transport chain

ETC – Electron transport chain

GCN2 – General control non-derepressible 2

HAP28 – Heat- and acid-stable phosphoprotein

HMOX1 - Heme oxygenase 1

HRI – Heme-regulated eIF2α kinase

Hs105 – Heat shock protein 105 kDa

Hsp10 – Heat shock protein 10

Hsp60 – Heat shock protein 60

Hsp72 – heat shock-related 70 kDa protein 2

HSPB6 – Heat shock protein beta-6

IF1AX – Eukaryotic translation initiation factor 1A

IMM – Inner mitochondrial membrane

IMS – Intermembrane space

IPA – Ingenuity Pathway Analysis

ISR – Integrated stress response

LONP1 – Lon protease homolog 1

MAGMAS – Mitochondrial import inner membrane translocase subunit TIM16

MCU - Mitochondrial calcium uniporter

MFF – Mitochondrial fission factor

Mfn1 – Mitofusin 1

Mfn2 – Mitofusin 2

MIA - Mitochondrial intermembrane space assembly complex

MiD49 – Dynamic protein 49 kDa

MiD51 – Dynamic protein 51 kDa

MIM - Mitochondrial import complex

MIM – Mitochondrial import complex

MIP – Mitochondrial intermediate presequence protease

MLCL - Monolysocardiolipin

MPP – Mitochondrial processing peptidase

mPTP – Mitochondrial permeability transition pore

mtDNA – Mitochondrial DNA

mtHsp70 – Mitochondrial heat shock protein 70

MYH7 – Myosin heavy chain 7

NECT2 – Nectin-2

NOX - NADH oxidase

OMA1 – Metalloendopeptidase

OMM – Outer mitochondrial membrane

OPA1 – Dynamin-like 120 kDa protein

OXPHOS – Oxidative phosphorylation

PAM – Presequence associated motor complex

PERK – PKR-like ER kinase

PHB – Prohibitin

PHB2 – Prohibitin 2

PHB2 – Prohibitin 2

PKR – Protein kinase R

PP1R15A - protein phosphatase 1 regulatory subunit 15A

Proteostasis – Protein homeostasis

PYGM – Glycogen phosphorylase

ROS – Reactive oxygen species

RT-qPCR – quantitative real time PCR

SAM – Sorting and assembly machinery

SS-31 – Setzo-Schiller peptide 31

STX2 - Syntaxin-2

TIM22 – Translocase of the inner membrane 22

TIM23 – Translocase of the inner membrane 23

TNNI2 – Troponin I2

TNNT3 – Troponin T3

TOM – Translocase of the outer membrane

TRAP1 – Heat shock protein 75 kDa

TRIB3 – Tribbles Pseudokinase 3

TUNEL - terminal deoxynucleotidyl transferase dUTP nick end labeling

UPRmt – Unfolded protein response of mitochondria

WARS1 - tryptophan—tRNA ligase

XBP1 – X-box binding protein 1

XPNPEP3 – X-prolyl aminopeptidase 3

YME1L - YME1 like ATPase

Chapter 1: Introduction

1.1 Overview

The dilated cardiomyopathy with ataxia syndrome (DCMA) is an autosomal recessive mitochondrial disorder resulting from mutations in the *DNAJC19* gene (Davey et al., 2006). Common clinical characteristics of DCMA include elevated levels of 3-methylglutaconic acid (3-MGC) and 3-methylglutaric acid (3-MG) in body fluids, cardiac dysfunction, heart failure, cerebellar ataxia, and developmental delay (Machiraju et al., 2022). DCMA was first identified in the Canadian Dariusleut Hutterite population of southern Alberta but there have been subsequent cases identified worldwide. The DNAJC19 protein is understudied but is suspected to play a role in either mitochondrial protein import and/or in the metabolism of cardiolipin, a mitochondrial membrane phospholipid. This chapter outlines what is currently known about DCMA and the DNAJC19 protein, and how deficiency of this protein could lead to the observed patient phenotype.

1.2 DCMA

1.2.1 DCMA is a Mitochondrial Disease

Amongst their diverse functions, mitochondria play an imperative role in cellular energy production through oxidative phosphorylation (OXPHOS) (Hernando-Rodríguez & Artal-Sanz, 2018). When mitochondrial function is perturbed, it can result in selective removal of dysfunctional mitochondria through mitophagy or even apoptosis. Unsurprisingly, mitochondrial disorders are frequently associated with cardiac and neurological symptoms as these tissues have high energetic demands (El-Hattab & Scaglia, 2016).

There are two broad types of mitochondrial disease: primary and secondary. Primary mitochondrial diseases result from either mutations in mitochondrial DNA (mtDNA) or nuclear DNA that encode subunits of the electron transport chain (ETC) or impact OXPHOS complex assembly (Niyazov et al., 2016). One such example of a primary mitochondrial disease is Leigh syndrome that can result from mutations in either mtDNA or more commonly in nuclear DNA which encode subunits of various respiratory chain complexes (Lake et al., 2016). Leigh syndrome frequently presents with cardiac involvement in the form of hypertrophic cardiomyopathy, as well as neurologic involvement ranging from seizures and ataxia to cognitive impairment (Ruhoy & Saneto, 2014).

Secondary mitochondrial disease can be caused by mutations in genes that do not directly impact OXPHOS function or respiratory chain assembly but still result in mitochondrial dysfunction (Niyazov et al., 2016). For example, Barth syndrome is a mitochondrial disease caused by deficiency in the tafazzin enzyme due to mutations in the *TAZ* gene (Adès et al., 1993). This particular disorder leads to abnormal cardiolipin maturation thereby impacting mitochondrial structure and function (Ikon & Ryan, 2017). Barth syndrome presents with dilated cardiomyopathy, neutropenia, and elevated levels of 3-MGC in body fluids (Barth et al., 1999). These clinical characteristics are similar to another mitochondrial disease termed the dilated cardiomyopathy with ataxia syndrome (DCMA).

DCMA was first identified in the Hutterite population, where a single mutation in the *DNAJC19* gene (found on chromosome 3q26.33) resulted in deficiency of the DNAJC19 protein (Davey et al., 2006). Since DCMA is highly prevalent in the Hutterites of southern Alberta, the majority of described cases of DCMA result from the pathogenic variant found in this population which is a homozygous splice site mutation ($IVS_{3\text{-}1}G>C$). This particular mutation prevents

splicing of exon 4 leading to a premature stop codon and truncation of the DNAJC19 protein (Benson et al., 2017; Davey et al., 2006; Sparkes et al., 2007) (Figure 1).

Despite most described cases having this mutation, there has been a smaller subset of patients described with alternate mutations such as a homozygous one base pair (bp) deletion (c.300delA, p.Ala100fsX11) causing a frameshift mutation in two Finnish brothers (Ojala et al., 2012) (Figure 1). The elder of the two brothers had initially presented with motor developmental delay and partial respiratory chain enzyme deficiency. As for cardiac findings, the older brother was found to have left ventricular enlargement and a prolonged QT interval. Following treatment, he remained stable with no clinical cardiac symptoms. As for the younger brother, he presented with moderate muscular hypotonia, prolongation of the QT interval and compromised cardiac functions that eventually progressed to heart failure (Ojala et al., 2012). This case report and another case series (Machiraju et al. 2022) emphasize how the clinical characteristics of DCMA can drastically differ, even within families.

A homozygous five bp splice site deletion (c.280+1_280+5delGTAAG) was found to be the causative mutation for a young patient diagnosed at 12 years of age (Al Teneiji et al., 2016) (Figure 1). This was also the first reported patient with progressive cerebellar atrophy. In addition, she presented with global developmental delay, hypotonia, left ventricular dilation and reduced ejection fraction. Notably, the cardiac phenotype and levels of 3-MGC showed improvement with age despite no improvement in her neurological phenotype.

A Turkish boy was found to have a homozygous frameshift mutation (c.63delC, p.Tyr21*) (Ucar et al., 2017) (Figure 1). This patient presented with a systolic murmur and diminished ejection fraction that stabilized at 2 years of age. Other clinical characteristics included dystonia, spasticity, muscular atrophy, reduced cerebellar volume and progressive

cerebellar atrophy, much like the patient reported by Al Teneiji et al. (2016). Notably, this patient also presented with bilateral sensorineural hearing loss, further expanding the list and diversity of clinical characteristics of patients with DCMA.

A novel variant (c.159del [Phe54Leufs*5]) was recently reported in a patient from the Middle East (Al Tuwaijri et al., 2022) (Figure 1). Similar to other cases of DCMA, this patient presented with cardiomyopathy, seizures, developmental delay, cerebellar white matter changes, and elevated levels of 3-MGC and 3-methylglutaric acid (3-MG).

The most common clinical characteristics for patients with DCMA include dilated cardiomyopathy and elevated levels of 3-MGC and 3-MG in body fluids, usually 5-10 times greater than normal physiological levels (Al Teneiji et al., 2016). However, it is important to note that severity of these clinical characteristics can change over time, as observed by Ojala et al. (2012) and Al Teneiji et al. (2016). As new patients are identified, we are provided with a more comprehensive view of the clinical heterogeneity of this disease.

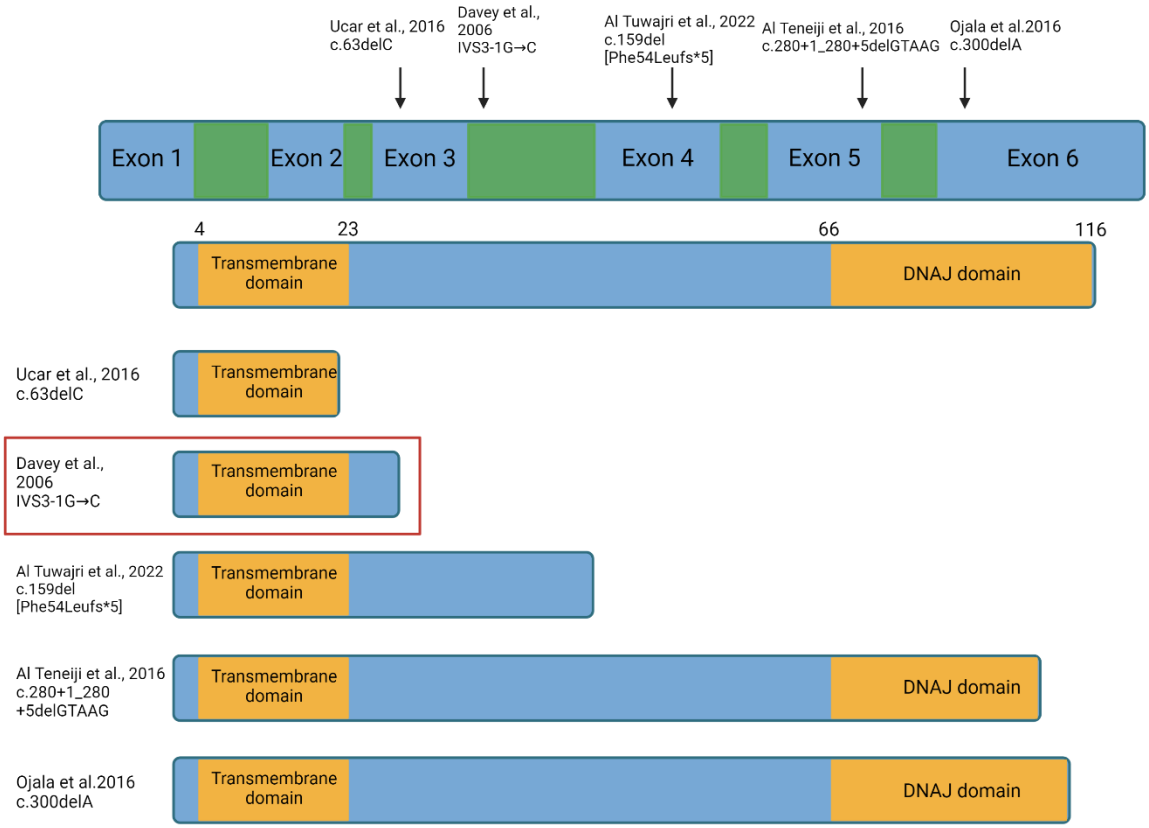

Figure 1. Impact of pathogenic variants in *DNAJC19* on protein structure. Location of known mutations (arrows) in exons and introns of *DNAJC19* (blue and green bands) are shown with resulting protein products shown by the blue and orange bands. Blue represents exons, green represents introns, and important domains within the protein product are represented by orange. The red box represents the mutation present in patient cells used for my study.

1.2.2 DNAJC19

DNAJC19 encodes the DnaJ heat shock protein family member C19 (DNAJC19), a J protein that localizes to the inner mitochondrial membrane (IMM) (Davey et al., 2006). J proteins are a family of molecular co-chaperones characterized by their J domain which consists of four helices, one of which enables interactions with the ATPase domain of heat shock protein 70 kDa (Hsp70) (Walsh et al., 2004). There are three types of J proteins, all of which contain a J domain. Type I (class A) and type II (class B) J proteins both have a glycine-rich region with their J domains near the N-terminus. However, type I J proteins have a Zn-finger domain, while type II does not (Kampinga et al., 2019; Walsh et al., 2004). Type III (class C) J proteins lack both the glycine-rich region and the Zn-finger domain meaning they are only characterized by their J domain at the C-terminus (Kampinga et al., 2019; Walsh et al., 2004). DNAJC19 contains only the J domain near the C-terminus, making DNAJC19 a type III J protein (Davey et al., 2006). Despite DNAJC19 being a J protein, the precise role of DNAJC19 has yet to be determined. DNAJC19 is suspected to play a role in protein import into mitochondria through the translocase of the inner membrane 23 (TIM23), based on interactions with mitochondrial heat shock protein 70 kDa (mtHsp70) (Figure 2) (Davey et al., 2006). However, DNAJC19 has also been proposed to be involved in cardiolipin remodeling through interactions with prohibitin proteins which form protein and lipid scaffolds on the IMM (Figure 2) (Richter-Dennerlein et al., 2014).

Mitochondria are comprised of around 99% nuclear-encoded proteins. This means that almost all of the mitochondrial proteome must be imported. Without proper protein import, numerous mitochondrial complexes, such as respiratory chain complexes, could not be formed, placing mitochondrial functions at risk (Schmidt et al., 2010). The TIM23 complex is responsible for the import of most matrix-localized proteins within mitochondria (Jensen & Dunn, 2002;

Wiedemann & Pfanner, 2017). Major components of this complex include mtHsp70, mitochondrial import inner membrane translocase subunit TIM16 (MAGMAS) and DnaJ heat shock protein family member C19 or C15 (DNAJC19 or DNAJC15) (Lu & Claypool, 2015; Sinha et al., 2016).

Supporting the role for DNAJC19 in mitochondrial protein import was a study indicating that DNAJC19 and MAGMAS form dimeric subcomplexes as indicated by a co-immunoprecipitation assay in HEK293T cells (Sinha et al., 2016). Additionally, this study found that DNAJC19 stimulates ATPase activity of mtHsp70, while MAGMAS inhibits ATPase activity (Sinha et al., 2010, 2016). Moreover, depletion of DNAJC19 resulted in the accumulation of presequence-containing unprocessed forms of mtHsp70, suggesting impaired mitochondrial protein import (Sinha et al., 2016). These findings were then confirmed in a more recent study using HeLa and HEK293T cells (Waingankar & D'Silva, 2021). Interestingly, DNAJC15 forms a distinct complex which positively regulates mtHsp70 similarly to DNAJC19 (Figure 2). However, it is suspected that DNAJC15 has a dispensable role while DNAJC19 serves a more crucial role, as downregulation of MAGMAS and DNAJC19 resulted in increased cell mortality (Sinha et al., 2016). Nonetheless, there is still the possibility that DNAJC15 could be playing a compensatory role for the loss of DNAJC19 in cells from patients with DCMA. These findings would suggest that DNAJC19 may be playing an important role in mitochondrial proteostasis through modulating protein import via the TIM23 complex.

As for cardiolipin metabolism, in HEK293T cells, DNAJC19 was reported to interact with prohibitin-2 (PHB2), a subunit of the prohibitin (PHB) complex (Richter-Dennerlein et al., 2014). Mitochondrial membranes are comprised of pools of cardiolipin (CL) which serve a multifaceted role in mitochondrial function (Dudek et al., 2019). CL can be highly diversified

depending on the attached fatty acid tails but, in the heart, linoleic acid is the predominant form (Hoch, 1992; Maguire et al., 2017). CL plays an important role in mitochondrial morphology by stimulating dynamin-related GTPases necessary for IMM fusion and fission events (Paradies et al., 2019). In addition, movement of CL from the IMM to the OMM signals for apoptosis and mitophagy (Birk et al., 2014). Beyond this, CL interacts with various complexes on the IMM such as respiratory chain supercomplexes, serving an important role in ATP production (Lu & Claypool, 2015). Unsurprisingly, deficiency in CL or errors in CL metabolism can lead to mitochondrial dysfunction. This is apparent in certain mitochondrial disorders arising from mutations in genes important for phospholipid remodeling, such as Barth Syndrome and MEGDEL syndrome (Ikon & Ryan, 2017; Wortmann, Vaz, et al., 2012).

Barth syndrome is of particular interest as it presents similarly to DCMA with elevated levels of 3-MGC, cardiomyopathy, and developmental delay (Adès et al., 1993; Barth et al., 1983). Notably, both DCMA and Barth syndrome are heterogenous diseases and share similar mitochondrial morphology trending towards fragmentation (Barth et al., 1983; Machiraju et al., 2019). Recently, more studies have been looking at mouse models of Barth syndrome to better understand the disease (Acehan et al., 2011; Sohn et al., 2022; Wang et al., 2023). In fact, one study found that genetic modifiers may impact phenotypic expression in Barth syndrome and alter mitochondrial quality control, resulting in the heterogeneity observed (Wang et al., 2023). Given the similarities between Barth syndrome and DCMA it is reasonable to think that the mechanism of disease could be similar.

Barth syndrome results from mutations in *TAZ* encoding the tafazzin enzyme which is important for cardiolipin remodeling (Barth et al., 2004). Tafazzin catalyzes the transfer of acyl chains, helping to maintain proper acyl chain composition for CL (Houtkooper et al., 2009).

Notably, monolysocardiolipin (MLCL) is produced from CL during acyl chain remodeling, but can be reacylated by tafazzin (Duncan, 2020; Xu et al., 2006). Thus, loss of tafazzin, such as in Barth syndrome leads to the accumulation of MLCL and a decrease in CL (Lu & Claypool, 2015). As a result, mitochondrial function and morphology is impaired in Barth syndrome (Acehan et al., 2007). Based on the phenotypic similarities between patients with Barth syndrome and those with DCMA, along with the important role of CL in mitochondrial function, it is possible that DNAJC19 might be involved in CL remodeling.

One study assessed the interactome of PHB2, a necessary subunit of the PHB complex used in cardiolipin remodeling using HEK293T cells (Richter-Dennerlein et al., 2014). This interactome identified DNAJC19 as an interacting partner (Figure 2). Beyond DNAJC19, subunits of OXPHOS and the TIM22 and TIM23 translocases were also enriched, suggesting PHB plays a more general role in IMM homeostasis (Richter-Dennerlein et al., 2014). This is consistent with other findings suggesting PHB complexes help stabilize membrane components and has even been reported as increasing under imbalances of proteostasis, such as activation of the unfolded protein response of mitochondria (UPRmt) (Signorile et al., 2019). This same study found that in DNAJC19 knockout cells, acyl chain composition of CL was altered, shifting towards longer and less saturated acyl chains, similar to what is observed in Barth syndrome (Richter-Dennerlein et al., 2014). However, there were no changes in overall CL levels or accumulation of MLCL, unlike what is seen with Barth syndrome.

Alternatively, studies looking at CL in DCMA patient-derived fibroblasts and induced pluripotent stem cells that were differentiated into cardiomyocytes did not find significant differences in CL composition (Machiraju et al., 2019; Rohani et al., 2020). Both studies looked at the levels of the long isoform of dynamin-like 120kDa protein (L-OPA1), a pro-fusion isoform

of the OPA1 protein which is regulated by CL and is important for mitochondrial fission and fusion. The study by Richter-Dennerlein et al. (2014) found that knocking down DNAJC19 resulted in the loss of L-OPA1, similar to what was found in patient-derived cells used by Rohani et al. (2020). This would suggest that the maintenance of mitochondrial structure is compromised by upstream processes leading to imbalances in OPA1 processing, whether that is caused directly by changes in the CL profile has yet to be elucidated.

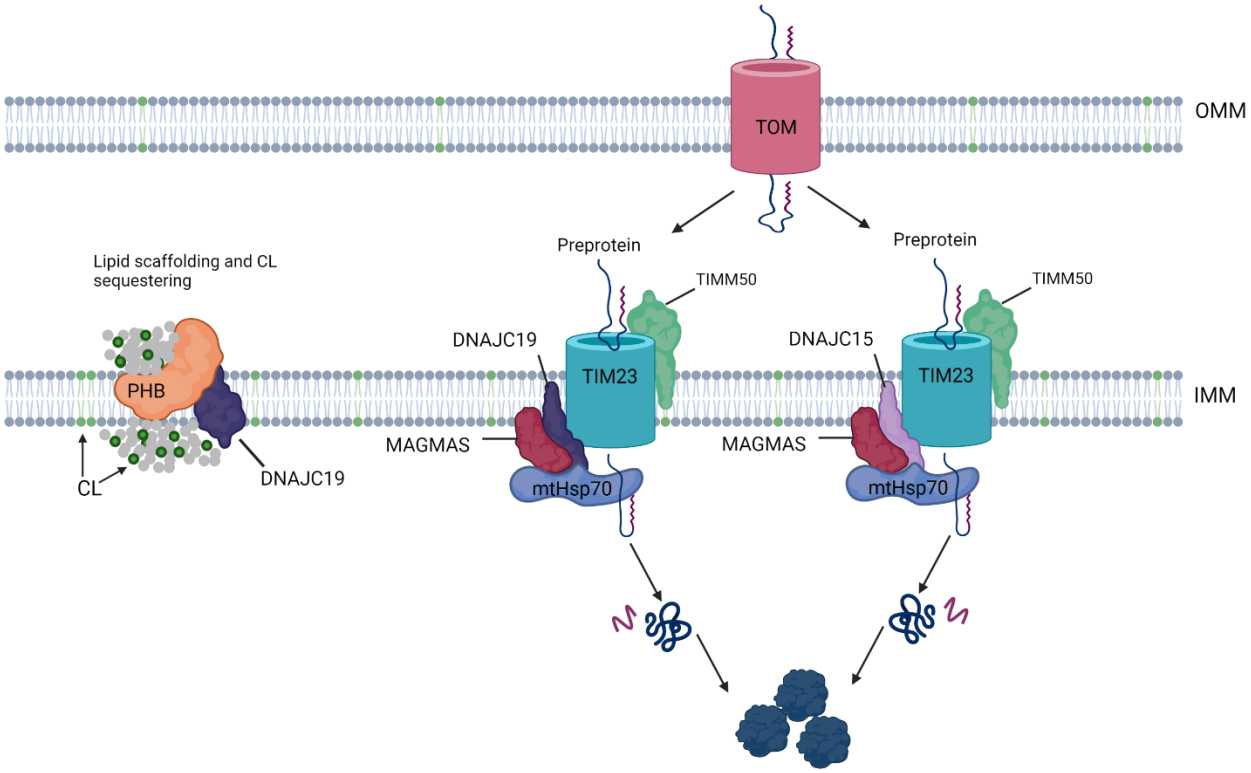

Figure 2. Suspected roles for DNAJC19 in cardiolipin remodeling or protein import. DNAJC19 as an interacting partner with the prohibitin (PHB) complexes along the inner mitochondrial membrane (IMM) could impact lipid scaffolding and cardiolipin sequestering/remodeling. Alternatively, DNAJC19 as an interacting partner with mitochondrial heat shock protein 70 kDa (mtHsp70) within the translocase of the inner membrane 23 (TIM23) could impact the import of mitochondrial proteins. Also shown is DnaJ heat shock protein family member C15 (DNAJC15) which is thought to modulate protein import similarly to DNAJC19 while forming a distinct complex. Created using BioRender.

1.3 Mitochondrial protein import

Mitochondria are comprised of two membranes separated by an intermembrane space (IMS). The outer mitochondrial membrane (OMM) allows ions and small molecules to pass freely, while larger molecules require translocases. The inner mitochondrial membrane (IMM) requires most molecules to pass through the use of translocases (Dudek et al., 2013). Mitochondrial DNA encodes only 13 proteins, while the rest need to be properly imported and folded to ensure healthy mitochondrial functions (El-Hattab & Scaglia, 2016). Thus, mitochondrial protein import must be tightly regulated and coordinated to ensure stability of the mitochondrial proteome.

Import of mitochondrial proteins follow three general pathways depending on the intended localization of the protein (Schmidt et al., 2010; Wiedemann & Pfanner, 2017). The presequence pathway sorts proteins intended for either the IMM or the matrix. The carrier pathway directs proteins for the IMM. The oxidative folding pathway is used for proteins residing in the IMS. Finally, outer membrane sorting and assembly machinery localizes proteins to the OMM (Bolender et al., 2008; Wiedemann & Pfanner, 2017).

The presequence pathway uses two main translocases, the translocase of the outer membrane (TOM) and the translocase of the inner membrane (TIM) (Bolender et al., 2008). This pathway identifies proteins with certain presequences that targets them for the IMM, matrix, or IMS. The TOM complex is used to pull proteins through the OMM and into the IMS. Comprised of three major subunits, Tom20 binds hydrophobic regions on preproteins, Tom22 binds positively charged residues, and Tom40 forms the β-barrel to move proteins into the IMS (Becker et al., 2010; Prasai, 2017). Proteins that are to be inserted into the IMM are recognized by their hydrophobic anchor and then transferred to the TIM22 complex (Chacinska et al., 2009). These proteins include most translocase subunits and other proteins destined for the IMM that

are not carrier proteins (Bolender et al., 2008). All other proteins that are to be imported into the matrix will be passed to TIM23 (Jensen & Dunn, 2002; Wiedemann & Pfanner, 2017). One major subunit of the TIM23 complex is mtHsp70 which serves as an ATPase to move proteins into the matrix. The presequence associated motor (PAM) complex regulates mtHsp70 ATPase activity, where the MAGMAS subunit inhibits activating activity of the DNAJC19 or DNACJ15 subunit (Davey et al., 2006; Sinha et al., 2016). Importantly, PAM not only regulates mtHsp70, but also assists in localization of subunits, helping TIM23 to assemble. Following entry to the matrix through TIM23, presequences on these proteins are cleaved by the mitochondrial processing peptidase (MPP) (Schmidt et al., 2010). In select cases, preproteins require secondary cleavage for stability. This is performed by X-prolyl-aminopeptidase 3 (XPNPEP3) which removes a single destabilizing N-terminal amino acid, or by the mitochondrial intermediate presequence protease (MIP) which removes an N-terminal octapeptide (Gakh et al., 2002; Singh et al., 2017). Lastly, following presequence removal, these proteins can be folded into their fully functional forms.

The carrier pathway uses the TIM22 complex to insert preproteins into the IMM, particularly metabolite carriers used in the transport of polar molecules (Chacinska et al., 2009). Importantly, these proteins do not contain a presequence like those following the presequence pathway that are destined for the IMM, instead they have multiple transmembrane domains that enable them to be incorporated into the IMM (Needs et al., 2021). Nonetheless, these proteins are still imported through TOM but instead are passed to TIM22 following entry to the IMS, rather than TIM23. This pathway is also responsible for the integration of certain subunits of the TIM23 translocase like Tim23 and Tim17 (Jensen & Dunn, 2002; Sokol et al., 2014).

Proteins that are destined to reside within the IMS can follow the oxidative folding pathway. The main complex involved in this pathway is the mitochondrial intermembrane space assembly (MIA) complex (Stojanovski et al., 2012). Many proteins found in the IMS contain disulfide bridges and it is believed that the cysteine motives found on preproteins are what targets them to the IMS (Milenkovic et al., 2009). Proteins first pass through the OMM via TOM where they are then sent to the MIA complex. The main component of the oxidative folding pathway is Mia40 which binds proteins using a transient disulfide bonded intermediate to stabilize them and promote their retention within the IMS (Stojanovski et al., 2012).

Import of proteins destine for the OMM relies on various signals and sequences (Chacinska et al., 2009). The OMM has two types of proteins that integrate into the membrane: β-barrel proteins which form pores allowing other molecules to be passed through, and α-helical segments comprised of hydrophobic regions allowing integration into the membrane (Schmidt et al., 2010). Both types of proteins are first transported into the IMS through TOM, much like proteins following the presequence pathway. Once inside the IMS the sorting and assembly machinery (SAM) complex is responsible for inserting β-barrel proteins into the OMM through recognition of their β signal (Pfanner et al., 2004). The SAM complex is formed of the β-barrel Sam50 subunit and two peripheral membrane proteins, Sam35 and Sam37 (Becker et al., 2008). Notably, this same machinery is used to assemble subunits of the TOM translocase (Becker et al., 2010). As for α-helical proteins, their incorporation into the OMM is less understood in humans (Doan et al., 2020). OMM α-helical proteins are recognized by either a signal-anchor sequence, C-terminal anchor, or internal signal (Chacinska et al., 2009). Nonetheless, these proteins pass through the OMM using TOM and are passed to the mitochondrial import (MIM) complex where they are then inserted into the OMM (Needs et al., 2021).

1.4 Mitochondrial protein homeostasis (proteostasis)

Protein homeostasis, or proteostasis, is a dynamic process that ensures the stability of individual proteins comprising the proteome (Hamilton & Miller, 2017). Mitochondrial proteostasis is maintained through the regulation of synthesis, folding, targeting, and degradation of mitochondrial proteins (Arrieta et al., 2019; Wachoski-Dark et al., 2022). Mitochondria are responsible for the production of the majority of cellular energy through ATP generation via OXPHOS. Considering the abundant energetic demands of the heart, dysregulation of mitochondrial proteostasis and mitochondrial processes has been linked to cardiac ageing, as well as heart failure (Smyrnias et al., 2019; Tocchi et al., 2015).

Errors in protein import, folding, degradation and targeting of proteins entering and within mitochondria can result in the accumulation of proteins and misfolded proteins which disrupt mitochondrial proteostasis (Arrieta et al., 2019). When mitochondrial proteostasis is perturbed there can be severe consequences to mitochondrial functions. Mitochondria house the ETC used to generate ATP necessary for cell vitality (Murphy et al., 2016). Oxidative stress resulting from defective electron transport functions in turn lead to accumulation of harmful reactive oxygen species (ROS) (Melber & Haynes, 2018). Accumulation of ROS and oxidative stress further exacerbates protein misfolding, disrupting mitochondrial proteostasis in a cyclical manner (Dietl & Maack, 2017).

In addition to energy production, mitochondria play an important role in calcium handling which is necessary for cardiac contractility (Dedkova & Blatter, 2013). Calcium enters mitochondria through the mitochondrial calcium uniporter (MCU) which is regulated by the mitochondrial membrane potential and thus is closely tied to ATP production (Dedkova &

Blatter, 2013). In fact, increased mitochondrial calcium uptake through the MCU results in stimulation of ATP synthesis (Tarasov et al., 2012). However, calcium signaling also serves an important role in cell death through the mitochondrial permeability transition pore (mPTP) (Bauer & Murphy, 2020).

Overloading of calcium, as well as accumulation of ROS allows the mPTP to open which collapses the mitochondrial membrane potential, inhibiting ATP synthesis and allowing rupturing the OMM (Bonora & Pinton, 2014). This permeabilization of the OMM allows for release of pro-apoptotic factors like cytochrome *c* into the cytosol where it can signal for apoptosis (Kinnally et al., 2011). Notably, peroxidation of CL by elevated calcium and H_2O_2 also leads to opening of the mPTP allowing cytochrome *c* to enter the cytosol and recruit pro-apoptotic factors (Birk et al., 2014). From this, it is evident that changes in the mitochondrial proteome that impair formation of important complexes or result in oxidative stress and ROS accumulation can have detrimental consequences on mitochondrial functions.

1.5 The unfolded protein response of mitochondria (UPRmt)

The unfolded protein response of mitochondria (UPRmt) is activated during mitochondrial stress resulting from or causing aggregated proteins within mitochondria or perturbed mitochondrial proteostasis. This response is best characterized in *C. elegans* but recent work has advanced our understandings of the mammalian UPRmt (Melber & Haynes, 2018). Disruptions in mitochondrial protein import and folding are sufficient to cause activation of the UPRmt, along with other stressors such as increases in ROS production and decreased ATP production (Oliveira & Hood, 2018; Qureshi et al., 2017; Rolland et al., 2019). However, the efficiency of protein import into mitochondria is suggested to be a key negative regulator of UPRmt (Melber

& Haynes, 2018). This is due to stress activated transcription factor atfs-1 ATFS-1 in *C. elegans* being targeted to mitochondria under normal physiological conditions wherein it is degraded. During mitochondrial stress, ATFS-1 will accumulate in the cytosol where the nuclear localization sequence will direct it to the nucleus to induce transcription of genes involved in the UPRmt (Melber & Haynes, 2018). This shows how closely tied the UPRmt is to protein import, however, these findings have not been confirmed in mammals. Nonetheless, activation of the UPRmt in both *C. elegans* and mammals works to restore mitochondrial proteostasis through the upregulation of genes encoding proteases to degrade misfolded proteins and chaperones to refold unfolded proteins (Arrieta et al., 2019). In addition, in *C. elegans*, the UPRmt has been shown to limit transcriptional activity of OXPHOS genes, suspected to reduce ROS production (Melber & Haynes, 2018; Nargund et al., 2015). While these findings have not been confirmed in mammals, there are studies that suggest mitochondrial translation is indeed limited (Münch, 2018)

Activation of the UPRmt in mammals relies on three bZIP transcription factors: activating transcription factor 4 (*ATF4*), activating transcription factor 5 (*ATF5*), and the C/EBP homologous protein (*CHOP*) (Figure 3). Importantly, activation of the UPRmt and these transcription factors requires activation of another stress response called the integrated stress response (ISR) (Zhou et al., 2008) (Figure 3). The ISR is activated under broad categories of environmental and cellular stress, such as viral infections, oncogene activation, glucose or amino acid deprivation, or protein accumulation (Pakos-Zebrucka et al., 2016). Depending on which stress the cell is facing, various kinases will work to phosphorylate eukaryotic translation initiation factor 2 alpha (eIF2α), which is required for most eukaryotic translation initiation. Phosphorylation of eIF2α results in an overall reduction in protein synthesis while allowing translation of select genes to help in recovery (Pakos-Zebrucka et al., 2016). Four various

kinases can phosphorylate eIF2α depending on the stress signal (Figure 3) (Costa-Mattioli & Walter, 2020). General control non-derepressible 2 (GCN2) phosphorylates in response to amino acid deprivation, mitochondrial stress, and oxidative stress (Costa-Mattioli & Walter, 2020; Mick et al., 2020). Double-stranded RNA-dependent protein kinase (PKR) phosphorylates in response to viral infections. Heme-regulated eIF2α kinase (HRI) phosphorylates in response to heme deprivation, mitochondrial stress, and heat shock. Lastly, PKR-like ER kinase (PERK) phosphorylates in response to endoplasmic reticulum (ER) stress and particularly unfolded protein accumulation within the ER (Melber & Haynes, 2018; Pakos-Zebrucka et al., 2016). Following phosphorylation of eIF2α there is activation of *ATF4* which is used in both the ISR and the UPRmt. Within the ISR, *ATF4* will upregulate various genes depending on the type of stress the cell is facing.

While there are numerous genes that are upregulated by *ATF4* within the ISR, there are a select few that are upregulated by various activating stressors (Figure 4). Asparagine synthetase (*ASNS*) is used in asparagine synthesis and is known to be upregulated during protein limitation, while heme oxygenase 1 (*HMOX1*) is an anti-oxidase which serves a role in response to oxidative stress (Dey et al., 2015; Pakos-Zebrucka et al., 2016). *XBP1* (X-box binding protein 1) is another transcription factor that upregulates select genes to address ER stress by increasing ER chaperones and components of the ER-associated degradation pathway (Elouil et al., 2007). Notably, the ER-associated degradation pathway serves to degrade accumulated misfolded proteins within the ER, playing an important role in protein quality control, similar to that of the UPRmt (Hampton, 2002). Lastly, TRIB3 (tribble pseudokinase) works using a negative feedback loop to regulate *ATF4* and terminate the ISR (Jousse et al., 2007). In the UPRmt, *ATF4* serves to activate two other transcription factors: *ATF5* and *CHOP* where they will translocate to the

nucleus to upregulate genes encoding proteases and chaperones (Figure 4) (Melber & Haynes, 2018).

There are two branches of the UPRmt, each of which is regulated by either *ATF5* or *CHOP* (Figure 3). The CHOP branch upregulates genes encoding chaperones like heat shock protein 10 (Hsp10) and heat shock protein 60 (Hsp60) which work to refold misfolded proteins (Oliveira & Hood, 2018; Zhao et al., 2002). The best characterized protease that is activated by CHOP is the caseinolytic mitochondrial matrix peptidase proteolytic subunit (CLPP) which will degrade any accumulated proteins (Zhao et al., 2002). Alternatively, the ATF5 branch activates the mitochondrial heat shock protein 70 (mtHsp70) that assists in protein import and protein folding in the matrix (Fiorese et al., 2016). This branch also activates proteases like lon protease homolog (LONP1) and YME1 like ATPase (YME1L) (Arrieta et al., 2019). YME1L is known to inactivate metalloendopeptidase (OMA1) which thereby prevents cleavage of OPA1 into the short isoform (Anand et al., 2014; Consolato et al., 2018). Importantly, both branches can be activated at the same time and serve a similar role to assist the cell in regaining mitochondrial proteostasis. For example, both YME1L and CLPP help maintain OXPHOS under stress through cleavage of dysfunctional ETC subunits (Ishizawa et al., 2019; Stiburek et al., 2012).

The UPRmt and the ISR have both been suggested to impact cardiac function. Notably, the ISR has been shown to be involved in cardiovascular disease through kinases such as PERK and GCN2 (Santos-Ribeiro et al., 2018). Increases in PERK, eIF2α, and ATF4 were considered detrimental wherein their downregulation led to cardioprotection though antiapoptotic and antioxidative effects (Santos-Ribeiro et al., 2018). Similarly, GCN2 was suggested to be involved with other comorbidities of cardiac disease, such as pulmonary hypertension and diabetes (Jung et al., 2015). Alternatively, the UPRmt has been found to have a cardioprotective

effect in mouse models through amelioration of left ventricular function and improving cardiomyocyte survival (Smyrnias et al., 2019). Particularly, activation of the UPRmt in an ATF5-dependent manner was shown to be cardioprotective in a mouse model of cardiac ischemia-reperfusion (I/R) injury (Wang et al., 2019). Additionally, loss of certain components of the UPRmt, such as YME1L, leads to heart failure in mice (Wai et al., 2015). Meanwhile, upregulation of certain components such as LONP1 attenuates ROS production and can protect against I/R injury (Kuo et al., 2015; Venkatesh et al., 2019). However, studies have also shown that the UPRmt can be maladaptive and can exacerbate cardiac dysfunction. For example, deletion of CLPP was shown to be beneficial and attenuated mitochondrial cardiomyopathy (Seiferling et al., 2016). Meanwhile release of Hsp60 from mitochondria was associated with increased cardiomyocyte apoptosis in a murine model of heart failure (Lin et al., 2007). Thus, we can see how the UPRmt plays an important role in cardioprotection through maintenance of mitochondrial function, but may also be maladaptive under certain circumstances (Liu et al., 2022).

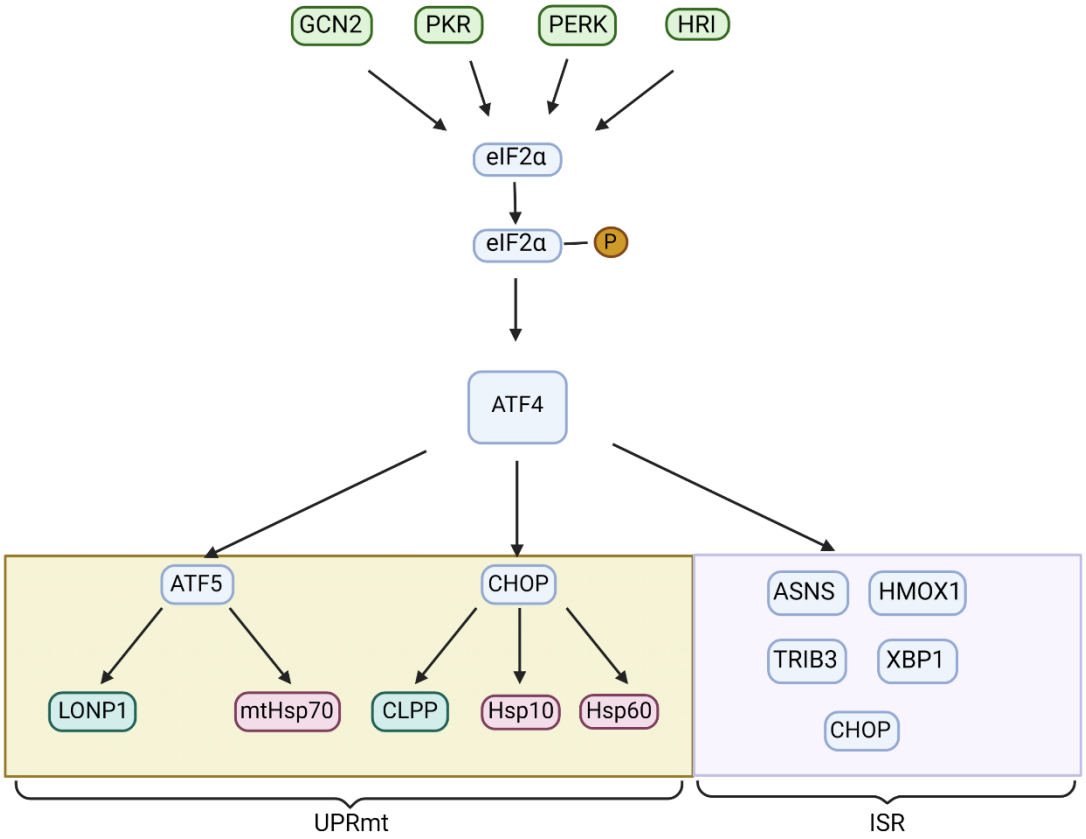

Figure 3. Activation of the integrated stress response (ISR) and the unfolded protein response of mitochondria (UPRmt) following phosphorylation of eukaryotic translation initiation factor 2 α (eIF2α). Kinases responsible for phosphorylation of eukaryotic translation initiation factor α (eIF2α) are the general control non-derepressible 2 (GCN2), protein kinase R (PKR), PKR-like ER kinase (PERK), heme-regulated eIF2α kinase (HRI). Phosphorylation of eIF2α subsequently activates activating transcription factor 4 (ATF4) which can activate the UPRmt through activating transcription factor 5 (ATF5) and C/EBP homolgous protein (CHOP). ATF5 and CHOP subsequently activate lon protease homolog 1 (LONP1), mitochondrial heat shock protein 70 kDa (mtHsp70), caseinolytic mitochondrial matrix peptidase proteolytic subunit (CLPP), heat shock protein 60 kDa (Hsp60), and heat shock protein 10 kDa (Hsp10). The ISR can also be activated leading to activation of asparagine synthetase (ASNS), heme oxygenase 1 (HMOX1), tribbles pseudokinase 3 (TRIB3), x-box binding protein 1 (XBP1), and CHOP. Created using BioRender.

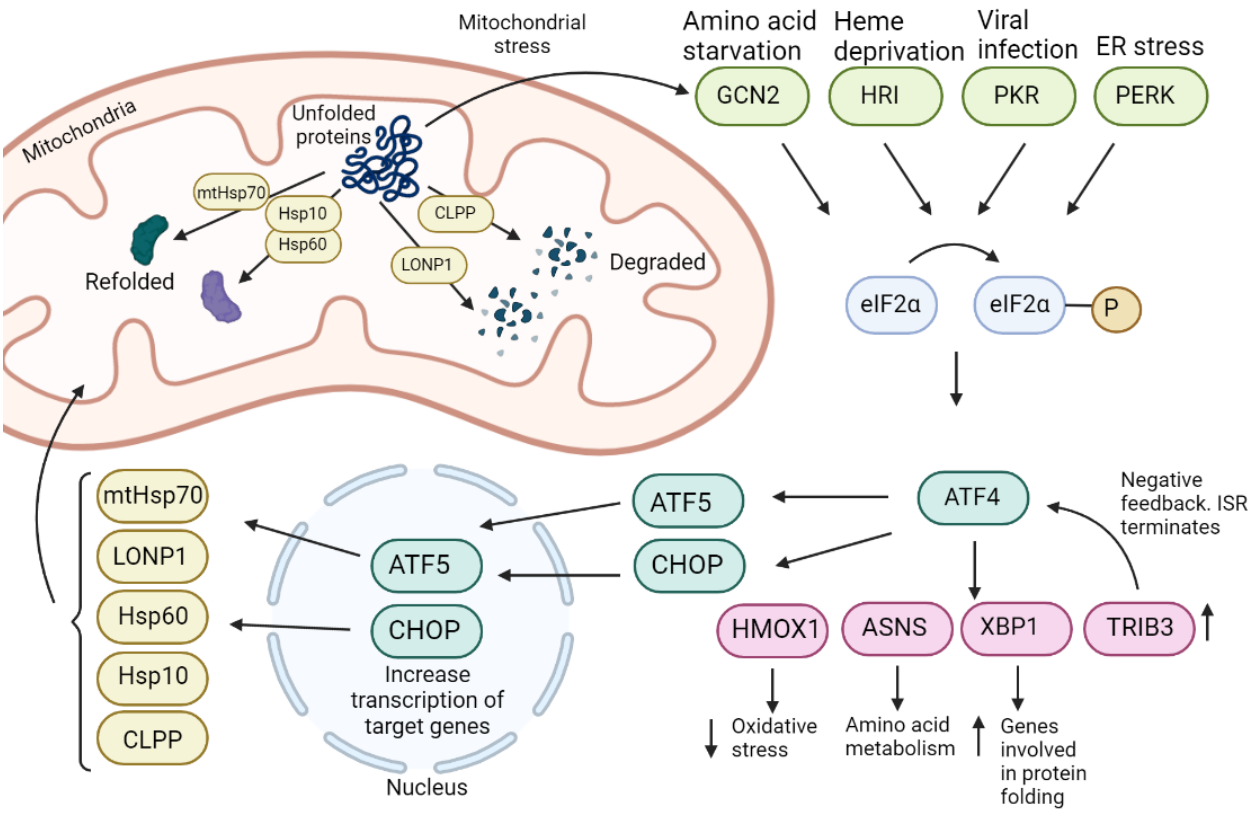

Figure 4. The integrated stress response (ISR) and the unfolded protein response of mitochondria (UPRmt) are linked. Unfolded proteins cause mitochondrial stress which can signal to the general control non-derepressible 2 (GCN2). Other kinases responsible for activation of the ISR include heme-regulated eIF2α kinase (HRI), protein kinase R (PKR), and PKR-like ER kinase (PERK). These kinases then phosphorylate eukaryotic translation initiation factor 2 α (eIF2α) which upregulates activating transcription factor 4 (ATF4). ATF4 can then upregulated heme oxygenase 1 (HMOX1), asparagine synthetase (ASNS), x-box binding protein 1 (XBP1), or tribbles pseudokinase 3 (TRIB3) for the ISR. Alternatively, ATF4 can upregulate the UPRmt through activating transcription factor 5 (ATF5) or C/EBP homolgous protein (CHOP) which will increase transcription of target genes encoding proteins like mitochondrial heat shock protein 70 kDa (mtHsp70), lon protease homolog 1 (LONP1), heat shock protein 60 kDa (Hsp60), heat shock protein 10 kDa (Hsp10), or caseinolytic mitochondrial matric peptidase proteolytic subunit (CLPP). These proteins will then serve to address the unfolded mitochondrial proteins through degradation or refolding. Created using BioRender.

1.6 Mitochondrial Membrane Fission and Fusion

Mitochondria play critical roles in the maintenance and production of cellular energy and signaling. The unique structure of mitochondria being comprised of an OMM and IMM are what enable these organelles to effectively perform their necessary functions (Giacomello et al., 2020). Mitochondria are able to alter their morphology and distribution within the cell through the process of fission and fusion (Youle & van der Bliek, 2012). These two processes encompass mitochondrial dynamics and are crucially important to respond to and cope with cellular and environmental stressors (Youle & van der Bliek, 2012). Maintenance of mitochondrial dynamics allows for the clearing of damaged mitochondria and the restoration of functional mitochondria.

Mitochondrial membrane dynamics are governed by conserved protein machinery (Ehses et al., 2009). Dynamin-related proteins (DRPs) are GTPase proteins that play a key role in mitochondrial membrane shaping and maintenance. The key protein that mediates fission is the dynamin-related protein 1 (Drp1) that is recruited to mitochondria by other proteins like mitochondrial fission factor (Mff), mitochondrial fission protein 1 (Fis1) and mitochondrial dynamic proteins 49 kDa and 51 kDa (MiD49 and MiD51) (Losón et al., 2013). Specifically, multimers of Drp1 subsequently promote GTPase activity and lead to mitochondrial fission (Hu et al., 2017). Meanwhile, mitochondrial fusion is also regulated by GTPases.

Mitochondrial fusion of the OMM and the IMM are regulated by different proteins. Mitofusin 1 and 2 (Mfn1 and Mfn2, respectively) are responsible for mediating fusion of the OMM, while OPA1 mediates fusion of the IMM (Youle & van der Bliek, 2012). Similar to Drp1, dimerization and activation of GTPase activity is crucial for functionality of the mitofusin proteins to promote fusion (Cao et al., 2017). However, while OPA1 is critically important for fusion, it can also be involved in mitochondrial fission and has been shown as necessary for

mitochondrial bioenergetics and cristae formation (Del Dotto et al., 2017). OPA1 undergoes proteolytic processing into long or short isoforms (L-OPA1 and S-OPA1, respectively) (Song et al., 2007). Particularly, cleavage of OPA1 into S-OPA1 results in a loss of GTPase activity (Anand et al., 2014). The ratio of long to short isoforms of OPA1 is what determines fusion rather than fission, with an increase in L-OPA1:S-OPA1 being considered pro-fusion (Song et al., 2007). Cleavage of OPA1 can occur at two different splice sites, S1 or S2. YME1L, a *i*-AAA protease, works to cleave OPA1 at S2, while OMA1 a peptidase on the IMM, cleaves at S1 (Anand et al., 2014). Importantly, cleavage at S2 by YME1L is considered to be important for cristae structure and the maintenance of mitochondrial bioenergetics (Anand et al., 2014; Mishra et al., 2014). However, cleavage at S1 by OMA1 results in increased fission, mitochondrial fragmentation, and a loss of mitochondrial bioenergetics (Gilkerson et al., 2021). OMA1 is activated under conditions of stress such as depletion of the mitochondrial membrane potential or a reduction in ATP production (Baker et al., 2014).

1.7 SS-31 as a potential therapeutic

The Szeto-Schiller (SS) peptides were discovered while looking at dermorphin analogs to target the μ opioid receptor (Szeto & Schiller, 2011). These peptides are readily taken up into mitochondria where they target the IMM. It is thought that due to their selectivity, they would assist in treating mitochondrial disease and mitochondrial dysfunction. SS-31 (D-Arg-2′6′-dimethylTyr-Lys-Phe-NH2) was created by altering the order of amino acid residues in SS-02, preventing 2',6'-dimethyl-L-tyrosine (Dmt) from being the N-terminal residue. The goal was to maintain the free radical scavenging ability of Dmt, while allowing Tyr to be the N-terminal amino acid which is essential for opioid activity. However, changing the Dmt position in SS-31

resulted to lower binding affinity for the μ opioid receptor. Thus, while SS-31 is suboptimal for opioid receptor targeting, it still works to scavenge free radicals, reducing ROS and preventing membrane depolarization and subsequent autophagy (Szeto, 2014; Szeto & Birk, 2014; Szeto & Schiller, 2011). Specifically, SS-31 interacts with CL to prevent peroxidative damage (Szeto & Birk, 2014). CL interacts with cytochrome *c* which can be loosely bound under normal physiological conditions, allowing the transfer of cytochrome *c* between complex II and IV in the ETC (Birk et al., 2014). However, during pathological conditions where ATP decreases, cytochrome *c* becomes tightly bound with CL and leads to peroxidation and subsequent apoptosis (Birk et al., 2014; Kagan et al., 2009). SS-31 selectively binds CL, inserting itself into the cytochrome *c* and CL complex to inhibit peroxidation. Through this interaction SS-31 is able to scavenge ROS, increase ATP synthesis and reduce electron leak, making it a plausible candidate for the treatment of mitochondrial diseases (Birk et al., 2013; Chavez et al., 2020; Zhao et al., 2017).

In fact, SS-31 has been tested in numerous animal models for the treatment of cognitive impairment (Zhao et al., 2019; Zuo et al., 2020), Alzheimer's disease (Calkins et al., 2011; Reddy et al., 2017), and heart failure (Lu et al., 2017; Suo et al., 2022). Due to preclinical findings proving SS-31 to be beneficial, it is being used in many clinical trials. Treatment with SS-31 showed a dose-dependent increase in distance walked for a walking test in patients with primary mitochondrial myopathy, along with a decrease in reported fatigue and muscle complaints (Karaa et al., 2018). Of particular interest to us, a clinical trial of SS-31 to treat Barth syndrome has shown significant improvements in a walking test to measure fatigue along with improvement in some cardiac parameters like improved left ventricular stroke volume (Reid Thompson et al., 2021). Notably, these changes suggest that SS-31 may be beneficial in the

treatment of Barth syndrome. Given the similarity between Barth Syndrome and DCMA, SS-31 could also be a potential therapeutic for the treatment of DCMA.

Rohani et al. (2020) looked at SS-31 to ameliorate mitochondrial fragmentation in DCMA patient-derived induced pluripotent stem cells (iPSCs) that were differentiated into cardiomyocytes. Particularly, patient iPSCs were found to have highly fragmented mitochondria with disorganized cristae. In addition, a lower ratio of L-OPA1 to S-OPA1 was noted alongside mitochondrial fragmentation. Indeed, addition of SS-31 reversed mitochondrial fragmentation and improved cristae formation (Rohani et al., 2020). SS-31 was also found to reduce L-OPA1 processing, restoring the ratio of isoforms back to control levels (Machiraju et al., 2019; Rohani et al., 2020). These findings were similar to another study using a mouse model of Alzheimer's disease wherein they showed a decrease in mRNA and protein levels of pro-fission genes along with an increase in fusion genes following treatment with SS-31 (Reddy et al., 2017). Another study confirmed imbalances in the OPA1 isoform ratio in DCMA patient fibroblasts which was ameliorated by addition of SS-31 (Machiraju et al., 2019). This same study also found elevated levels of ROS production which was reduced upon treatment with SS-31 (Machiraju et al., 2019). These findings further suggest SS-31 could be a potential therapeutic for the treatment of mitochondrial disorders and particularly the treatment of DCMA.

1.8 Hypothesis

Hypothesis: I hypothesize that deficiency of DNAJC19 negatively impacts mitochondrial protein homeostasis.

Aim 1: Assess the impact of DNAJC19 deficiency on the mitochondrial proteome of healthy control and patient fibroblasts.

Aim 2: Assess activation of genes involved in the mitochondrial unfolded protein response (UPRmt) in healthy control and patient fibroblasts.

Aim 3: Assess cellular stress responses to toxins and therapeutics using SS-31, tauroursodeoxycholic acid (TUDCA), and 3-methylglutaconic acid (3-MGC).

The rationale for this hypothesis was based on previous findings that supported the role of DNAJC19 in mitochondrial protein import due to associations with mtHsp70 within the TIM23 complex and the lack of changes in CL in DCMA patient cells. If DNAJC19 is involved in protein import, or perhaps even involved in protein folding through interactions with mtHsp70 as a chaperone, then loss of this protein would be detrimental to the mitochondrial proteome. If mitochondria cannot effectively import or process incoming proteins, then mitochondrial functions become compromised as the mitochondrial proteome cannot be maintained. This mitochondrial dysfunction would form the basis for the pathophysiology of DCMA.

Chapter 2: Materials and Methods

2.1 Fibroblast culture

The Alberta Precision Laboratories' Genetics & Genomics facility at the Alberta Children's Hospital, the Coriell Institute for Medical Research, and ThermoFisher Scientific provided fibroblast cultures that were isolated from patient skin biopsies. A total of nine separate

fibroblast cell lines were used, with each control, mild, and severe having three separate cell lines (Table 1). Control fibroblast cell lines are from hDFa lines or human dermal fibroblast adult lines which had been isolated from healthy adults, C1 and C2, respectively. The final control fibroblast cell line (C3) was isolated from a healthy control age matched to fibroblasts from patients with severe DCMA. Severe cell lines are from patients with DCMA that presented with severe cardiac dysfunction (S1-S3), while mild fibroblast cell lines are from patients with DCMA that presented with mild cardiac dysfunction (M1-M3). Mild DCMA was characterized by a left ventricular function within normal limits, thus, the left ventricular ejection fraction was >50%. Severe DCMA was characterized by left ventricular dysfunction, meaning that patients had a left ventricular ejection fraction <50% requiring medical therapy or had an early death related to heart failure.

Cultures were grown on T75 treated tissue culture flasks at 37 ˚C in a 5% CO_2 incubator. All fibroblast culture work was done in a class II biosafety cabinet. A full list of reagents used for fibroblast cell culture and other assays can be found in Table 2. Fibroblasts were maintained with Eagle's Minimum Essential Medium (EMEM) containing 25 mM glucose, 2 mM glutamine, phenol red, 100 U/mL penicillin-streptomycin, and 10% fetal bovine serum (FBS) (Sigma-Aldrich, ThermoFisher Scientific). Sodium bicarbonate was added to EMEM to maintain a stable pH around 7.4 when supplied with 5% CO_2 in the incubator (Kostidis et al., 2017). Medium was changed every 3-5 days until cells reached ≥80% confluency at which they were either collected or passaged.

Passaging and collection of confluent, adherent cells was done first by washing twice with 1X phosphate buffered saline (PBS) (pH7.4; ThermoFisher Scientific), followed by the addition of 1.5 mL of 0.5 g/L trypsin-0.2 g/L EDTA solution (Sigma-Aldrich) and incubated for

three minutes at 37 ˚C. To inhibit the action of trypsin once cells had started to detach, 10 mL of cell culture medium was added. The cell suspension was centrifuged at 100 x g for 5 minutes. The resultant cell pellet was either collected for downstream processing or resuspended in EMEM to be passaged. If the cell pellet was to be frozen for future use the pellet was resuspended in freezing medium containing 10-20% dimethyl sulfoxide (DMSO) (Gibco). Frozen cells were cooled overnight at -80 ˚C in a 2-propanol bath to cool at -1 ˚C/min then transferred to liquid nitrogen for long-term storage.

Table 1. Established fibroblast cell lines and their corresponding phenotype based on patient cardiac dysfunction. Cardiac phenotype was determined by left ventricular dysfunction. Severe phenotype was determined by a left ventricular ejection fraction (LVEF) <50% requiring medical therapy or leading to an early death related to heart failure. Mild phenotype was determined by a LVEF within normal limits (>50%). Age in years refers to the patient age at the time of fibroblast collection.

Cell line name	Cardiac Phenotype	Patient Sex	Age (Years)
C1	Control	Unknown	Adult
C2	Control	Unknown	Adult
C3	Control	Male	1.5
S1	Severe DCMA	Female	1.5
S2	Severe DCMA	Female	1.5
S3	Severe DCMA	Female	1.5
M1	Mild DCMA	Female	1.2
M2	Mild DCMA	Male	13
M3	Mild DCMA	Male	2.8

Table 2. List of reagents utilized throughout the methods, including the catalog number and company name.

Reagent	Catalog Number	Company
Eagle's Minimum Essential Medium	M2279	Sigma-Aldrich
L-Glutamine (200mM)	25030081	Gibco
Penicillin-Streptomycin	15140-122	Gibco
Phosphate Buffered Saline 10X	A25742	Lonza
Trypsin-EDTA	25200056	Gibco
Recovery Cell Culture Freezing Medium	12648-010	Gibco
FBS, Qualified, One Shot format	A3160702	Gibco
Mitochondria Isolation Kit for Cultured Cells	89874	Thermo Scientific
RIPA Lysis and Extraction Buffer	89900	Thermo Scientific
Pierce™ BCA Protein Assay Kit	23227	Thermo Scientific
12% Mini-PROTEAN® TGX™ Precast Protein Gels	4561044	Bio-Rad
Bio-Safe™ Coomassie Stain	1610786	Bio-Rad
Trizma base	T6066	Sigma-Aldrich
Tween 20	P9416	Sigma-Aldrich
Laemmli SDS sample buffer	J60015	Alfa Aesar
Immun-Blot PVDF Membrane	1620177	Bio-Rad
B-Tubulin Loading Control Monoclonal Antibody	MA5-16308	Invitrogen
VDAC1 Antibody	ab14734	Abcam
Hsp60 Antibody	12165S	Cell Signalling
Drp1 Antibody	8570S	Cell Signalling
OPA1 Antibody	612607	BD Biosciences
Goat anti-Mouse IgG (H+L) Secondary Antibody, HRP	31430	Invitrogen
Anti-rabbit IgG, HRP-linked Antibody	7074S	Cell Signalling
Pierce™ ECL Western Blotting Substrate	32106	Thermo Scientific
High-Capacity cDNA Reverse Transcription Kit	4368814	Applied Biosystems
RNaseOUT™ Recombinant Ribonuclease Inhibitor	10777019	Invitrogen
PowerUp SYBR Green Master Mix	A25742	Applied Biosystems
DeadEnd Fluorometric TUNEL System	G3250	Promega
ProLong™ Gold Antifade Mountant with DAPI	P36931	Invitrogen
CyQUANT LDH Cytotoxicity Assay	C20300	Invitrogen

2.2 Mitochondrial Isolation

Mitochondrial isolation was performed using a mitochondria isolation kit for cultured cells (ThermoFisher Scientific). Cell pellets were collected and combined from two T75 culture flasks using the trypsinization protocol described in fibroblast culture. Briefly, cells were lysed, vortexed and differentially centrifuged to isolate mitochondria. Once collected, the mitochondrial pellet was placed on ice and immediately processed for protein extraction following the method below.

2.3 Protein Extraction and Quantification

Whole cell protein was extracted using RIPA lysis buffer (ThermoFisher Scientific) with the addition of phosphatase inhibitors and protease inhibitors (Sigma-Aldrich). For the lysis of a cell pellet obtained from a T75 culture flasks, 150 µL of RIPA buffer was added. Mitochondrial protein was extracted in the same manner from mitochondrial pellets using only 40 µL of RIPA buffer. Following the addition of RIPA buffer, the pellet was resuspended by thorough pipetting and left to rock at 4 ˚C for 30 minutes. Subsequently, samples were centrifuged at 12,000 x g for 30 minutes at 4 ˚C. Supernatant was then collected and the pellet discarded. Samples were then stored at -80 ˚C.

Following protein extraction, protein was quantified using the Pierce BCA Protein Assay Kit (ThermoFisher Scientific). For the BCA assay, standards were created as outlined in the online protocol (ThermoFisher). The working reagent was prepared based on the total volume required, wherein 50 parts of the BCA reagent A was mixed with 1 part reagent B. Standards or unknown samples were loaded onto a microplate along with the working reagent and incubated

at 37 ˚C for 30 minutes prior to measuring absorbance at 562 nm using the SpectraMaxi3x Multi-Mode Microplate Reader (Molecular Devices). A standard curve was prepared and used to determine the protein concentration in each sample.

2.4 1D liquid chromatography with tandem mass spectrometry (LC-MS/MS)

Mitochondria were isolated from healthy control and patient fibroblasts at 90% confluency as outlined above. Mitochondrial protein was extracted using 40 µL RIPA buffer and subsequently quantified using a BCA assay. Following instructions from the Southern Alberta Mass Spectrometry Facility (SAMS), 167 µg of mitochondrial protein was loaded into the wells of a 12% prepared mini-protean TGX gel (BioRad) and ran at 150V until the dye front reached 1.5 cm (Figure 5). The run was stopped at 1.5 cm and the gel was rinsed in ultra pure water for 5 minutes, or until the background was clear. The gel was then stained with Coomassie blue for 1.5 hours and subsequently washed three times in ultra pure water for 5 minutes each. Bands from each lane were cut into 0.5 cm sections using a sterile scalpel blade and placed in sterile 1.5 mL centrifuge tubes with ultra pure water. Samples were submitted to the SAMS facility for analysis where the bands were first digested with trypsin. Following trypsinization, peptides were analyzed on an Orbitrap Fusion Lumos Tribrid mass spectrometer (Thermo Scientific) operated with Xcalibur (version 4.4.16.14) and coupled to a Thermo Scientific Easy-nLC (nanoflow Liquid Chromatography) 1200 system. Samples were searched against a database for *Homo sapiens* using Mascot (Matrix Science, London, UK; version 2.7.0) with a maximum missed trypsin cleavage of 1, parent ion tolerance of 10 PPM, and a fragment ion tolerance of 0.60 Da. Proteins were identified using significant threshold parameters of a protein probability of 99% along with a peptide probability of 95% and a minimum of 2 unique peptides per sample. From

my proteomic data the false discovery rate (FDR) was calculated at 0.4%. Results of the 0.5 cm bands were combined for each lane and data was provided to me in the form of a Mascot file which could be imported into Scaffold (v4.3.4, Proteome Software Inc.) for interpretation and analysis.

Total spectrum counts were quantified within Scaffold software and used for downstream analysis. From quantitative values, fold changes for cells collected from patients with mild and severe cardiac phenotypes were calculated in relation to control counts. A one-way ANOVA with Tukey's test was used for statistical analysis, where a p value < 0.05 was considered statistically significant. Mitochondrial proteins were identified through cross-referencing MitoCarta3.0. Data was input and analyzed further using Ingenuity Pathway Analysis (IPA) (QIAGEN Inc., https://www.qiagenbioinformatics.com/products/ingenuitypathway-analysis). Due to the low number of mitochondrial proteins, fold changes and p values were input into IPA for all identified proteins with a fold change ±2 and a core analysis was performed. Top canonical pathways and disease pathways were returned with downstream analyses. Subsequently these same proteins were then input into Metascape (Zhou et al., 2019) for additional pathway analysis.

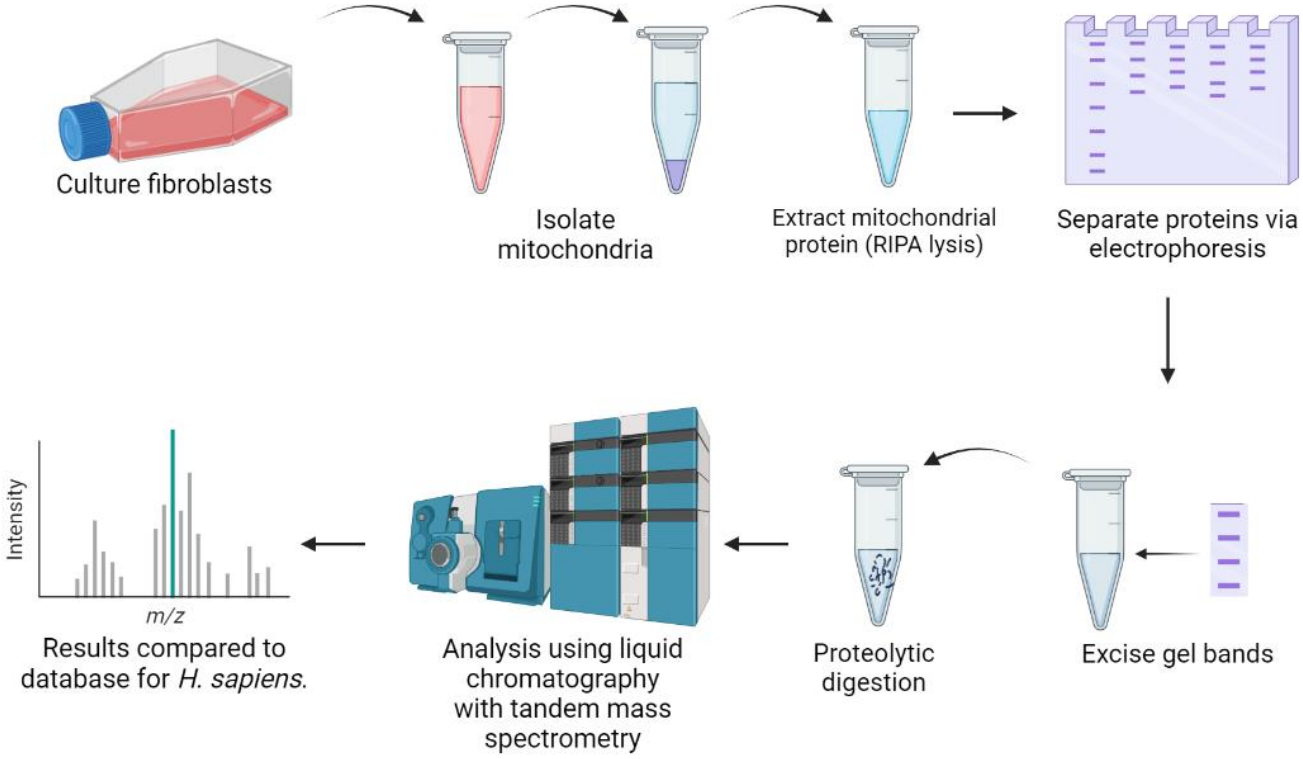

Figure 5. 1D liquid chromatography with tandem mass spectrometry. Created using BioRender.

2.5 Western Blotting

All western blotting buffers were prepared in the lab from 10X solutions. The 10X running buffer was prepared by adding 800 mL of ultra pure water to 30.2 g of Tris base (Sigma-Aldrich), 144.0 g of glycine (Sigma-Aldrich), and 10.0 g of SDS (Sigma-Aldrich) then ultra pure water was added to a final volume of 1 L. The 10X transfer buffer was prepared by adding 800 mL of ultra pure water to 30.2 g of Tris base (Sigma-Aldrich), and 144.0 g of glycine (Sigma-Aldrich) then topped to a final volume of 1 L. The 1X transfer buffer was prepared by adding 100 mL of 10X transfer buffer to 200 mL of methanol (Sigma-Aldrich) and 700 mL of ultra pure water. To prepare 10X Tris-buffered saline (TBS) 24.0 g of Tris base (Sigma-Aldrich) and 88.0 g of NaCl (Sigma-Aldrich) were dissolved in 900 mL of ultra pure water, followed by adjusting the pH to 7.6 and a final volume of 1 L with ultra pure water. The 1X Tris-buffered saline with 0.1% Tween 20 detergent (TBST) was prepared by adding 100 mL of 10X TBS and 1 mL of Tween 20 detergent (Sigma-Aldrich) to 900 mL of ultra pure water.

Mini-protean TGX gel 8% or 10% with 15 µL wells (Bio-Rad) were used in conjunction with the Mini Trans-Blot Cell (Bio-Rad). Once protein concentrations for desired samples had been calculated, 40 µg of protein was added to 4X laemmli SDS buffer (Alfa Aesar) and heated at 70 ˚C for ten minutes to denature proteins. Once denatured, samples were loaded onto the gel and placed in the tank with 1X running buffer. Gels were run at 100V for around one and a half hours, or until the dye front reached the end of the gel.

Once electrophoresis finished, the gel was removed and prepared for wet transfer. This required the removal and soaking of the gel in pre-chilled 4 ˚C 1X transfer buffer for 10 minutes along with filter paper and sponges. Immun-Blot PVDF membranes (Bio-Rad) cut to the size of the gel were wet with methanol for thirty seconds prior to immersing in 1X transfer buffer for 10

minutes. The transfer cassette was assembled as follows: negative side down, sponge, filter paper, gel, membrane, filter paper, sponge, positive side up. The membrane was placed in such a way to ensure no air bubbles were left between the gel and the membrane; this is necessary for an optimal transfer. Once closed, the cassette was placed in the tank which was rested on ice and filled with pre-chilled 1X transfer buffer. The wet transfer then occurred in a climate-controlled room at 4 ˚C overnight at 30V.

Once transferred, the membrane was removed and blocked in 5% milk diluted in TBST for 1 hour while rocking at room temperature. This ensured that antibodies did not bind non-specifically to the membrane. Following blocking, the membrane was rinsed three times with 1X TBST for 5 minutes. Primary antibody was then diluted in 5% milk with TBST (1:1000 for Drp1, OPA1, VDAC1, and Hsp60. 1:3000 for β-tubulin), covered with saran wrap, and left to rock overnight at 4˚C. The next day the membrane was washed three more times with 1X TBST to remove excess antibody solution. Secondary antibody was then added at 1:10 000 and left to rock for 1 hour at room temperature. Lastly, the membrane was washed three more times with 1X TBST before adding enhanced chemiluminescence (ECL) substrate (ThermoFisher Scientific) for 1 minute prior to imaging. Membranes were then imaged using the iBright CL1500 Imaging System (ThermoFisher Scientific).

2.6 Quantitative real-time PCR (qRT-PCR)

2.6.1 RNA extraction

Fibroblasts were collected at confluency, yielding around 8.4 x 10^6 cells. RNA was extracted from cell pellets using the standard protocol provided with the RNeasy Mini Kit (Qiagen). Once

extracted, the purity and concentration of RNA was determined using the NanoPhotometer N50 Touch (Implen), wherein an A260/280 and A260/230 greater than 2.0 was considered pure (ThermoFisher Scientific). RNA was then stored at -80 ˚C for future use.

2.6.2 Conversion of RNA to cDNA

RNA was converted to complementary DNA (cDNA) from 2 µg of total RNA per 20 µL reaction using the Invitrogen High-Capacity cDNA Reverse Transcription Kit (ThermoFisher Scientific). The determined amount of RNA was then diluted in RNase-free water to a final volume of 10 µL. To this, 0.5 µL of RNaseOUT (ThermoFisher Scientific) and 1 µL of DNase I (ThermoFisher Scientific) were added to diluted RNA and incubated at 37 ˚C for 30 minutes using the Bio-Rad T100 thermal cycler (Bio-Rad). After 30 minutes, 1 µL of STOP buffer (ThermoFisher Scientific) was added and the solution was incubated at 65 ˚C for 10 minutes to stop the reaction. During this time, 10 µL of master mix was prepared by adding 2 µL of RT 10X buffer, 0.8 µL of 25X dNTPs, 2 µL of 10X RT random primers, 1 µL of RNaseOUT, 1 µL of MultiScribe reverse transcriptase, and 3.2 µL of DEPC water (ThermoFisher Scientific). Following the 10-minute incubation period, 10 µL of the master mix was added and the solution was placed in the thermal cycler for reverse transcription using the optimized cDNA settings. The settings are as follows; Step 1 occurred at 25 ˚C for 10 minutes, Step 2 occurred at 37 ˚C for 120 minutes, Step 3 occurred at 85 ˚C for 5 minutes, Step 4 occurred at 4 ˚C for an infinite hold time. Once complete the concentration of cDNA was measured using the NanoPhotometer N50 Touch (Implen) and then was stored at -20 ˚C for future use.

2.6.3 qRT-PCR

First, the primer mix was prepared for each primer by adding 20 µL of the forward primer and 20 µL of the reverse primer to 60 µL of DEPC water (Table 3). Excess primer mix could then be stored at 4 ˚C for future use. Master mix was prepared by adding 0.3 µL of primer mix and 5 µL of SYBR Green Powerup MasterMix (Applied Biosystems) to 0.7 µL of DEPC water. To a 384-well PCR plate 4 µL of 10X dilute cDNA using sterile DEPC water was added followed by 6 µL of master mix. The plate was then briefly spun to mix the cDNA and master mix and remove any air bubbles. Amplification was performed in triplicates using the QuantStudio 5 Real Time PCR system (ThermoFisher Scientific). Settings were as follows: 50 ºC for 2 minutes, 95 ºC for 2 minutes, then 95 ºC for 1 second, 60 ºC for 30 seconds; this was done for 40 cycles, followed by 95 ºC for 1 second, 60 ºC for 20 seconds, and 95 ºC for 1 second. Gene expression was calculated relative to a housekeeping gene (GAPDH) using the $2^{-\Delta\Delta CT}$ method.

Table 3. Primer sequences used for each gene analyzed using RT-qPCR.

Gene	Sequence
ATF5	Forward CTGGCTCCCTATGAGGTCCTTG
	Reverse GAGCTGTGAAATCAACTCGCTCAG
ATF4	Forward CAGCAAGGAGGATGCCTTCT
	Reverse CCAACAGGGCATCCAAGTC
mtHsp70	Forward AAGGCGGGATTATGCATCAGA
	Reverse TTCCAACAAGTCGCTCACCA
Hsp10	Forward ATCGGGTTCTAAAGGAAAGGGTG
	Reverse TCTAGAACTACTTTGGTGCCTCC
Hsp60	Forward GATGCTGTGGCCGTTACAATG
	Reverse GTCAATTGACTTTGCAACAGTCACAC
CHOP	Forward GGAACCTGAGGAGAGAGTGTTC
	Reverse CTGCCATCTCTGCAGTTGGA
LONP1	Forward CATTGCCTTGAACCCTCTC
	Reverse ATGTCGCTCAGGTAGATGG
CLPP	Forward AAGCACACCAAACAGAGCCT
	Reverse AAGATGCCAAACTCCTGGG
XBP1	Forward ACGGGACCCCTAAAGTTCTG
	Reverse GCTACTCTGTTTTTCAGTTTCCTCC
HMOX1	Forward CAGCAACAAAGTGCAAGATCCTG
	Reverse TGCCTGCATGTGCTTTTCGT
TRIB3	Forward TTTTCACAGACCCCGCCG
	Reverse GACGGGGTACACCTTGCAG
ASNS	Forward AAGCTGTCCACATCCCTGG
	Reverse GTGATTGAAGAAAATCTGGGCGT
GAPDH	Forward TGGGCAGCCGTTAGGAAAG
	Reverse CGCCCAATACGACCAAATCAGA

2.7 TUNEL Apoptosis Assay

The DeadEnd Fluorometric TUNEL System (Promega) was used to determine the percentage of apoptotic cells in control and DCMA patient fibroblasts. Cells were grown in T25 tissue culture treated flasks until they reached 80% confluency. A cell pellet was collected and resuspended in 500 µL of media. A drop of this cell suspension was then placed onto a glass coverslip. Cells were then fixed in 4% methanol-free formaldehyde in PBS and then subsequently washed three times. Triton X-100 in 0.2% solution was then used to permeabilize the cells. The coverslips were then washed again in PBS. Equilibration buffer was prepared and added for 10 minutes at room temperature. Following equilibration, Terminal Deoxynucleotidyl Transferase, Recombinant enzyme (rTdT) incubation buffer was added and a plastic coverslip was placed on top to allow even distribution of the incubation buffer. 2X SSC was then added prior to a final three washes in PBS. Coverslips were then mounted onto slides in ProLong Gold Antifade Mountant with DAPI (Invitrogen) to stain nuclei. Slides were then imaged using the 20X objective of an Olympus VS110-S5 Slide Scanner (Olympus). The images were then analyzed using ImageJ (Schneider et al., 2012) to perform object-based colocalization analysis using JACoP to determine co-localization of DAPI and TUNEL staining.

2.8 LDH Cytotoxicity Assay

Cytotoxicity was measured for control and DCMA patient cells using the CyQUANT LDH Cytotoxicity Assay (Invitrogen). Briefly, 8000 cells were determined to be the optimal number to plate in a 96-well tissue culture plate. As such, 8000 cells in 100 µL were plated and left overnight in a cell culture incubator at 37 ˚C with 5% CO_2. The following day, the treated group

was treated with 100 µM TUDCA for 24 hours. To the set of triplicates labeled as the Maximum LDH controls, 10X lysis buffer was added and incubated for 45 minutes at 37 ˚C. Following incubation, 50 µL of each sample medium was transferred to a clear flat-bottom 96-well plate. To each well, 50 µL of reaction mixture was added and the plate was incubated for 30 minutes at room temperature. Stop solution was then added and absorbance was measured at 490 nm and 680 nm using the SpectraMaxi3x Multi-Mode Microplate Reader. The percentage cytotoxicity was then calculated using the equation in the online protocol (Invitrogen).

2.9 Statistics

All graphs and statistics were generated using GraphPad Prism 9.4.1. A p value < 0.05 was considered statistically significant and data was displayed as mean ± SEM. Significance within groups was determined using a one-way ANOVA with Tukey's test. Significance between treatment groups was determined using a paired t-test. Meanwhile, significance between independent groups was determined using an unpaired two-tailed t-test.

Chapter 3: Results

3.1 Proteomic analysis of control and DCMA patient fibroblasts

The whole proteome of control and DCMA patient cells was assessed to determine if there were significant changes to the overall number and type of proteins identified between samples. Initially, I attempted to generate pure mitochondrial isolates that would enable insight into the mitochondrial proteome, rather than the whole proteome. Due to issue with generating pure mitochondrial fractions, what was thought to be mitochondrial isolates were more likely total protein isolates and will be referred to as such. The generated mitochondrial isolates/total protein isolates were low in purity with a mitochondrial enrichment factor of only 6%, while whole cell lysates yielded a mitochondrial enrichment factor of 4% relative to total protein (Figure 6). In addition, abundance of VDAC1, a common mitochondrial marker, was found to be similar between total protein isolates and whole cell lysates, again suggesting low mitochondrial enrichment (Figure 7). To verify the consistency of mitochondrial isolations I performed western blotting for VDAC1 abundance using separate samples than those submitted for proteome analysis (Figure 8). Densitometric analysis did not reveal statistically significant changes in levels of VDAC1 protein within or between groups, aside from cells from patients with severe DCMA (Figure 8C). Furthermore, upon visual analysis of individual isolates, it is apparent that mitochondrial isolation had variable success in how much mitochondria were isolated (Figure 8B). From this, it is evident that what I hoped were mitochondrial isolates are more representative of whole cell lysate. Thus, for all future mention of proteomic data it is imperative to note that I am discussing total protein identified in what was intended to be mitochondrial isolates but will be referred to as total protein isolates to avoid confusion with the whole cell lysate that was submitted for comparison. As such, all proteins from the total protein isolates

were used in downstream analysis, and not only mitochondrial proteins. This meant that due to the limitations in generating a pure mitochondrial fraction, I analyzed the total proteome and not the mitochondrial proteome for all patient and control fibroblasts.

Proteomic analysis was performed on the total protein isolates for control and patient fibroblasts using 1D liquid chromatography with tandem mass spectrometry and analysis was performed using Scaffold software (v.4.3.4, Proteome Software Inc.) wherein subtle changes to the proteome of patient cells were identified. The thresholds used for protein identification were a protein threshold of 99%, a minimum number of 2 unique peptides, and a peptide threshold of 95%. This resulted in a false discovery rate (FDR) of 0.4%. The total number of proteins identified using significant threshold parameters was 2406. Out of the 2406 proteins identified, only 156 were identified as mitochondrial proteins which again confirms the relative lack of enrichment as discussed above. In downstream analysis, only proteins that had total spectrum counts greater than 0 in two of three replicates were kept, leading to a total of 2043 proteins to be considered in downstream analysis.

Around one quarter of all proteins identified were suggested to be involved in protein metabolism, while the next largest category was signal transduction (Figure 9). Of the mitochondrial proteins, 33 showed a ±2-fold change in fibroblasts from patients with mild DCMA, while there were 46 identified with a ±2-fold change in fibroblasts from patients with severe DCMA. However, only 3 proteins in each of the two phenotypes were found to be significantly different from control levels (Table 4 & Table 5). Due to the low number of mitochondrial proteins identified, pathway analysis using only these proteins could not be reliably performed.

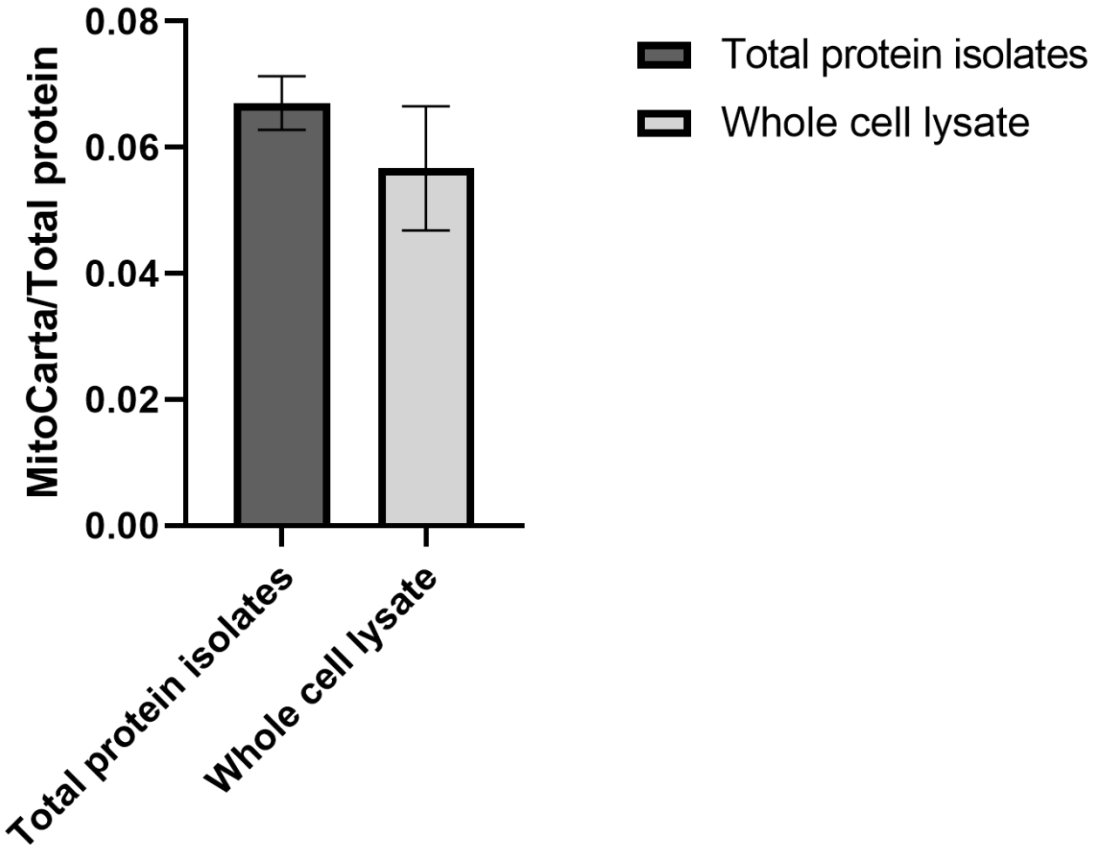

Figure 6. Total protein isolates and whole cell lysate have a similar mitochondrial enrichment factor. Mitochondrial enrichment factor was derived from the ratio of mitochondrial protein to total protein shared between control and patient fibroblasts (n =3/group for total protein isolates, n = 3/group for whole cell lysate). Mitochondrial proteins were identified by matching proteins to the MitoCarta3.0 database. Bars represent the mean ± SEM. No significant difference were determined using an unpaired two-tailed t-test.

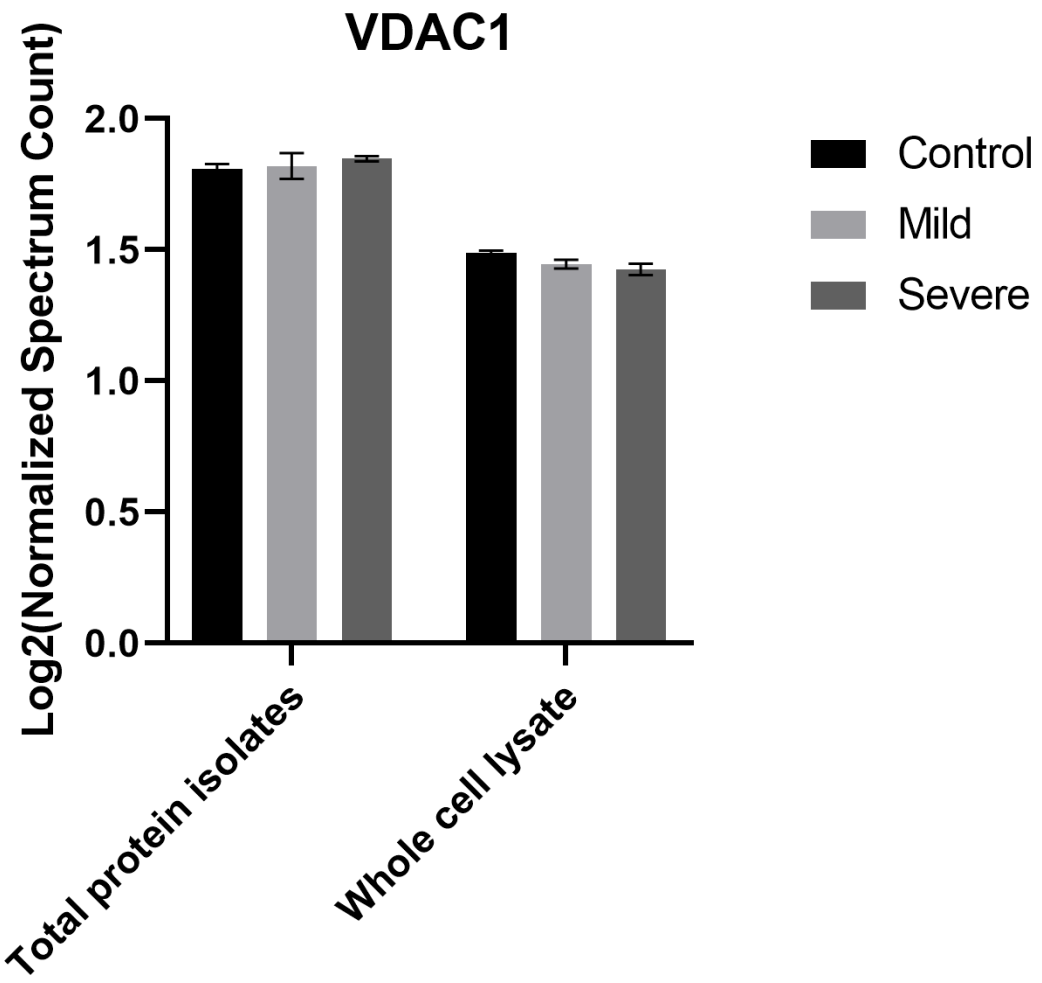

Figure 7. Similar levels of voltage-dependent anion-selective channel 1 (VDAC1) identified between total protein isolates and whole cell lysate using 1D LC-MS/MS. Log base 2 of normalized spectrum counts were calculated for each group (n = 3/group for total protein isolates; n = 3/group for whole cell lysate). Samples were collected from both total protein isolates and whole cell lysates. Proteins were identified and analyzed using Scaffold software. Bars represent the mean ± SEM. No significant differences were detected between groups by using a one-way ANOVA or between isolate groups by using an unpaired two-tailed t-test.

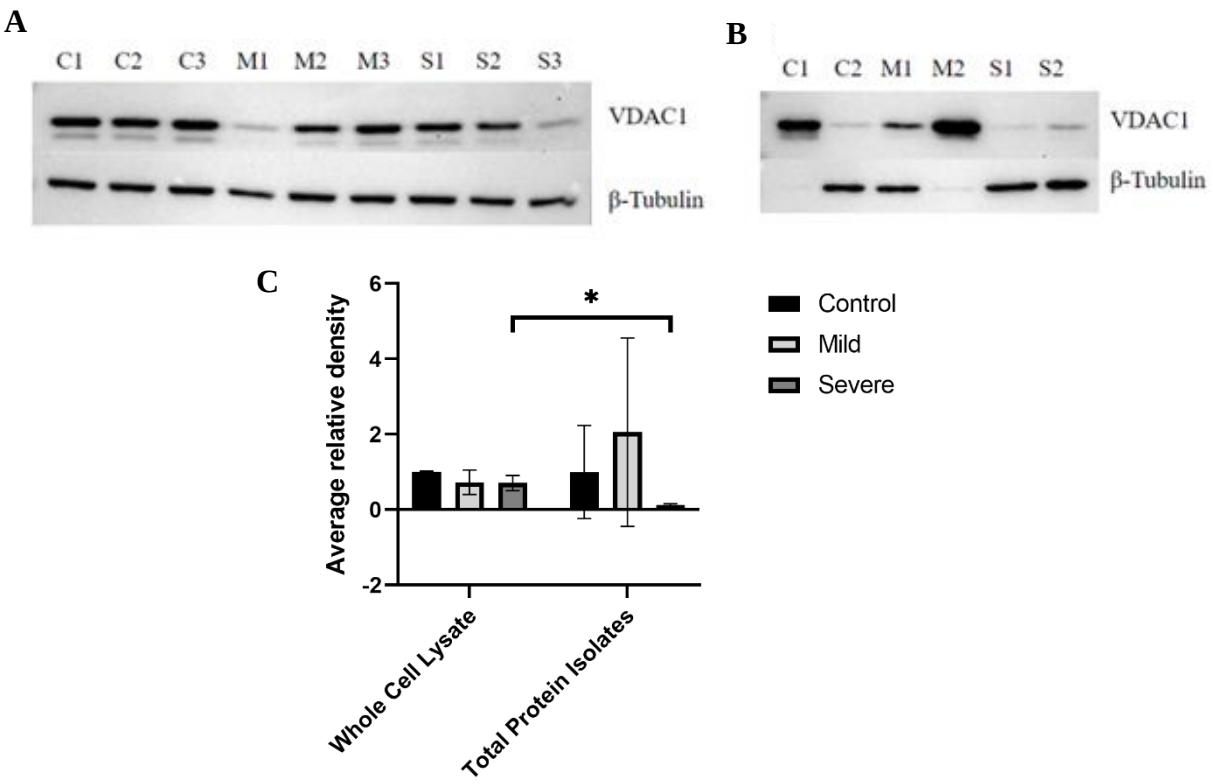

Figure 8. Western blot analysis and quantification of voltage-dependent anion-selective channel 1 (VDAC1) protein abundance in control and patient fibroblasts shows variability in generating a pure mitochondrial fraction. (A) Western blot for the determination of VDAC1 from whole cell lysate (n = 3 per group). (B) Western blot for the determination of VDAC1 from total protein isolates (n = 2 per group). (C) Quantification of VDAC1 protein levels normalized to β-tubulin. Bars represent the mean ± SEM. P values within groups were calculated using a one-way ANOVA and Tukey's test. Changes between isolate groups were detected using an unpaired two-tailed t-test. * $p < 0.05$.

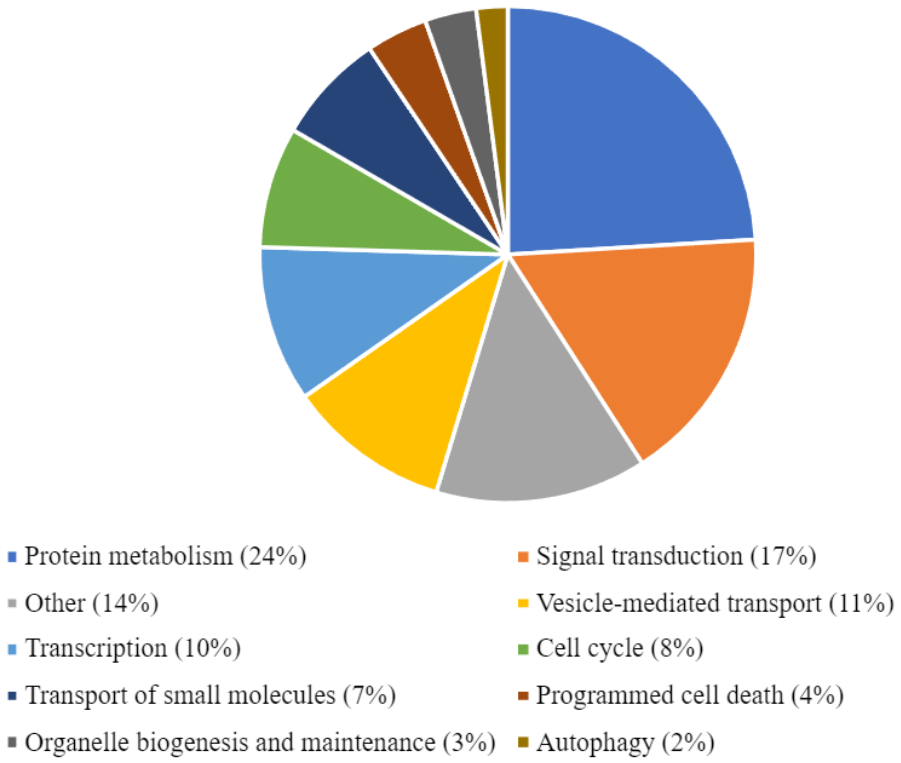

Figure 9. Classification of proteins identified with 1D liquid chromatography with tandem mass spectrometry. Total input of 2043 proteins being identified between control, mild, and severe patient fibroblasts (n = 3 for each group). Proteins grouped using Reactome.

In addition, DNAJC19 was not identified within the generated proteomic dataset. Nonetheless, I was able to identify a number of differentially expressed proteins in DCMA patient cells. When looking at differentially expressed proteins, fibroblasts from patients with mild cardiac dysfunction showed 324 proteins with a fold change ±2, 27 of these proteins were significantly different when compared to control cells (Table 4) (Figure 10). Meanwhile, 353 proteins were identified with a ±2-fold change in fibroblasts collected from patients with a severe cardiac phenotype, with 57 being statistically significant in comparison to control cells (Table 5) (Figure 11). Interestingly, there were 4 differentially expressed proteins that were identified to be shared between cells with mild and severe cardiac phenotypes (Table 4 & Table 5). These proteins are eukaryotic translation initiation factor 1A (IF1AX), syntaxin-2 (STX2), complement decay-accelerating factor (DAF), and nectin-2 (NECT2).

Of the differentially expressed proteins, the 27 identified in mild were insufficient to perform pathway analysis on. However, inputting the 57 proteins identified in cells from patients with severe cardiac dysfunction into Metascape (Zhou et al., 2019) identified 5 predicted pathway networks based on protein-protein interactions (Figure 12). Of these pathways the most confident predictions related to metanephros development, heart contraction, and glycogen metabolism (Figure 12).

When looking at all proteins with a ±2-fold change in cells from patients with mild and severe cardiac dysfunction and not accounting for statistical significance, metabolism of RNA was the most confident prediction (Figure 13 & Figure 14). In cells from patients with mild cardiac dysfunction, protein localization and proteolysis were also predicted pathways (Figure 13). As for cells from patients with severe DCMA, cellular homeostasis and membrane fission were notable predictions (Figure 14).

Table 4. List of differentially expressed proteins with a p value less than 0.05 present in DCMA fibroblasts from patients with mild cardiac dysfunction. Proteins were identified using 1D liquid chromatography with tandem mass spectrometry. Fold changes were calculated compared to controls. An unpaired two-tailed t-test was used to calculate p values.

Protein Name	Reference Number (UniProt)	Fold Change	p value
Ubiquitin carboxyl-terminal hydrolase isozyme L5 (UCHL5)	Q9Y5K5	35.4	4.00×10^{-3}
Mitochondrial dicarboxylate carrier, mitochondrial (DIC)	Q9UBX3	34.7	1.11×10^{-2}
Chromobox protein homolog 1 (CBX1)	P83916	32.4	2.75×10^{-3}
Diacylglycerol kinase alpha (DGKA)	P23743	25.3	1.88×10^{-2}
Vacuolar protein sorting 13 C homolog (VP13C)	Q709C8	25.3	2.52×10^{-3}
Elongin-B (ELOB)	Q15370	21.1	2.06×10^{-3}
Eukaryotic translation initiation factor 1A (IF1AX)	P47813	4.86	4.94×10^{-2}
28S ribosomal protein S34, mitochondrial (RT34)	P82930	4.78	2.57×10^{-2}
GPI transamidase component PIG-S (PIGS)	Q96S52	4.63	4.62×10^{-2}
NADH dehydrogenase [ubiquinone] flavoprotein 2, mitochondrial (NDUV2)	P19404	3.11	4.47×10^{-2}
Mesencephalic astrocyte-derived neurotrophic factor (MANF)	P55145	2.74	1.46×10^{-2}
Lysosome-associated membrane glycoprotein 2 (LAMP2)	P11279	3.68×10^{-1}	1.21×10^{-2}
Kin of IRRE-like protein 1 (KIRR1)	Q96J84	3.47×10^{-1}	4.80×10^{-2}
Nuclear migration protein nudC (NUDC)	Q9Y266	3.42×10^{-1}	4.00×10^{-2}
Syntaxin-2 (STX2)	P32856	3.42×10^{-1}	9.68×10^{-3}
Complement decay-accelerating factor (DAF)	P08174	3.26×10^{-1}	2.67×10^{-2}
Nectin-2 (NECT2)	Q92692	3.20×10^{-1}	4.98×10^{-2}
Protein S100-A8 (S10A8)	P05109	3.16×10^{-1}	4.63×10^{-2}
Gamma-enolase (ENOG)	P09104	2.47×10^{-1}	4.16×10^{-2}
Junctional adhesion molecule B (JAM2)	P57087	2.02×10^{-1}	3.19×10^{-2}
Rap1 GTPase-GDP dissociation stimulator 1 (GDS1)	P52306	1.89×10^{-1}	3.03×10^{-2}
Zinc-alpha-2-glycoprotein (ZA2G)	P25311	1.48×10^{-1}	4.84×10^{-2}
Aldo-keto reductase family 1 member C1 (AK1C1)	Q04828	1.34×10^{-1}	4.29×10^{-2}

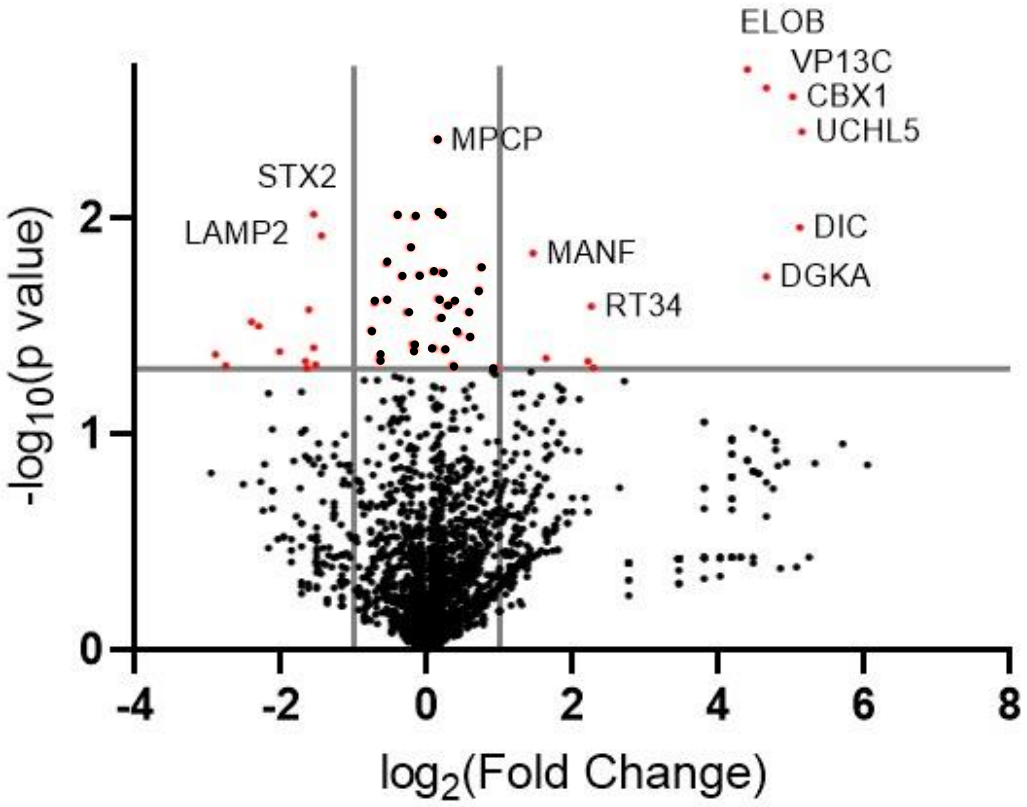

Figure 10. Differentially expressed proteins in fibroblasts from DCMA patients with a mild cardiac phenotype. Proteins identified using 1D liquid chromatography with tandem mass spectrometry for mild patient fibroblasts were compared to control fibroblasts to yield a fold change. Non-axial horizontal line indicates p value equal to 0.05, while non-axial vertical lines indicate ±2-fold change. Red dots indicate proteins that show a statistically significant change relative to control and are completely listed in Table 4.

Table 5. List of differentially expressed proteins with a p value less than 0.05 present in DCMA fibroblasts from patients with severe cardiac dysfunction. Proteins were identified using 1D liquid chromatography with tandem mass spectrometry. Fold changes were calculated compared to controls. An unpaired two-tailed t-test was used to calculate p values.

Protein Name	**Reference Number (UniProt)**	**Fold Change**	**p value**
Glycogen phosphorylase (PYGM)	P11217	87.9	7.97×10^{-3}
Collagen alpha-1(XI) chain (COBA1)	P12107	84.7	1.59×10^{-3}
Fibrillin-1 (FBN1)	P35555	57.7	7.30×10^{-5}
Dedicator of cytokinesis protein 5 (DOCK5)	Q9H7D0	44.8	1.10×10^{-4}
Coiled-coil domain-containing protein 80 (CCD80)	Q9H0W5	44.2	4.60×10^{-4}
Lysosomal alpha-glucosidase (LYAG)	P10253	43.7	1.25×10^{-3}
Titin (TITIN)	Q8WZ42	42.5	2.05×10^{-2}
Eukaryotic translation initiation factor 3 subunit K (EIF3K)	Q9DBZ5	32.4	3.47×10^{-3}
Protein ABHD14B (ABHEB)	Q96IU4	30.5	2.89×10^{-2}
D-aminoacyl-tRNA deacylase 1 (DTD1)	Q8TEA8	29.5	6.99×10^{-3}
Vacuolar-sorting protein SNF8 (SNF8)	Q96H20	28.2	1.51×10^{-2}
Coiled-coil domain-containing protein 124 (CC124)	Q96CT7	21.1	1.74×10^{-3}
Tyrosine-protein phosphatase non-receptor type 13 (PTN13)	Q12923	21.1	1.74×10^{-3}
LIM and calponin homology domains-containing protein 1 (LIMC1)	Q9UPQ0	8.64	2.99×10^{-3}
Ubiquitin carboxyl-terminal hydrolase isozyme L1 (UCHL1)	P09936	8.37	3.18×10^{-3}
Calcineurin B homologous protein 1 (CHP1)	Q99653	6.59	1.04×10^{-2}
Eukaryotic translation initiation factor 1A (IF1AX)	P47813	6.53	6.25×10^{-3}
Programmed cell death protein 6 (PDCD6)	O75340	5.76	4.75×10^{-2}

Coatomer subunit zeta-2 (COPZ2)	Q9P299	4.78	$2.83x10^{-2}$
Histone H1.0 (H10)	P07305	4.21	$1.72x10^{-2}$
Troponin I, fast skeletal muscle (TNNI2)	P48788	4.21	$1.72x10^{-2}$
Prostaglandin E synthase 3 (TEBP)	Q15185	4.13	$9.41x10^{-3}$
SEC23-interacting protein (S23IP)	Q9Y6Y8	3.40	$3.95x10^{-2}$
Proteasome subunit beta type-2 (PSB2)	P49721	2.85	$1.89x10^{-2}$
Collagen alpha-2(V) chain (CO5A2)	P05997	2.78	$4.07x10^{-2}$
Serine/threonine-protein kinase Nek9 (NEK9)	Q8TD19	2.74	$2.478x10^{-2}$
CTP synthase 1 (PYRG1)	P17812	2.59	$2.81x10^{-2}$
GTP-binding protein Rheb (RHEB)	Q15382	2.55	$3.53x10^{-2}$
Metalloproteinase inhibitor 3 (TIMP3)	P35625	2.52	$4.53x10^{-2}$
Retinol dehydrogenase 10 (RDH10)	Q8IZV5	2.36	$2.45x10^{-2}$
Protein NipSnap homolog 2 (NIPS2)	O75323	2.30	$3.78x10^{-2}$
Troponin T, fast skeletal muscle (TNNT3)	P45378	2.30	$3.97x10^{-2}$
Dynamin-1-like protein (DNM1L)	O00429	2.28	$6.20x10^{-3}$
Translationally-controlled tumor protein (TCTP)	P13693	2.25	$4.77x10^{-2}$
Laminin subunit beta-2 (LAMB2)	P55268	2.10	$3.90x10^{-3}$
26S proteasome non-ATPase regulatory subunit 14 (PSDE)	O00487	2.04	$2.83x10^{-2}$
Glycogen [starch] synthase, muscle (GYS1)	P13807	2.00	$4.80x10^{-2}$
Lon protease homolog, mitochondrial (LONM)	P36776	$5.00x10^{-1}$	$2.60x10^{-2}$
Acetyl-CoA acetyltransferase, mitochondrial (THIL)	P24753	$4.78x10^{-1}$	$8.53\ x10^{-3}$
Nectin-2 (NECT2)	Q92692	$4.46x10^{-1}$	$2.67x10^{-2}$
Charged multivesicular body protein 4b (CHM4B)	Q9H444	$4.14x10^{-1}$	$4.65x10^{-2}$
Charged multivesicular body protein 6 (CHMP6)	Q96FZ7	$3.42x10^{-1}$	$3.39x10^{-2}$
Syntaxin-2 (STX2)	P32856	$3.42x10^{-1}$	$3.20x10^{-2}$
Transient receptor potential cation channel subfamily M member 4 (TRPM4)	Q8TD43	$3.34x10^{-1}$	$4.86x10^{-2}$
Calcium-binding protein 39 (CAB39)	Q9Y376	$2.88x10^{-1}$	$3.71x10^{-3}$
Complement decay-accelerating factor (DAF)	P08174	$2.80x10^{-1}$	$2.14x10^{-2}$

RNA-binding protein EWS (EWS)	Q01844	$2.57x10^{-1}$	$4.62x10^{-2}$
Synaptopodin-2 (SYNP2)	Q9UMS6	$2.55x10^{-1}$	$4.92x10^{-2}$
Tissue factor (TF)	P13726	$2.29x10^{-1}$	$4.83x10^{-2}$
Cytochrome P450 20A1 (CP20A)	Q6UW02	$1.58x10^{-1}$	$3.31x10^{-2}$
Mannose-1-phosphate guanyltransferase alpha (GMPPA)	Q96IJ6	$1.58x10^{-1}$	$1.90x10^{-2}$
Epoxide hydrolase 1 (HYEP)	P07099	$1.15x10^{-1}$	$3.91x10^{-2}$
Aldehyde dehydrogenase X, mitochondrial (AL1B1)	P30837	$9.27x10^{-2}$	$5.11x10^{-3}$

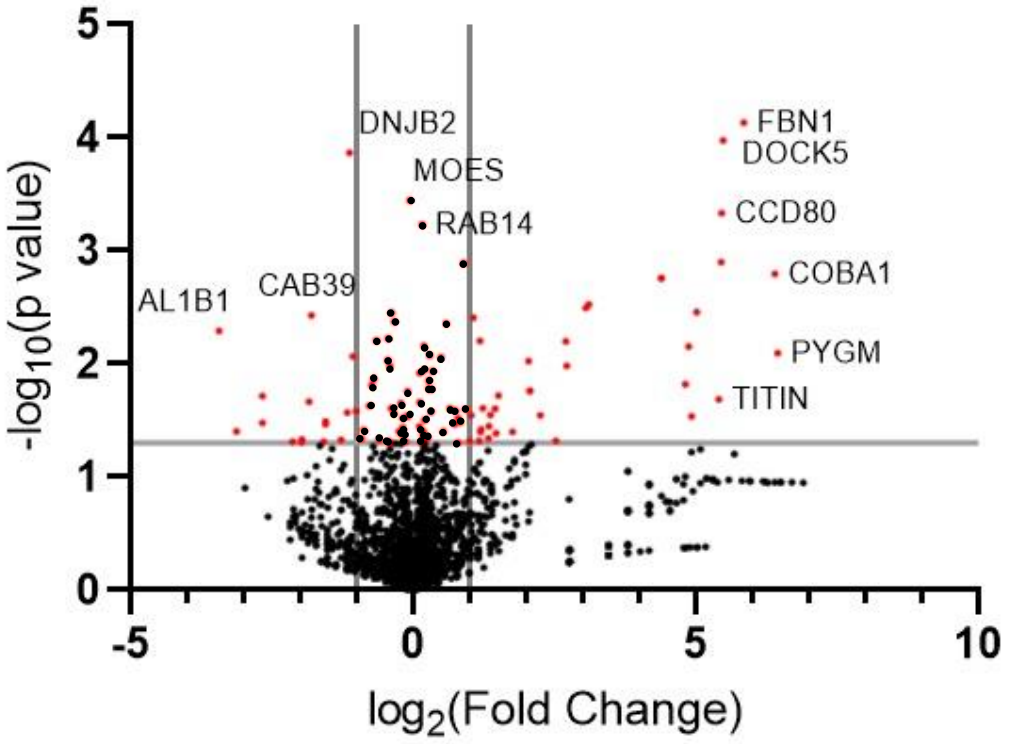

Figure 11. Differentially expressed proteins in fibroblasts from DCMA patients with a severe cardiac phenotype. Proteins identified using 1D liquid chromatography with tandem mass spectrometry for severe patient fibroblasts were compared to control fibroblasts to yield a fold change. Non-axial horizontal line indicates p value equal to 0.05, while non-axial vertical lines indicate ±2-fold change. Red dots indicate proteins that show a statistically significant change relative to control and are completely listed in Table 5.

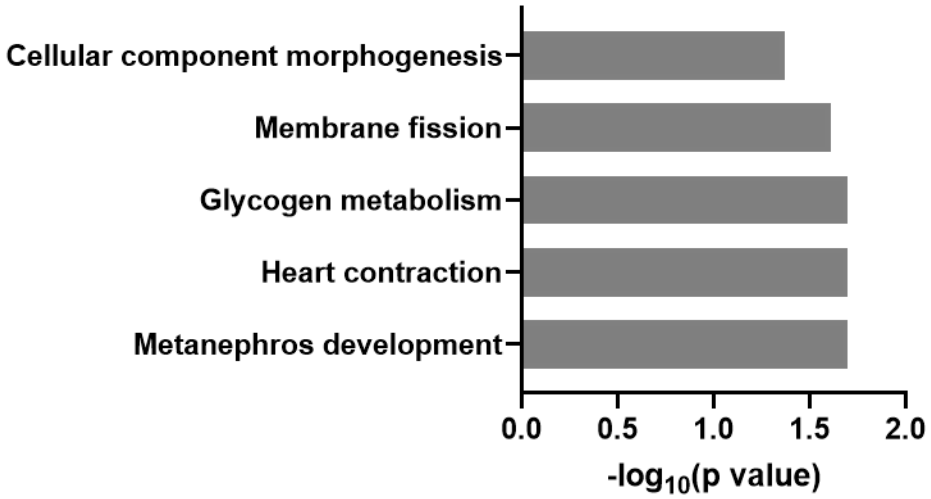

Figure 12. Pathways identified from differentially expressed proteins in fibroblasts from DCMA patients with a severe cardiac phenotype. Proteins were identified using 1D liquid chromatography with tandem mass spectrometry. Differentially expressed proteins with a ±2-fold change and p value less than 0.05.

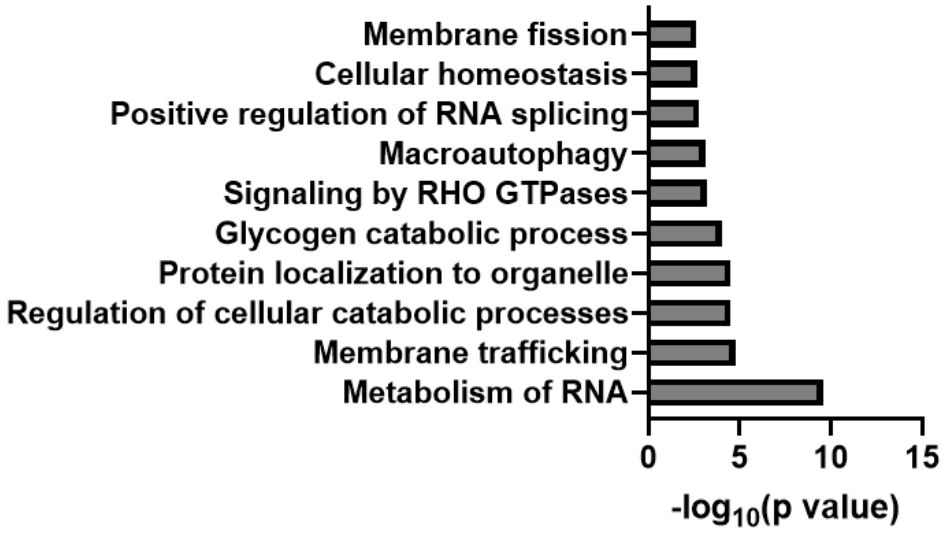

Figure 13. Top 10 pathways identified in fibroblasts from DCMA patients with a severe cardiac phenotype using Metascape. Proteins were identified using 1D liquid chromatography with tandem mass spectrometry. Proteins with a ±2-fold change were identified and input into Metascape for pathway analysis. Confidence interval is identified by the -log(p value) wherein a higher number indicates a more confident prediction.

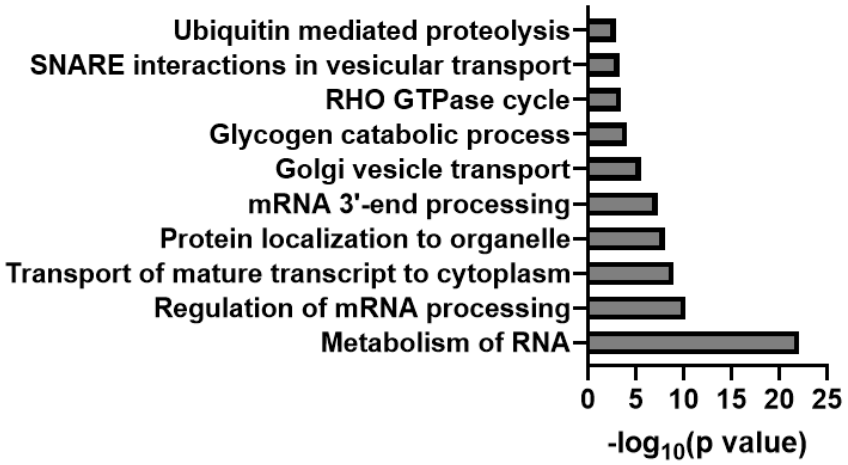

Figure 14. Top 10 pathways identified in fibroblasts collected from patients with a mild cardiac phenotype using Metascape. Proteins were identified using 1D liquid chromatography with tandem mass spectrometry. Proteins with a ±2-fold change were identified and input into Metascape for pathway analysis. Confidence interval is identified by the -log(p value) wherein a higher number indicates a more confident prediction.

3.2 Changes to proteins involved in mitochondrial membrane dynamics

Proteins related to mitochondrial membrane dynamics were investigated due to previous findings indicating increased mitochondrial fragmentation in DCMA patient cells, along with changes in the OPA1 isoform ratio (Machiraju et al., 2019). Thus, I considered that certain proteins involved in mediating mitochondrial membrane fission and fusion may be differentially expressed in proteomic data from DCMA patient fibroblasts. There were 5 notable proteins identified in the dataset that were related to mitochondrial membrane fission and fusion (Figure 15). Four of these proteins are involved in mitochondrial membrane fission: dynamin-2 (DYN2), dynamin-1-like protein (DNM1L), mitochondrial fission 1 protein (FIS1), and mitochondrial fission factor (MFF). The final protein is involved in mitochondrial membrane fusion: dynamin-like 120 kDa protein (OPA1). Of the 5 proteins identified, 2 showed significant changes, while all others remained close to control levels for protein abundance (Figure 15). DNM1L (Drp1) was increased by 1.9-fold in cells from patients with mild DCMA and 2.3-fold in cells from patients with severe DCMA. Meanwhile, OPA1 was decreased by 1.5-fold in fibroblasts from patients with mild cardiac dysfunction and 1.9-fold in fibroblasts from patients with severe cardiac dysfunction. All other 3 proteins identified did not present with notable increases or decreases to protein abundance. These results support previous observations that mitochondrial membrane dynamics are altered and suggests a trend towards increased fission following loss of DNAJC19.

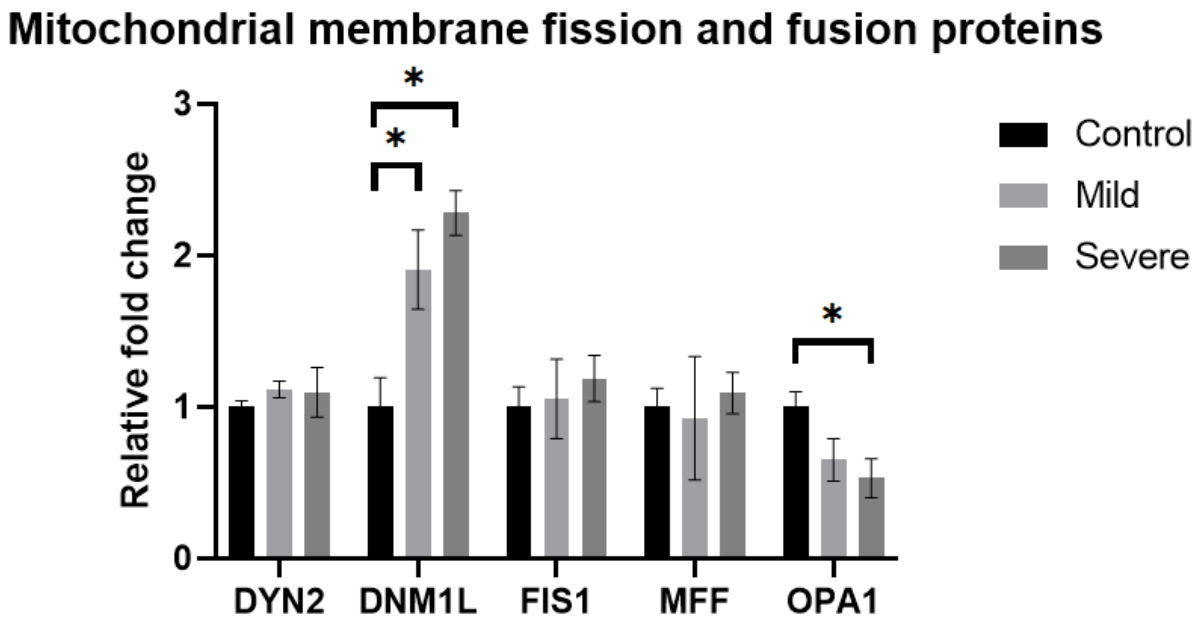

Figure 15. Changes to proteins involved in mitochondrial membrane fission and fusion suggest increased fission in DCMA patient cells. Fold change relative to control was calculated using the log base 2 values of total spectrum counts. Identified proteins include dynamin-2 (DYN2), dynamin-1-like protein (DNM1L), mitochondrial fission 1 protein (FIS1), mitochondrial fission factor (MFF), and dynamin-like 120 kDa protein (OPA1). Proteins were identified for control, mild and severe patient fibroblasts using 1D LC-MS/MS and analyzed using Scaffold software (n = 3 for each group). Changes between groups were detected using a one-way ANOVA and Tukey's test. Bars represent the mean ± SEM. * $p < 0.05$.

3.3 Proteome analysis shows predicted increases in eukaryotic initiation factor 2 (EIF2) signaling

Ingenuity pathway analysis (IPA) (QIAGEN Inc.) was used to aid in the analysis of the proteome of control and patient fibroblasts. IPA was used to organize the identified proteins into pathways to better understand how changes in the abundance of these proteins impacted the various pathways that they are part of (Figure 16). Results were normalized to control cells, and all proteins with a ±2-fold change were input to IPA using the fold changes, the log base 2 values, and the p values. Looking at the top 10 upregulated pathways, eukaryotic initiation factor 2 (EIF2) signaling was predicted to increase the greatest in cells from patients with severe and mild cardiac dysfunction, with Z-scores of +6.45 and +7.14, respectively (Figure 16). Notably, EIF2 signaling is involved in mRNA translation and consequently impacts protein synthesis. The top predicted downregulated pathway for patient cells was the RHOGDI signaling pathway with a Z-score of -3.71 in fibroblasts from patients with severe cardiac dysfunction and -3.5 in fibroblasts from patients with mild cardiac dysfunction (Figure 16). RHOGDI signaling encompasses the signaling cascades of various Rho GTPases that are involved in regulating numerous cellular processes such as cell morphology, division, and migration.

Pathways were verified by inputting the same proteins used in IPA analysis into Metascape (Zhou et al., 2019). The top predicted pathway for patient fibroblasts with mild and severe phenotypes was the metabolism of RNA (Figure 13, Figure 14). Regulation of mRNA processing and transcription were also identified in fibroblasts from patients with a mild cardiac phenotype (Figure 14). As for fibroblasts from patients with severe cardiac dysfunction, pathways involved in metabolism such as regulation of catabolic processes and glycogen

catabolism were predicted pathways. Notably, cellular homeostasis and membrane fission were also predicted pathways in fibroblasts from patients with severe DCMA (Figure 13).

Further analysis of the EIF2 signaling pathway using IPA indicated a predicted increase in endoplasmic reticulum stress, cardioprotection, amino acid synthesis and transport, and vascularization (Figure 17a). As for downregulated pathways, uptake of D-glucose was predicted to be inhibited based on the changes in molecules relevant to the EIF2 signaling pathway (Figure 17a). Specifically, cells from patients with a mild cardiac phenotype had 82/224 proteins associated with the EIF2 pathway, while cells from patients with a severe phenotype had 81/224 proteins identified. When looking at the proteins that were predicted to be altered within the pathway, there was predicted increases in proteins involved in the ISR and the UPRmt. Particularly, ATF4, ATF5, TRIB3, HSPA9 (Hsp70), and DDIT3 (CHOP) were predicted to be increased (Figure 17b). Together, these results suggest that the ISR and UPRmt stress pathways may be activated within patient cells.

Other pathways of interest were the phagosome formation pathway, which was the second most upregulated pathway predicted by IPA (Figure 16). Of the proteins identified within our dataset, 39/159 matched this pathway in cells from patients with mild and severe cardiac dysfunction. Of these proteins, four subunits of the adaptor protein complexes were identified, along with four of the myosin heavy chain proteins. From changes in these identified proteins, IPA predicted there to be increased actin remodeling and increased phagocytosis which may impact immunity and clearance of damaged cells.

Following phagosome formation, oxidative phosphorylation was the third top predicted upregulated pathway (Figure 16). This pathway had 34/111 proteins identified within our dataset in cells from patients with mild cardiac dysfunction and 31/111 proteins identified in cells from

patient with severe cardiac dysfunction. Within this pathway, multiple subunits of complex I were shown to be increased (specifically 8 subunits of the NADH:ubiquinone oxidoreductase), with the most significant increase being identified in the NADH dehydrogenase subunit 4, along with 5 of the subunits involved in the ATP synthase complex. These changes were then predicted to lead to increased ATP production within patient cells which may be important to ensure adequate energy production during stress or may even impact cellular metabolism in patient cells.

As for downregulated pathways, the top predicted downregulated pathway was the RHOGDI signaling pathway (Figure 16). Within cells collected from patients with severe DCMA, 27/183 proteins were identified to fit within this pathway. As for cells collected from patients with mild cardiac dysfunction, there were 18/183 identified proteins. Of these proteins there were significant changes in myosin heavy chain 4 and 7, and myosin light chain 11. These changes were then predicted by IPA to lead to increased cytoskeletal reorganization and actin linkage which may suggest an attempt to prevent further cellular damage.

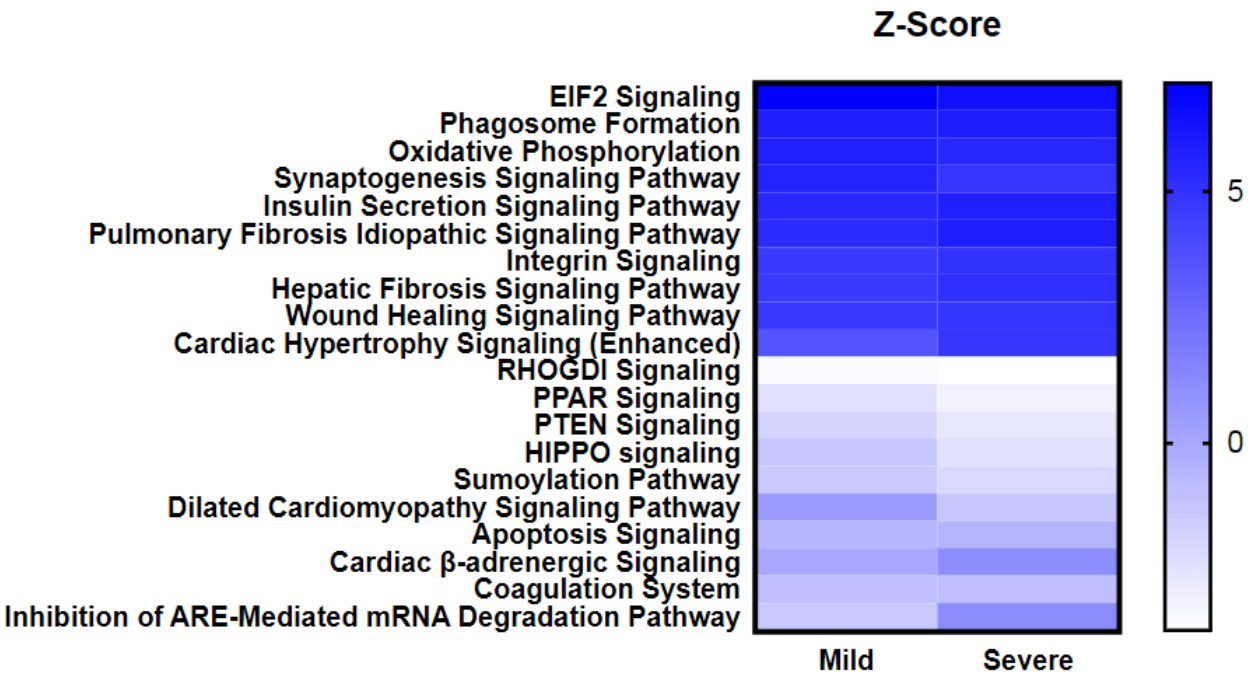

Figure 16. Top 20 differentially expressed canonical pathways in patient fibroblasts. Top canonical pathways predicted for proteomic data showing differential expression from total protein isolates using Ingenuity Pathway Analysis (IPA) software (n = 3 control, n = 3 mild, n = 3 severe). Z-score represents differential expression of proteins in mild and severe patient fibroblasts relative to control fibroblasts identified using 1D liquid chromatography with tandem mass spectrometry. A z-score above 2 is considered upregulated, while a z-score below -2 is considered downregulated.

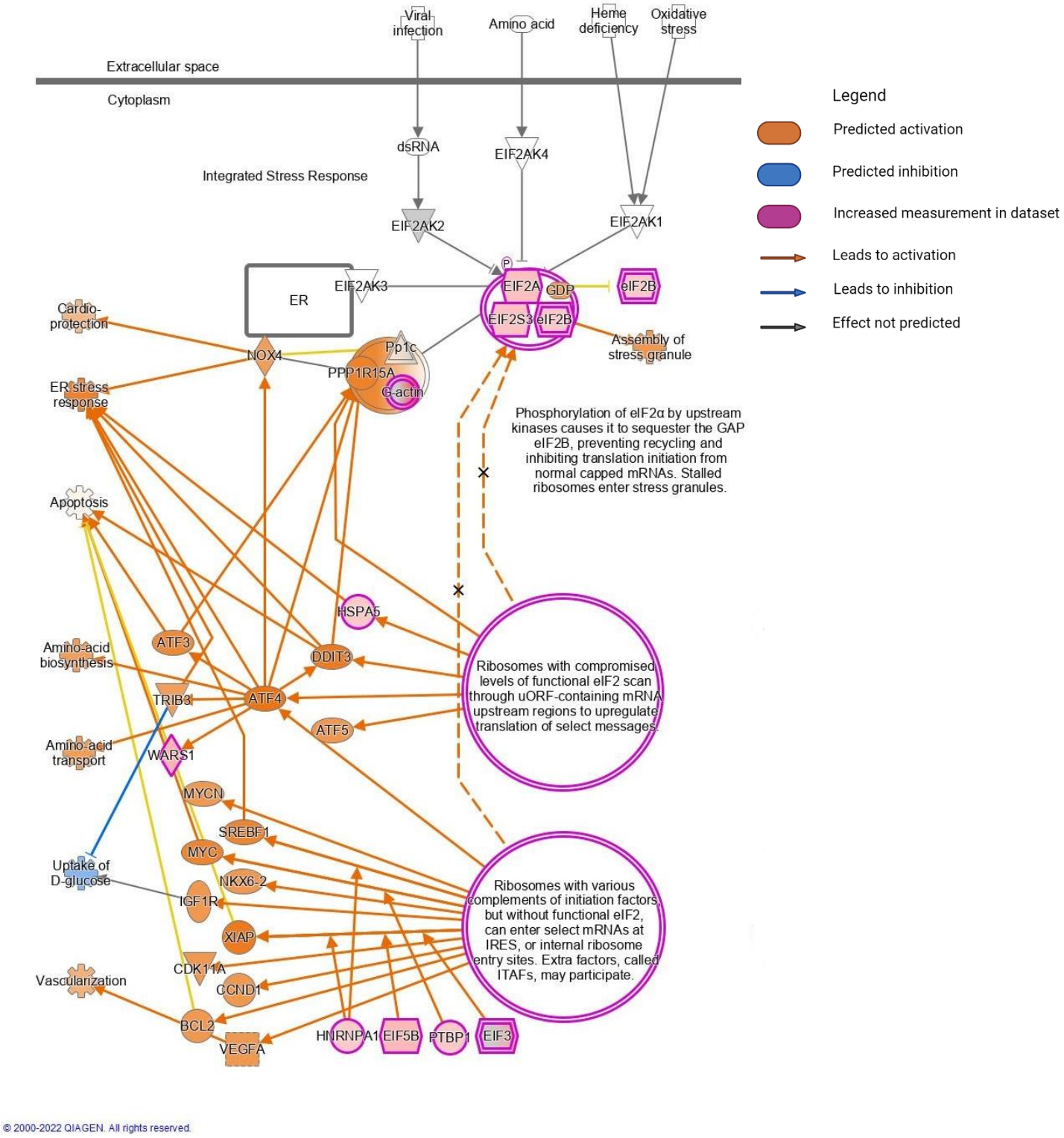

Figure 17a. Canonical pathway predictions for eukaryotic translation initiation factor 2 (EIF2) signaling pathway. Predicted activation and inhibition of molecules involved in the EIF2 signaling pathway and how these changes could alter other biological processes.

Predictions based on input of proteomic data collected from total protein isolates from control and patient fibroblasts using 1D liquid chromatography with tandem mass spectrometry showing differential expression into Ingenuity Pathway Analysis (IPA) software (n = 3 per group).

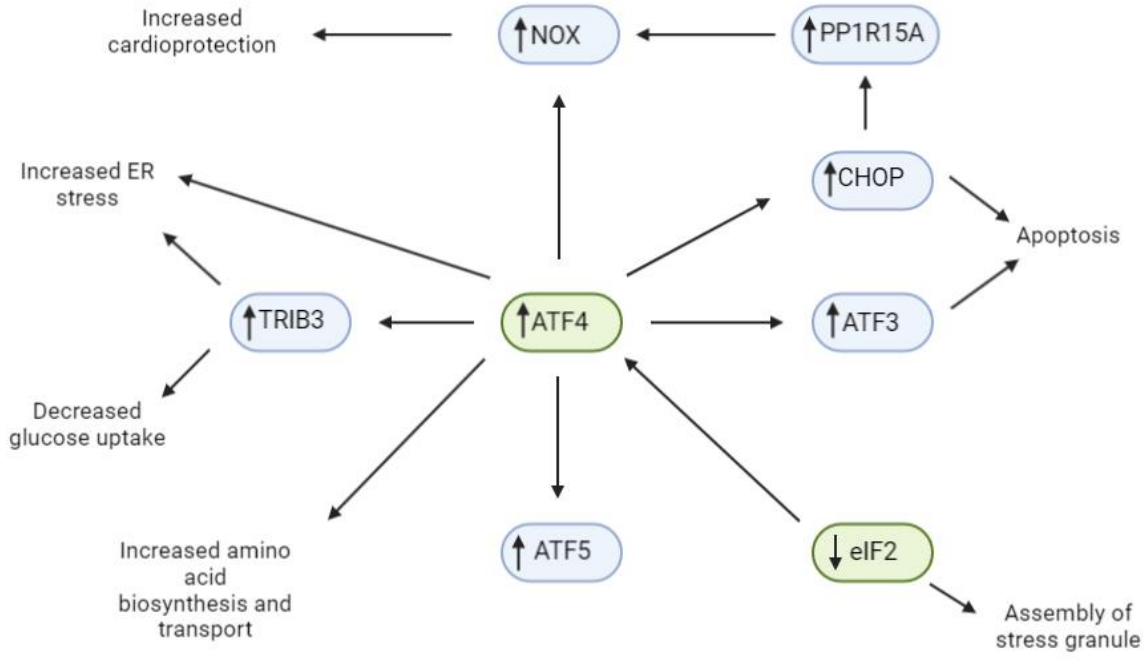

Figure 17b. Simplified predictions for the eukaryotic initiation factor 2 (EIF2) signaling pathway. Key proteins identified within the EIF2 signaling pathway generated by Ingenuity Pathway Analysis (IPA) software. These select proteins are also involved in various stress responses such as the unfolded protein response of mitochondria (UPRmt) and/or the integrated stress response (ISR), making them of notable interest. Proteins identified were tribbles pseudokinase 3 (TRIB3), activating transcription factor 4 (ATF4), activating transcription factor 5 (ATF5), activating transcription factor 3 (ATF3), eukaryotic translation initiation factor 2 (eIF2), C/EBP homologous protein (CHOP), protein phosphatase 1 regulatory subunit 15A (PP1R15A), and NADH oxidase (NOX). Green represents key regulators of these stress responses, while blue represents their targets. Created using BioRender.

3.4 Differential expression of proteins involved in dilated cardiomyopathy signaling

A particular pathway that was of interest identified by IPA and predicted to be downregulated was the dilated cardiomyopathy (DCM) signaling pathway (Figure 16). IPA predicted that the DCM signaling pathway was downregulated in fibroblasts from patients with severe and mild DCMA, correlating to a Z-score of -2.6 and -1.6, respectively. There were 21/148 identified proteins within cells from patients with severe DCMA, however, there were only 12 proteins identified in cells from patients with mild DCMA. Five proteins involved in the DCM signaling pathway were shared between the samples (Figure 18). Of these proteins the largest changes were in troponin I2 (TNNI2), troponin T3 (TNNT3), and myosin heavy chain 7 (MYH7). TNNT3 increased significantly by 2.2-fold, while TNNI2 increased significantly by 4.2-fold in cells from patients with severe cardiac dysfunction. However, MYH7, while not statistically significant, did increase by nearly 2-fold in cells from patients with mild and severe DCMA. From these changes IPA predicted there to be a decrease in heart muscle contractility and contractility of cardiac cells, along with an increase in cardiomyocyte apoptosis and mitochondrial dysfunction. Thus, further investigation into proteins predicted to cause these changes would be useful to better understand how these cellular changes are linked to cardiac dysfunction in patients with DCMA.

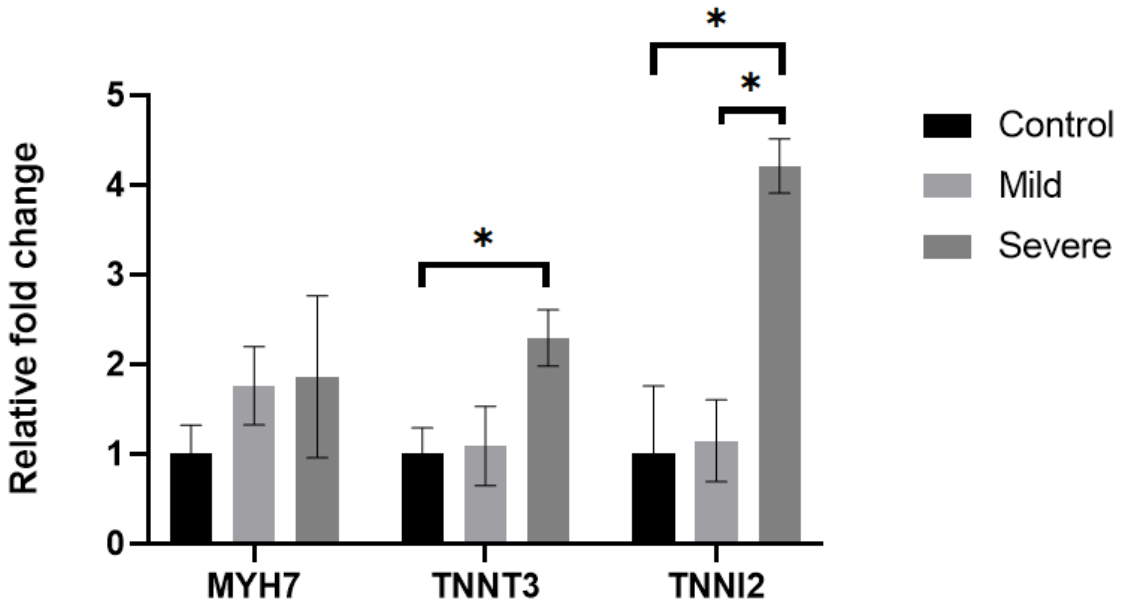

Figure 18. Proteins involved in the dilated cardiomyopathy signaling pathway from cells collected from patients with severe cardiac dysfunction. Fold change relative to control was calculated using the log base 2 values of total spectrum counts. Identified proteins include myosin heavy chain 7 (MYH7), troponin T3 (TNNT3), and troponin I2 (TNNI2). Proteins were identified for control and patient fibroblasts using 1D liquid chromatography with tandem mass spectrometry and analyzed using Scaffold software (n = 3 for each group). Bars represent the mean ± SEM. Changes between groups were detected using a one-way ANOVA and Tukey's test. * $p < 0.05$.

3.5 Changes in abundance of proteins involved in the ISR and the UPRmt

Following initial data collection and IPA analysis, I sought to investigate proteins that could be involved in either the ISR or UPRmt from my proteomic dataset. This was due to IPA having predicted that EIF2 signaling was upregulated. Considering that DNAJC19 may be involved in mitochondrial proteostasis, loss of DNAJC19 could subsequently lead to cellular stress and upregulation of stress response pathways. EIF2 signaling is crucially important for certain cellular stress responses, such as the ISR and UPRmt (Melber & Haynes, 2018). Thus, I considered that deficiency of DNAJC19 may result in activation of the ISR and/or the UPRmt.

A total of 10 proteins were identified to be part of either the ISR, UPRmt, or the UPR of the ER in the proteomic dataset from control and patient fibroblasts. Of these proteins, pro-apoptotic protein, bcl-2-associated x protein (BAX) was the only one that resulted in statisticallt significant changes. BAX protein levels increased nearly 1.5-fold in cells from patients with a mild cardiac phenotype and 2-fold in cells from patients with severe cardiac dysfunction, with the latter being statistically significant (Figure 19). Lon protease homolog 1 (LONP1) decreased 1.5-fold in cells from patients with severe DCMA when compared to the control (Figure 20). Eukaryotic translation initiation factor 2A (EIF2A) and asparagine synthetase (ASNS) increased 1.5-fold, while tryptophan—tRNA ligase (WARS1) increased 1.7-fold (Figure 21) in cells from patients with severe cardiac dysfunction. As for heme oxygenase 1 (HMOX1), protein levels in cells from patients with a severe phenotype were not much different from control levels, but cells from patients with a mild phenotype presented with a 1.5-fold increase in protein levels (Figure 21). While most of these results are not statistically significant, they represent only a small subset of molecules involved in these stress responses and thus are insufficient to claim activation or inhibition of these cellular stress responses without further testing.

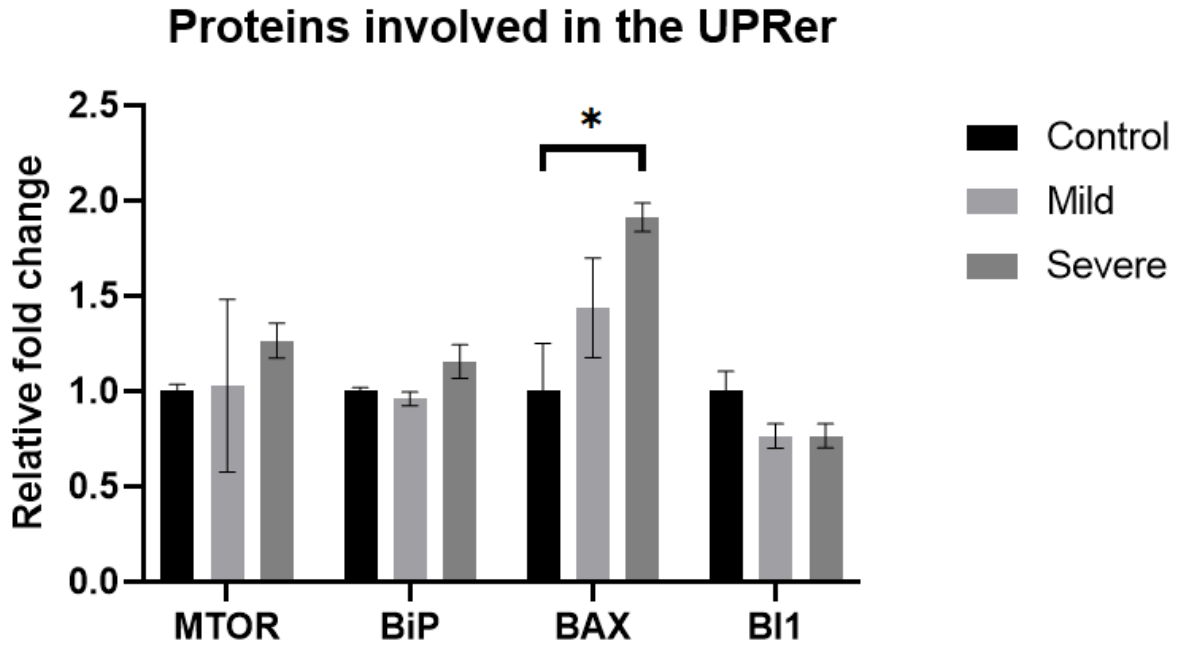

Figure 19. Proteins involved in the endoplasmic reticulum unfolded protein response. Fold change relative to control was calculated using the log base 2 values of total spectrum counts for proteins identified from control and patient fibroblasts using 1D liquid chromatography with tandem mass spectrometry (n = 3 for each group). Proteins identified for the endoplasmic reticulum unfolded protein response (UPRer) were mechanistic target of rapamycin (MTOR), binding immunoglobulin protein (BiP), Bcl-2-associated X protein (BAX), and bax inhibitor 1 (BI1). Proteins were analyzed using Scaffold software. Bars represent the mean ± SEM. Changes between groups were detected using a one-way ANOVA and Tukey's test. * $p < 0.05$.

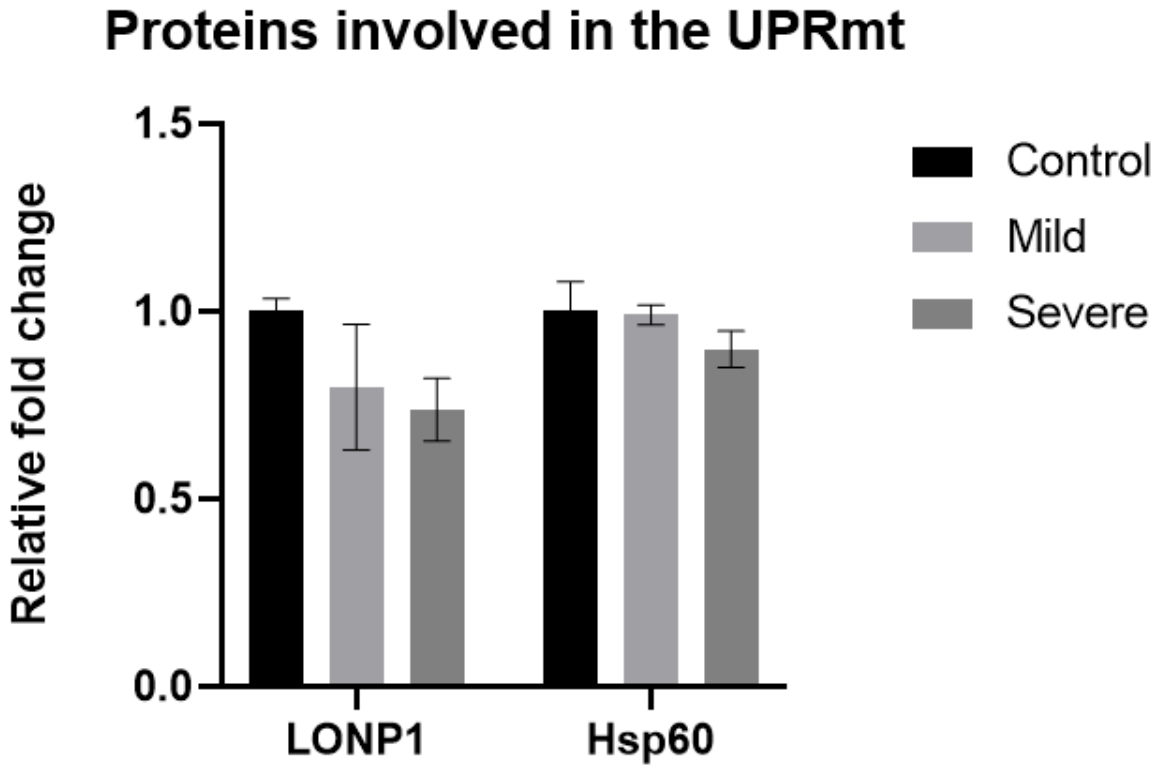

Figure 20. Proteins involved in the unfolded protein response of mitochondria. Fold change relative to control was calculated using the log base 2 values of total spectrum counts for proteins identified from control and patient fibroblasts using 1D liquid chromatography with tandem mass spectrometry (n = 3 for each group). Proteins identified for the unfolded protein response of mitochondria (UPRmt) include lon peptidase 1 (LONP1) and heat shock 60 kDa protein (Hsp60). Proteins were analyzed using Scaffold software. Bars represent the mean ± SEM. No significant changes were detected between groups using a one-way ANOVA.

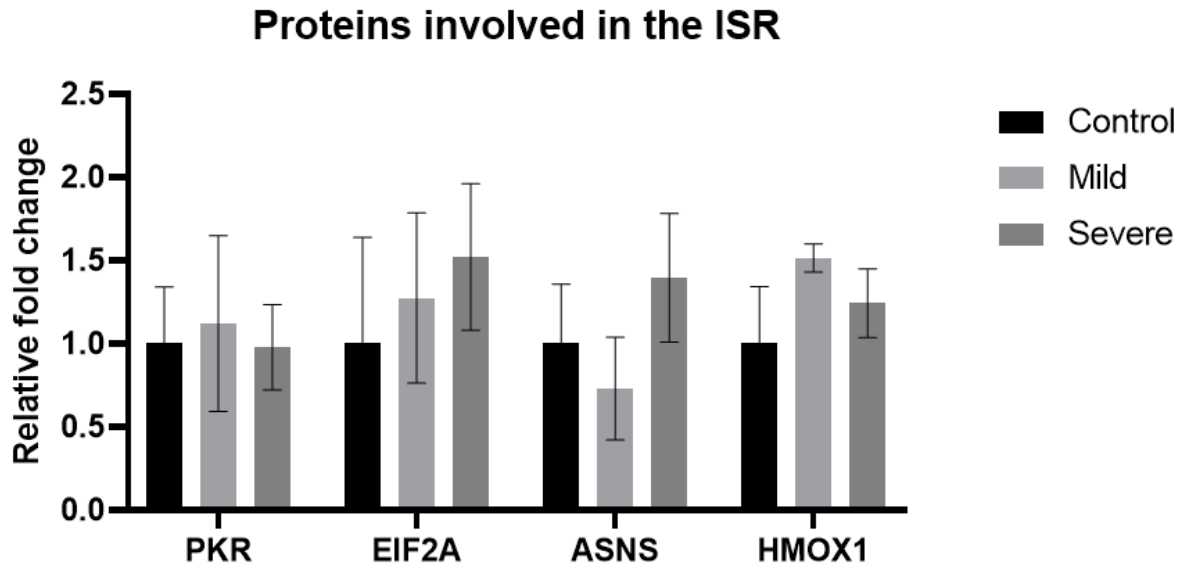

Figure 21. Identification of proteins involved in the integrated stress response. Fold change relative to control was calculated using the log base 2 values of total spectrum counts for proteins identified from control and patient fibroblasts using 1D liquid chromatography with tandem mass spectrometry (n = 3 for each group). Identified proteins include protein kinase R (PKR), eukaryotic translation initiation factor 2 subunit alpha (EIF2A), asparagine synthetase (ASNS), and heme oxygenase 1 (HMOX1) involved in the integrated stress response (ISR). Proteins were analyzed using Scaffold software. Bars represent the mean ± SEM. No significant differences were detected between groups by using a one-way ANOVA.

3.6 Differential expression of DNAJ proteins

DNAJC19 is a J protein and as such, shares overlapping functions with other J proteins. For example, DNAJC15 has been shown to perform a similar role to DNAJC19 through interactions with mtHsp70, though DNAJC15 is considered to serve a dispensable role (Sinha et al., 2016). As such, it is possible that loss of DNAJC19 would impact other DnaJ proteins. Upon analysis of DnaJ proteins identified through 1D LC-MS/MS, the majority of DnaJ proteins did not show statistically significant changes. Of the DnaJA proteins, there were no significant changes (Figure 22). However, DnaJ heat shock protein family (Hsp40) member B2 (DNJB2) was found to be decreased by 1.5-fold in cells from patients with mild cardiac dysfunction and 2-fold in cells from patients with severe cardiac dysfunction, with both changes being statistically significant (Figure 23). Meanwhile, DnaJ heat shock protein family (Hsp40) member C3 (DNJC3) increased nearly 1.7-fold in patient cells with mild and severe DCMA, however, this was not statistically significant (Figure 24). These results suggest that loss of DNAJC19 is insufficient to cause alterations in the abundance of other DnaJ proteins. However, this conclusion may be limited by the sensitivity of the assay used.

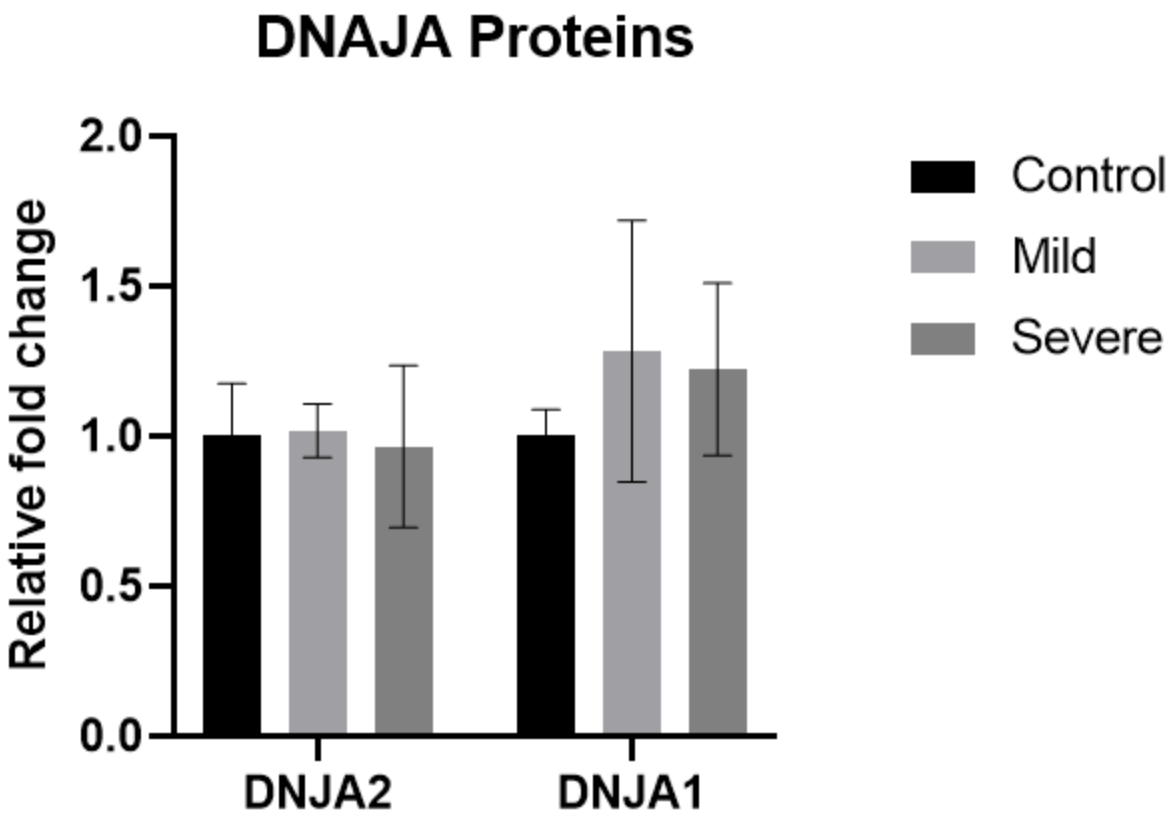

Figure 22. No significant changes in DNAJA proteins. Fold change relative to control was calculated for fibroblasts from patients with mild and severe DCMA using the log base 2 values of total spectrum counts (n = 3 for each group). Identifiable DnaJA proteins were DnaJ heat shock protein family (Hsp40) member A1 (DNJA1) and DnaJ heat shock protein family (Hsp40) member A2 (DNJA2). Proteins were analyzed using Scaffold software. Bars represent the mean ± SEM. No significant differences were detected in groups by using a one-way ANOVA.

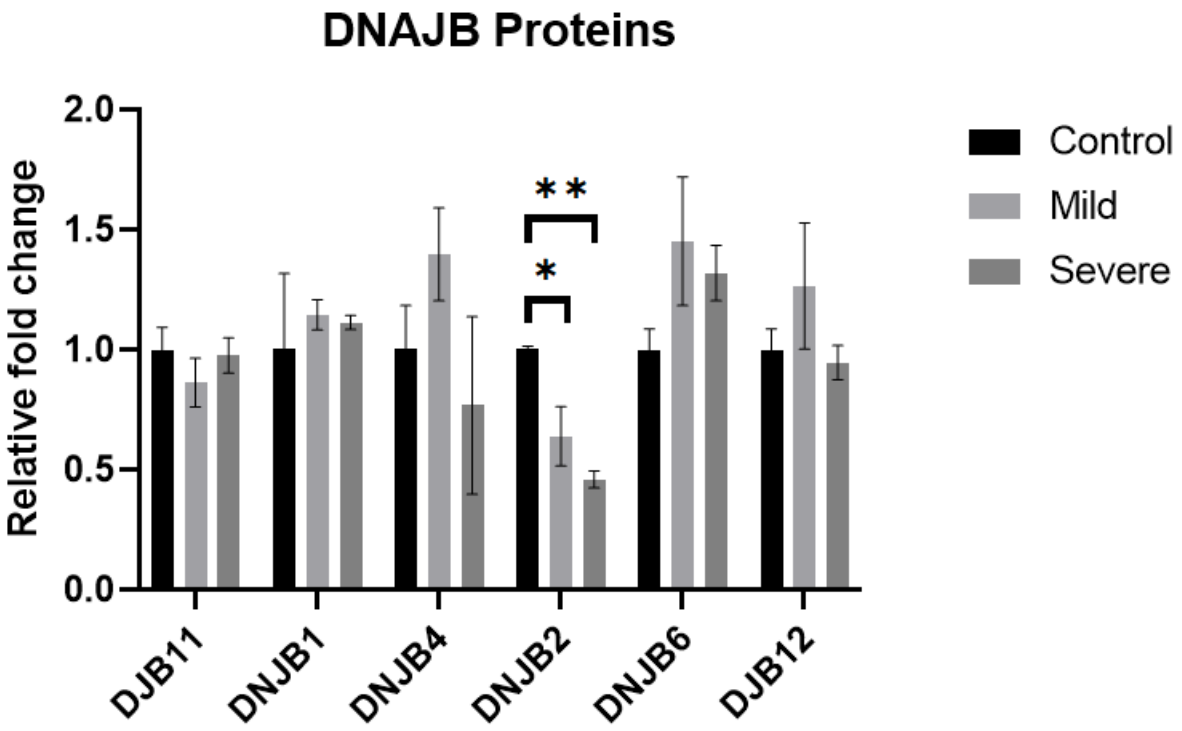

Figure 23. Changes in DNAJB proteins. Fold change relative to control was calculated using the log base 2 values of total spectrum counts for patient fibroblasts (n = 3 for each group). Identifiable DnaJB proteins were DnaJ heat shock protein family (Hsp40) member B11 (DNJB11), member B1 (DNJB1), member B4 (DNJB4), member B2 (DNJB2), member B6 (DNJB6), and member B12 (DJB12). Proteins were analyzed using Scaffold software. Bars represent the mean ± SEM. Changes between groups were detected using a one-way ANOVA and Tukey's test. * $p < 0.05$; ** $p < 0.01$.

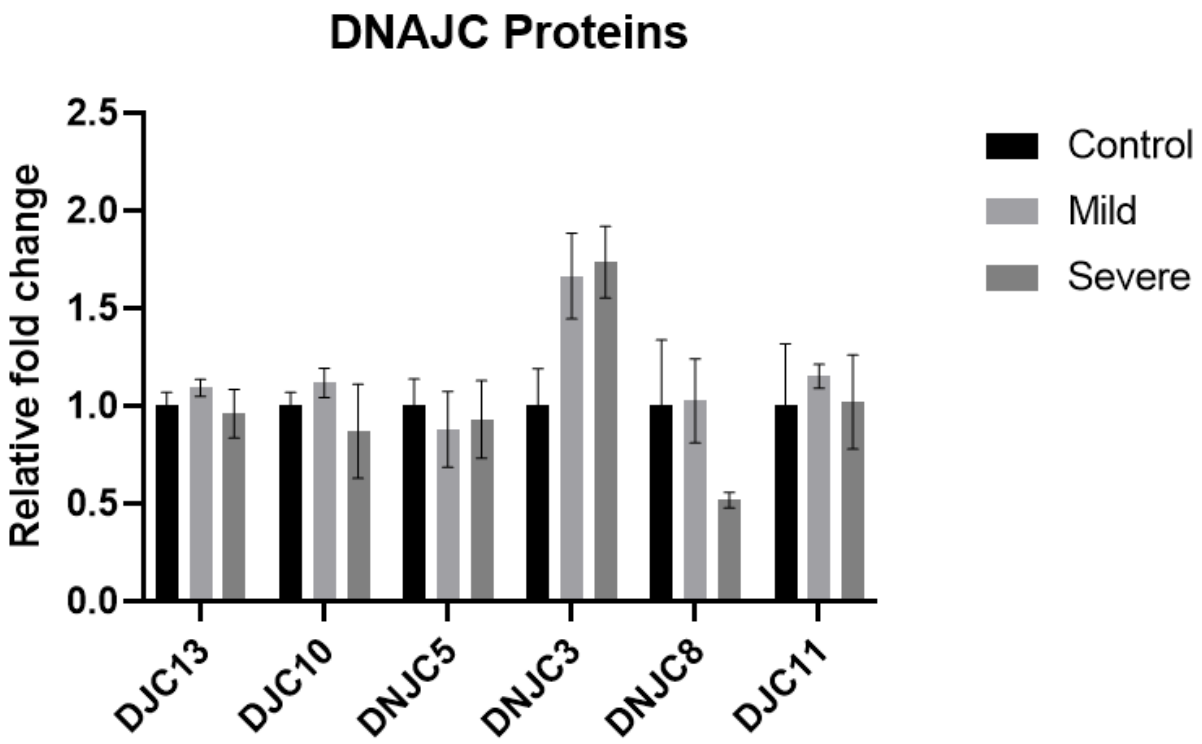

Figure 24. No significant changes in DNAJC proteins identified. Fold change relative to control was calculated using the log base 2 values of total spectrum counts for patient fibroblasts (n = 3 for each group). Identifiable DnaJC proteins were DnaJ heat shock protein family (Hsp40) member C13 (DJC13), member C10 (DJC10), member C5 (DNJC5), member C3 (DNJC3), member C8 (DNJC8), and member C11 (DNJC11). Proteins were analyzed using Scaffold software. Bars represent the mean ± SEM. No significant differences were detected in groups by using a one-way ANOVA.

3.7 Differential expression of heat shock proteins

Heat shock proteins are a class of proteins that are involved in protein maturation and are activated in response to various stressors (Miller & Fort, 2018). DNAJC19 has been shown to stimulate ATPase activity of mtHsp70 (Sinha et al., 2016). Thus, I considered that loss of DNAJC19 may impact specifically mtHsp70 but could also potentially affect other heat shock proteins that play an important role in regulating cellular stress. Analysis of the heat shock proteins in my proteomics dataset did not identify any heat shock proteins as showing statistically significant differences between control and DCMA patient fibroblasts.

However, despite not being considered statistically significant, heat shock-related 70 kDa protein 2 (HSP72) showed a 1.7-fold decrease in patient cells with mild DCMA and a 4-fold decrease in cells from patients with severe DCMA, which likely failed to achieve statistical significance due to substantial variation between samples (Figure 25). In addition, heat shock protein 75 kDa (TRAP1) exhibited a 1.3-fold increase in both groups of patient cells, though this again was not statistically significant (Figure 25). Lastly, heat shock protein beta-6 (HSPB6) was found to be 1.3-fold increased in mildly affected patient cells and 1.48-fold increased in severely affected patient cells (Figure 25). As for heat shock proteins that were identified to play a lesser role in stress responses, 28 kDa heat- and acid-stable phosphoprotein (HAP28) was found to be increased by 1.4- and 1.6-fold in cells from patients with a mild and severe cardiac phenotype, respectively (Figure 26). Meanwhile, heat shock protein 105 kDa (HS105) was 1.4-fold increased in cells from patients with severe DCMA but did not change in cells from patients with mild DCMA (Figure 26). All other heat shock proteins did not show any noticeable changes in protein levels when compared to controls. These results suggest that the abundance of heat shock proteins identified within our dataset are not altered due to deficiency of DNAJC19.

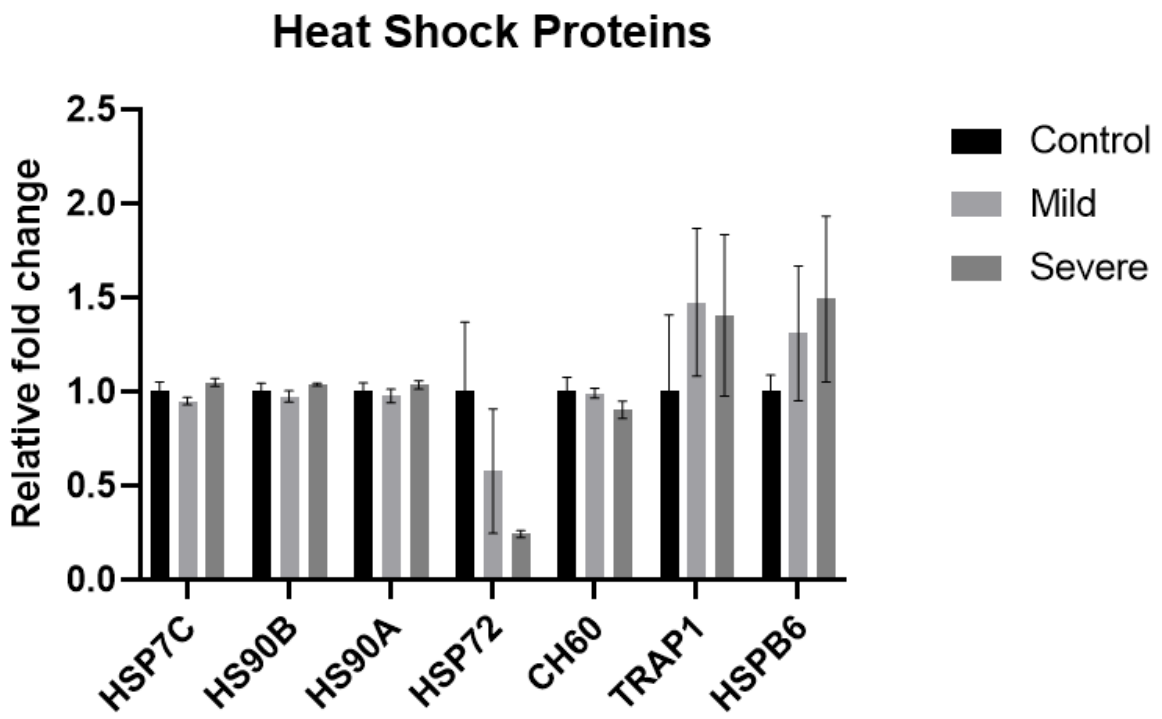

Figure 25. No significant changes in seven heat shock proteins involved in regulating cellular stress responses. Log base 2 of normalized spectrum counts for heat shock cognate 71 kDa protein (HSP7C), heat shock protein HSP 90-beta (HS90B), heat shock protein HSP 90-alpha (HS90A), heat shock-related 70 kDa protein 2 (HSP72), 60 kDa heat shock protein (CH60), heat shock protein 75 kDa (TRAP1), and heat shock protein beta-6 (HSPB6) (n = 3 for each group). Proteins were identified in control and patient fibroblasts using 1D liquid chromatography with tandem mass spectrometry and analyzed using Scaffold software. Bars represent the mean ± SEM. No significant differences were detected in groups by using a one-way ANOVA.

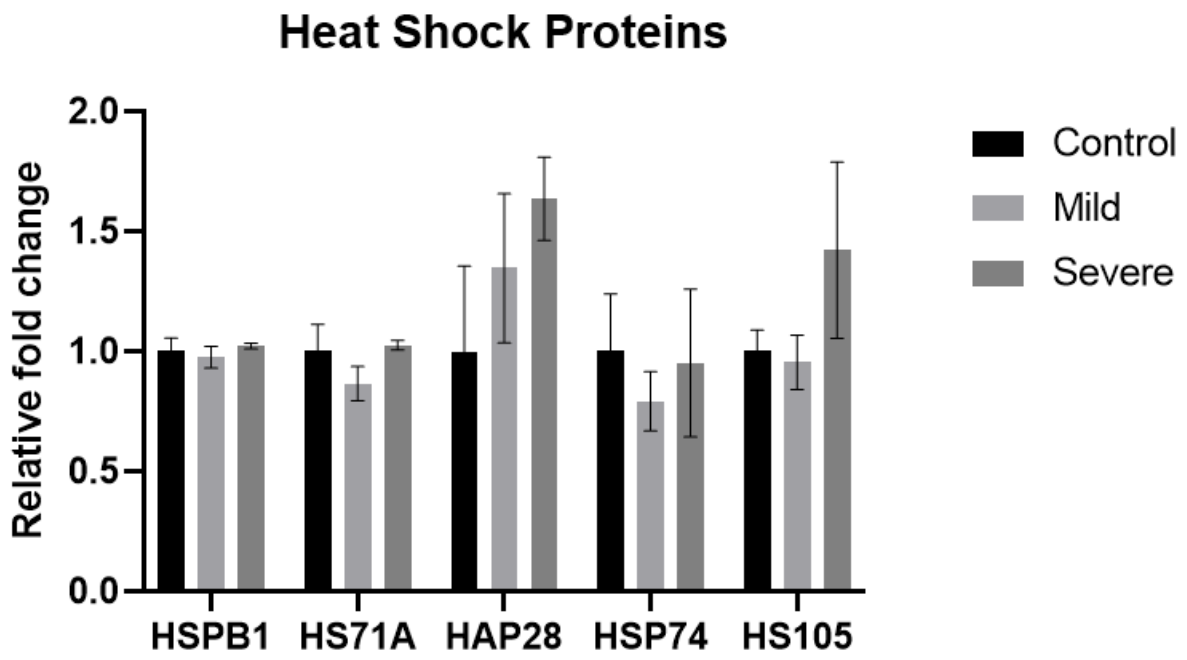

Figure 26. No significant changes to heat shock proteins identified using 1D liquid chromatography with tandem mass spectrometry that may be less involved in regulating cellular stress responses. Log base 2 of normalized spectrum counts for heat shock protein beta-1 (HSPB1), heat shock 70 kDa protein 1A (HS71A), 28 kDa heat- and acid-stable phosphoprotein (HAP28), heat shock 70 kDa protein 4 (HSP74), and heat shock protein 105 kDa (HS105). Proteins were detected in control and patient cells using 1D liquid chromatography with tandem mass spectrometry and analyzed using Scaffold software (n = 3 for each group). Bars represent the mean ± SEM. No significant differences were detected in groups by using a one-way ANOVA.

3.8 Fibroblasts deficient in DNAJC19 show increased gene activation of the ISR

Following observations that EIF2 signaling may be upregulated in proteomic data, I sought to further assess activation of specific stress responses under control of EIF2 signaling, including the ISR and the UPRmt. Gene expression analysis for a subset of genes involved in the ISR was performed using RT-qPCR. Fibroblasts treated with 500 µM of 2,4-dinitrophenol (DNP), a direct mitochondrial membrane uncoupler (Yoneda et al., 2004), for 24 hours were used as a positive control for ISR activation. The positive control showed a 4- or 5-fold increase for the activator of the ISR, *ATF4*, and three of the downstream targets, *ASNS*, *HMOX1*, and *XBP1* (Figure 27). Untreated fibroblasts from patients with a mild cardiac phenotype did not show any significant increase in gene expression for genes involved in the ISR. Meanwhile, untreated fibroblasts from patients with severe cardiac dysfunction exhibited a 2-fold increase in expression of both *ATF4* and *ASNS*, and a 7-fold increase in *XBP1* expression, all of which were statistically significant. These results indicate that genes involved in the ISR are upregulated in cells from patients with severe DCMA, suggesting ISR activation and indicating that patient cells are likely facing increased stress.

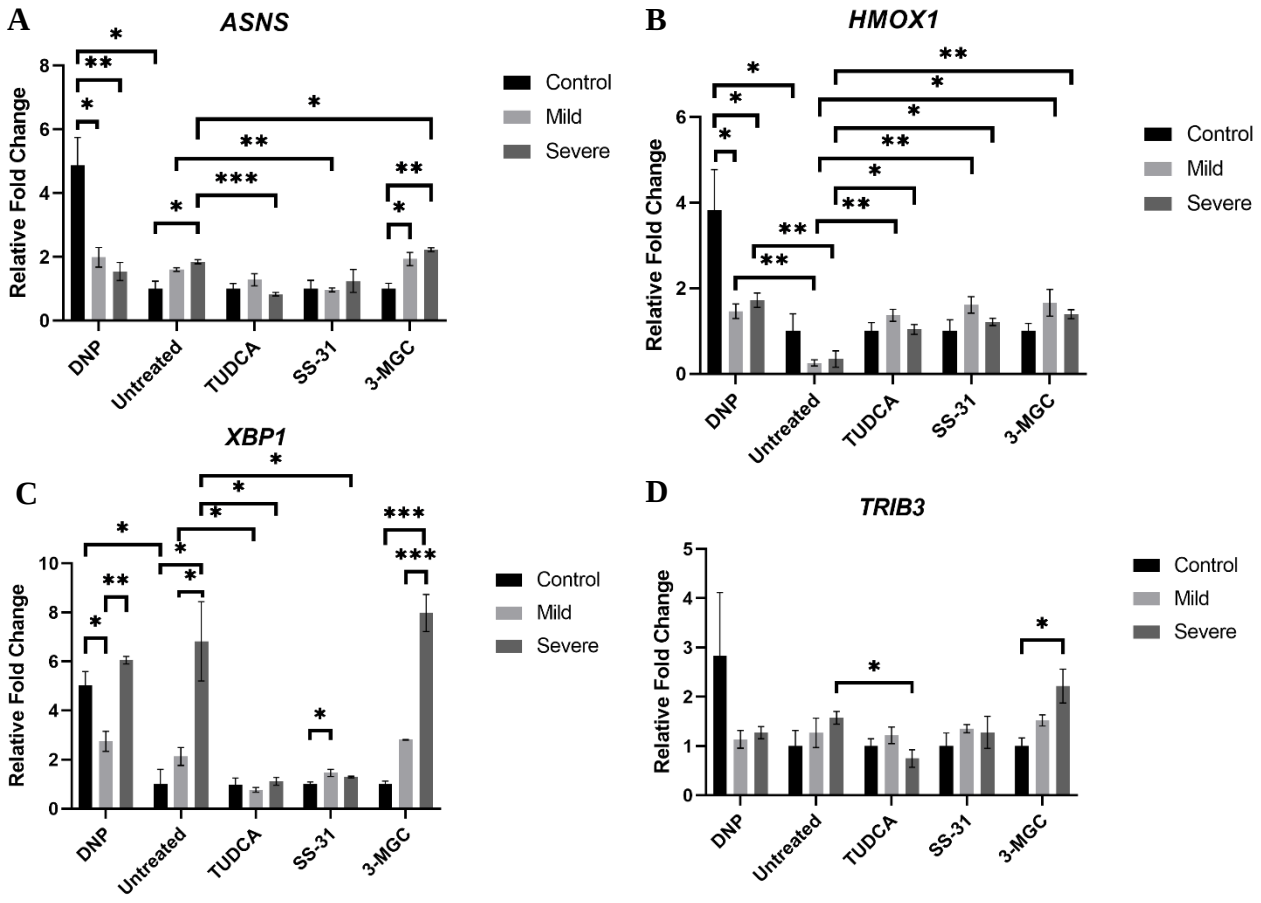

Figure 27. Upregulation of genes in the integrated stress response in DCMA patient fibroblasts. Changes in gene expression for genes involved in the integrated stress response (ISR) regulated by activating transcription factor 4 (*ATF4*) (n = 3 for each group). Relative fold change of ISR genes [(A) asparagine synthetase (*ASNS*), (B) heme oxygenase 1 (*HMOX1*), (C) x-box binding protein 1 (*XBP1*), (D) tribble pseudokinase 3 (*TRIB3*)] in control and patient fibroblasts. Positive control was generated by treating control fibroblasts with 500 µM 2,4-dinitrophenol (DNP) for 24 hours. Attenuation of the ISR was attained by treating patient fibroblasts with 100 µM of tauroursodeoxycholic acid (TUDCA) or 100 µM of SS-31 for 24 hours. Addition of 3-methyglutaconic acid (3-MGC) to control and patient fibroblasts at 2400 nM for 24 hours did not exacerbate the ISR. Bars represent the mean ± SEM. P values within groups were calculated using a one-way ANOVA and Tukey's test. Changes between treatment groups were compared using a paired t-test. * $p < 0.05$; ** $p < 0.01$; *** $p < 0.001$.

3.9 DNAJC19-deficient fibroblasts have increased UPRmt gene activity

The UPRmt is another cellular stress response closely linked to EIF2 signaling and more specifically to protein-based stress in mitochondria, including perturbed mitochondrial proteostasis (Melber & Haynes, 2018). Thus, gene expression data using RT-qPCR served to identify activation of the UPRmt which would support a role for DNAJC19 in the maintenance of mitochondrial proteostasis. Fibroblasts were treated with 500 μM of 2,4-dinitrophenol (DNP) for 24 hours and used as a positive control for UPRmt activation. The positive control exhibited between a 4-fold and 12-fold increase for all three activators of the UPRmt and their downstream targets, with the exception of *Hsp10* which exhibited no change (Figure 28 & Figure 29). Fibroblasts from patients with mild cardiac dysfunction that were untreated showed a significant 2-fold and 1.5-fold increase in gene expression for *CLPP* (Figure 29B) and *Hsp60* (Figure 29C), respectively. Meanwhile, cells from patients with severe DCMA that were untreated showed a significant 2- to 4-fold increase in gene expression for all three activators of the UPRmt, *ATF4*, *ATF5*, and *CHOP* (Figure 28A, Figure 28B, Figure 29A), as well as their downstream targets *mtHsp70* and *CLPP* (Figure 28C & Figure 29B). However, gene expression was not significantly altered for *LONP1, Hsp60* and *Hsp10* (Figure 28 & Figure 29). These results indicate that gene expression is increased for both the ATF5 and CHOP branches of the UPRmt in a step-wise manner with significant upregulation being apparent in cells from patients with severe DCMA. Activation of the UPRmt then suggests a role for DNAJC19 in the maintenance of the mitochondrial proteome.

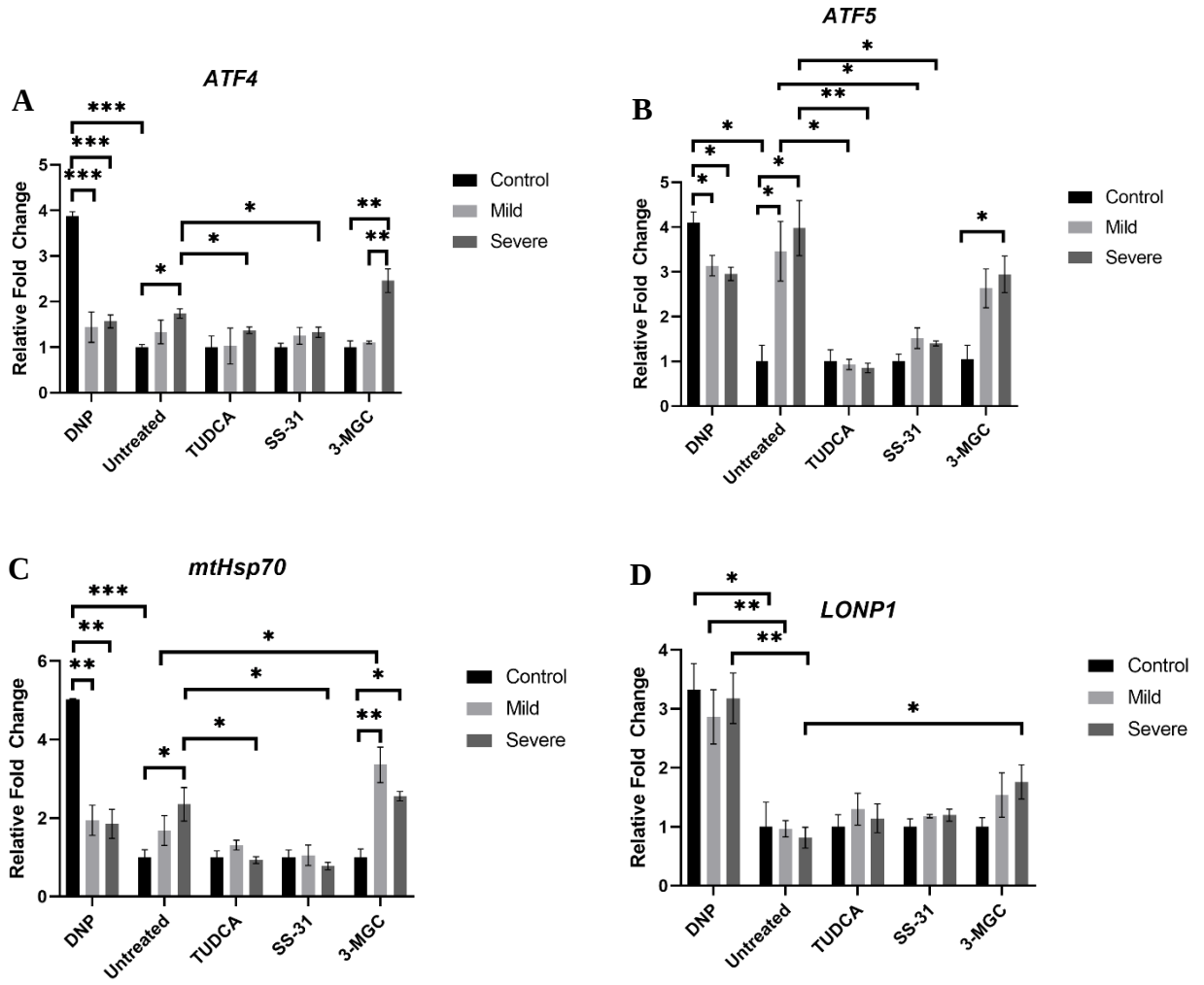

Figure 28. Upregulation of genes in the ATF5 branch of the mitochondrial unfolded protein response in DCMA patient fibroblasts. Changes in gene expression for genes involved in the unfolded protein response of mitochondria (UPRmt) regulated by (A) activating transcription factor 4 (*ATF4*) and (B) activating transcription factor 5 (*ATF5*) (n = 3 for each group). Relative fold change of UPRmt genes [(C) mitochondrial heat shock protein 70 (*mtHsp70*), (D) lon protease homolog 1 (*LONP1*)] in control and patient fibroblasts. Positive control was generated by treating control fibroblasts with 500 µM 2,4-dinitrophenol (DNP) for 24 hours. Attenuation of the UPRmt was attained by treating patient fibroblasts with 100 µM of tauroursodeoxycholic acid (TUDCA) or 100 µM of SS-31 for 24 hours. Addition of 3-methyglutaconic acid (3-MGC) to control and patient fibroblasts at 2400 nM for 24 hours did not exacerbate the UPRmt. Bars represent the mean ± SEM. P values within groups were calculated using a one-way ANOVA and Tukey's test. Changes between treatment groups were compared using a paired t-test. * $p < 0.05$; ** $p < 0.01$; *** $p < 0.001$.

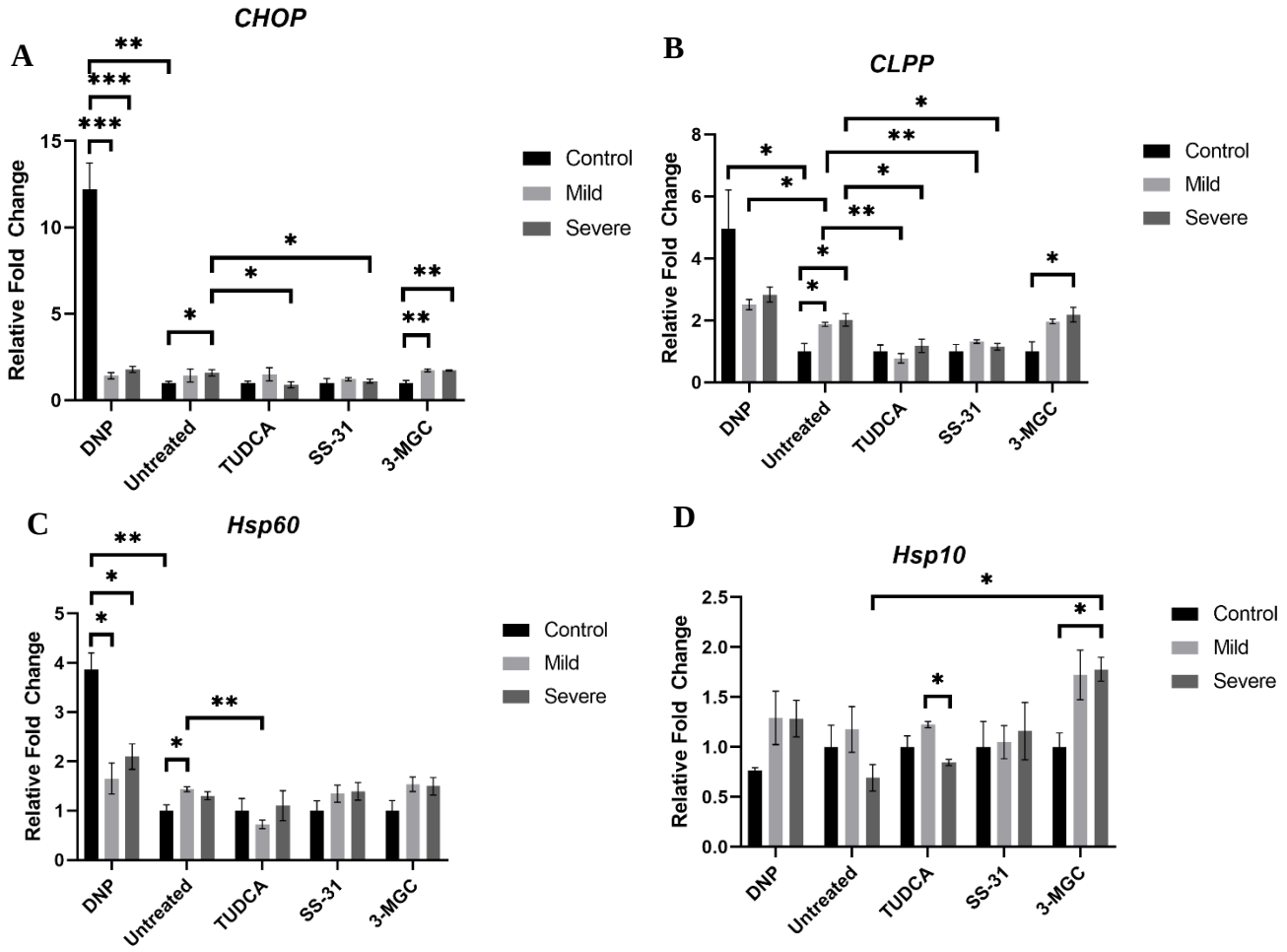

Figure 29. Upregulation of genes in the CHOP branch of the mitochondrial unfolded protein response in DCMA patient fibroblasts. Changes in gene expression for genes involved in the unfolded protein response of mitochondria (UPRmt) regulated by activating transcription factor 4 (*ATF4*) and (A) C/EBP homologous protein (*CHOP*) (n = 3 for each group). Relative fold change of UPRmt genes [(B) caseinolytic mitochondrial matrix peptidase proteolytic subunit (*CLPP*), (C) heat shock protein 60 (*Hsp60*), (D) heat shock protein 10 (*Hsp10*)] in control and patient fibroblasts. Positive control was generated by treating control fibroblasts with 500 µM 2,4-dinitrophenol (DNP) for 24 hours. Attenuation of the UPRmt was attained by treating patient fibroblasts with 100 µM of tauroursodeoxycholic acid (TUDCA) or 100 µM of SS-31 for 24 hours. Addition of 3-methyglutaconic acid (3-MGC) to control and patient fibroblasts at 2400 nM for 24 hours did not exacerbate the UPRmt. Bars represent the mean ± SEM. P values within groups were calculated using a one-way ANOVA and Tukey's test. Changes between treatment groups were compared using a paired t-test. * $p < 0.05$; ** $p < 0.01$; *** $p < 0.001$.

3.10 SS-31 blocks the increased expression of genes involved in the ISR

SS-31 is a mitochondrial targeting peptide that has been proposed to be beneficial for the treatment of a variety of mitochondrial disorders as it can reduce mitochondrial dysfunction (Zhao et al., 2017). Previously, SS-31 has been used to treat DCMA patient fibroblasts and was shown to reduce ROS production, restore the OPA1 isoform ratio, and reverse mitochondrial fragmentation (Machiraju et al., 2019). Based on these previous findings, I considered that SS-31 may serve to reduce or block activation of the ISR and the UPRmt in DCMA patient cells. Indeed, the ISR was measured following treatment of control and patient fibroblasts with 100 µM of SS-31 for 24 hours. The key regulator, *ATF4*, decreased significantly by 1.3-fold in cells from patients with severe DCMA relative to the untreated group. *XBP1* showed a significant 5-fold decrease in fibroblasts from patients with severe cardiac dysfunction, with no significant changes in cells from patients with mild DCMA relative to untreated groups (Figure 27C). *HMOX1* expression significantly increased in cells from patients with mild and severe DCMA by 6-fold and 3.5-fold, respectively, when compared to untreated patient cells (Figure 27B). However, these changes in *HMOX1* were not significantly different from control values (Figure 27B). As for *ASNS* there were no significant changes in cells from patients with severe cardiac dysfunction following treatment. However, treated fibroblasts from patients with mild cardiac dysfunction showed a 1.5-fold decrease in *ASNS* which was considered significant (Figure 27A). Lastly, there were no significant changes in *TRIB3* expression following treatment of fibroblasts from patients with mild and severe DCMA (Figure 27D). However, when expression of genes for the ISR in treated patient fibroblasts were compared to control cells only *XBP1* in cells from patients with mild DCMA was significantly increased. These results suggest that SS-31 serves to

block increases in gene expression for the ISR in DCMA fibroblasts and as such may reduce cellular stress.

3.11 SS-31 blocks UPRmt gene activation

Control and patient fibroblasts were treated with 100 μM of SS-31 for 24 hours and then activation of the UPRmt was measured. Following treatment with SS-31 there were no significant difference in gene expression for *Hsp60*, *Hsp10*, or *LONP1* in cells from patients with mild and severe DCMA (Figure 28 & Figure 29). However, *ATF4*, resulted in a near 2-fold decrease in gene expression in cells from patients with a severe cardiac phenotype following treatment with SS-31. *CHOP* and *mtHsp70* showed significant changes in gene expression in fibroblasts from patients with severe DCMA following treatment, resulting in a 1.5-fold and 2-fold decrease, respectively (Figure 29A & Figure 28C). In addition, *ATF5* and *CLPP* both showed significant changes in gene expression in cells from patients with mild and severe cardiac dysfunction relative to untreated groups (Figure 28B & Figure 29B). *ATF5* expression decreased by 2-fold in cells from patients with mild cardiac dysfunction and 2.8-fold in cells from patients with severe cardiac dysfunction, both of which were statistically significant (Figure 28B). Lastly, *CLPP* expression decreased by nearly 1.5-fold in cells from patients with mild and severe cardiac phenotypes (Figure 29B). Taken together, these results indicate that SS-31 serves to block activation of the UPRmt and maintain gene expression close to control levels, thus indicating its potential use as a therapeutic to reduce stress to the mitochondrial proteome.

3.12 TUDCA serves to block gene expression of the ISR

Tauroursodeoxycholic acid (TUDCA) has previously been shown to refold proteins within the cytosol, thereby reducing ER stress and activation of the UPR of the ER (Uppala et al., 2017). Additionally, TUDCA was found to interact with mitochondria preventing apoptosis and ameliorating mitochondrial dysfunction (Zangerolamo et al., 2021). Thus, if TUDCA can work within the cytosol while also impacting mitochondrial dysfunction it may serve to block activation of both the ISR and the UPRmt. The ISR was measured following treatment of control and patient fibroblasts with 100 µM of TUDCA for 24 hours. Following treatment with TUDCA, expression of *XBP1* decreased significantly by 2.7-fold in cells from patients with a mild phenotype, and 6-fold in cells from patients with a severe phenotype (Figure 27C). As for *ASNS*, treatment with TUDCA resulted in a 1.2-fold and 2.25-fold decrease in gene expression levels in cells from patients with mild and severe DCMA, respectively (Figure 27A). There were no significant differences in gene expression in cells from patients with mild cardiac dysfunction for *TRIB3* expression, but cells from patients with severe cardiac dysfunction showed a significant 2-fold decrease in the treated group (Figure 27D). Notably, *HMOX1* gene expression was increased nearly 2-fold in fibroblasts from patients with mild and severe DCMA following treatment (Figure 27B). Although these changes in *HMOX1* were significant when compared to untreated groups, they were not statistically significant when compared to controls (Figure 27B). These results suggest that TUDCA works to block activation of genes in the ISR and may serve as a therapeutic to reduce cellular stress.

3.13 TUDCA acts to downregulate genes expressed by the UPRmt

Control and patient fibroblasts were treated with 100 µM of tauroursodeoxycholic acid (TUDCA) for 24 hours and then activation of the UPRmt was measured. Following treatment

with TUDCA there was a significant 1.3-fold reduction in the expression of *ATF4* in fibroblasts from patients with severe DCMA (Figure 28A). In addition, both *ATF5* and *CHOP* gene expression significantly decreased in fibroblasts from patients with severe DCMA following treatment (Figure 28B & Figure 29A). *CHOP* expression decreased by 1.8-fold in cells from patients with severe cardiac dysfunction (Figure 29A). Meanwhile, *ATF5* expression decreased by nearly 5-fold and 3.5-fold in cells from patients with severe and mild cardiac dysfunction, respectively (Figure 28B). As for downstream targets of ATF5, *mtHsp70* decreased significantly by 2.5-fold in fibroblasts from patients with severe DCMA, whereas there were no significant differences in expression of *LONP1* for patient fibroblasts after treatment (Figure 28C & Figure 28D). Downstream target of CHOP, *CLPP* showed significant decreases in gene expression in fibroblasts from patients with mild and severe cardiac dysfunction after treatment, decreasing by 2.5-fold and 1.7-fold, respectively (Figure 29B). Meanwhile, following treatment *Hsp60* decreased significantly by 2-fold in fibroblasts from patients with mild DCMA, but no significant changes were identified in fibroblasts with severe DCMA. As for *Hsp10* gene expression, there were no significant changes in treated cells from patients with mild and severe DCMA relative to untreated cells (Figure 29C & Figure 29D). Taken together, these results indicate that TUDCA serves to prevent upregulation of genes within the UPRmt and may address cellular stress to enable patient cells to better cope with deficiency of DNAJC19.

3.14 Addition of TUDCA helps restore mitochondrial structure

Considering that SS-31 worked to ameliorate mitochondrial fragmentation and block activation of cellular stress responses, I thought that TUDCA may serve a similar role for mitochondrial membrane fission. Patient fibroblasts were treated with 100 µM of tauroursodeoxycholic acid

(TUDCA) for 24 hours prior to collection and protein extraction. In untreated cells there was a significant increase in Drp1 levels in cells from patients with severe DCMA when compared to control data (Figure 30). Following treatment with TUDCA, the abundance of Drp1 decreased 1.4-fold back to control levels.

Analysis of the ratio of OPA1 isoforms in untreated cells collected from patients with severe DCMA showed a significant decrease in the long isoform (L-OPA1) (Figure 31). The isoform ratio was then increased 1.25-fold and restored back to control levels following treatment with TUDCA (Figure 31). These results suggest that TUDCA works to restore changes observed in proteins that are involved in mitochondrial membrane fission through the reduction of fission proteins and the increase of fusion proteins.

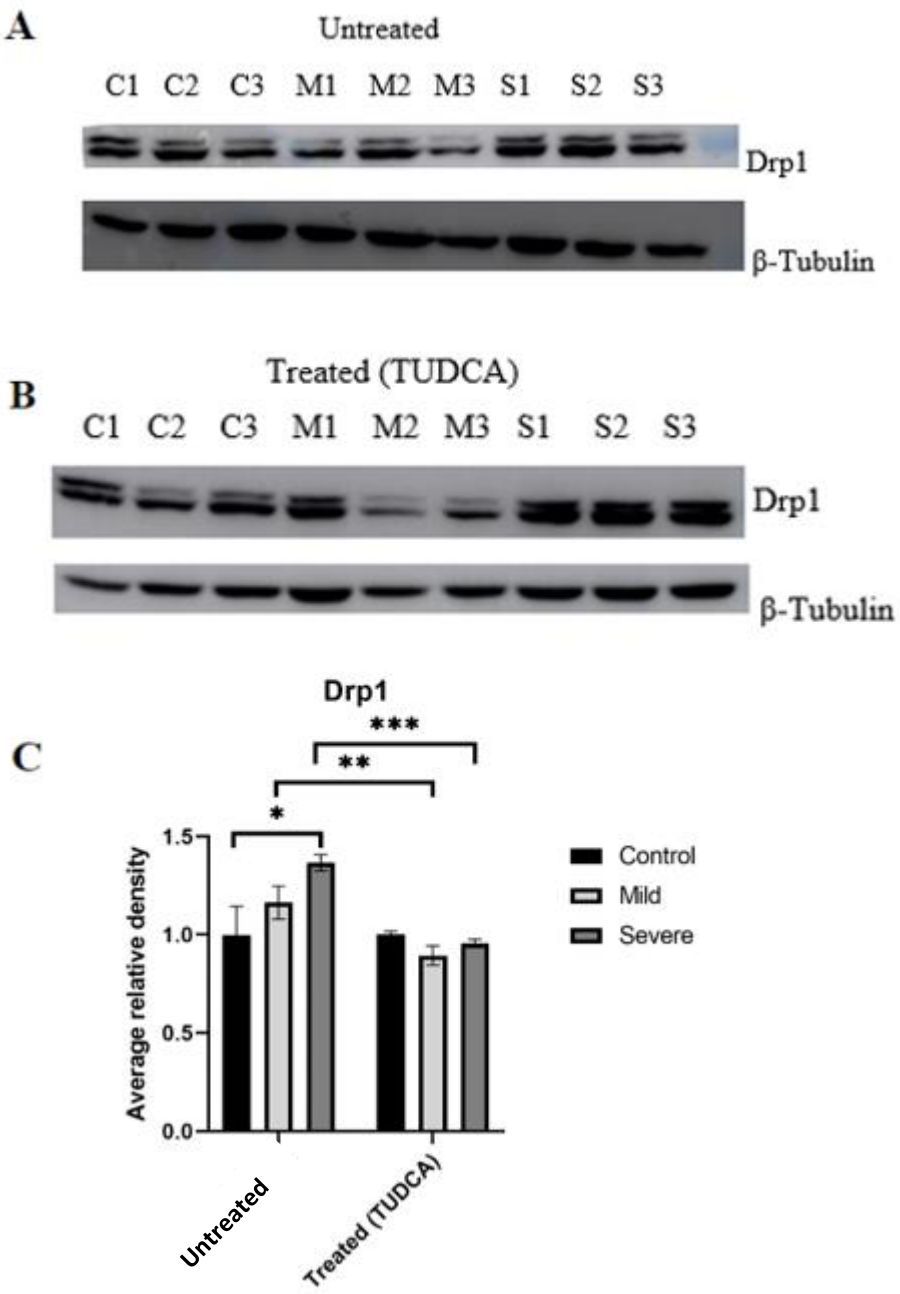

Figure 30. Increased Drp1 protein abundance in fibroblasts from patients with severe DCMA. (A) Western blot of untreated control (C1-C3) and DCMA patient fibroblasts (M1-M3, S1-S3) (n = 3 for each group). (B) Western blot of control and DCMA patient cells treated with 100 μM of TUDCA (tauroursodeoxycholic acid) for 24 hours to restore dynamin-related protein 1 (Drp1) protein abundance (n = 3 for each group). (C) Densitometric analysis of Drp1 for untreated and treated control and patient fibroblasts normalized to β-tubulin. P values within groups were calculated using a one-way ANOVA and Tukey's test. Changes between treatment groups were compared using a paired t-test. Bars represent the mean ± SEM. * $p < 0.05$; ** $p < 0.01$; *** $p < 0.001$.

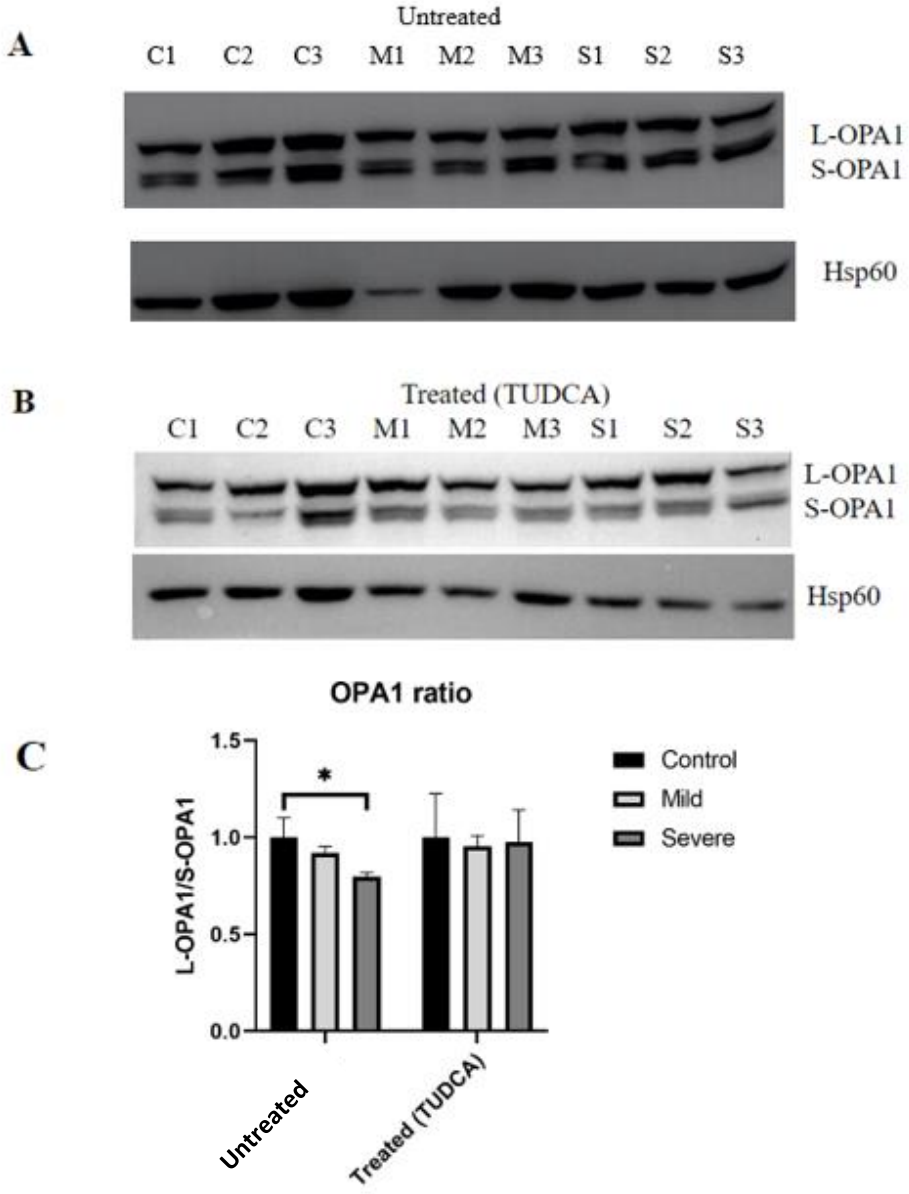

Figure 31. Decreased ratio of long to short OPA1 isoforms in fibroblasts from patients with severe DCMA. (A) Western blot of untreated control (C1-C3) and DCMA patient fibroblasts (M1-M3, S1-S3) depicting the long dynamin-like 120 kDa protein (OPA1) isoform (L-OPA1) and the short OPA1 isoform (S-OPA1). (B) Western blot of long and short OPA1 isoforms for treated control and DCMA patient fibroblasts. Fibroblasts were treated with 100 μM of tauroursodeoxycholic acid (TUDCA) for 24 hours to restore the OPA1 isoform ratio (n = 3 for each group). (C) Densitometric analysis of treated and untreated control and patient fibroblasts normalized to Hsp60. P values within groups were calculated using a one-way ANOVA and Tukey's test. Changes between treatment groups were compared using a paired t-test. Bars represent the mean ± SEM. * $p < 0.05$.

3.15 Incubation with 3-methylglutaconic acid does not exacerbate ISR gene expression in DCMA patient fibroblasts

Patients with DCMA have elevated levels of 3-methylglutaconic acid (3-MGC) in bodily fluids, around 2400 nM, making DCMA a disorder of 3-methylglutaconic aciduria (Davey et al., 2006; Machiraju et al., 2022). It was thought that the elevation in 3-MGC may be a causal agent of cellular stress within patient cells. The ISR was measured following treatment of control and patient fibroblasts with 2.4 µM of 3-MGC for 24 hours. Following treatment with 3-MGC, *HMOX1* expression significantly increased 6-fold and 4-fold in cells from patients with mild and severe DCMA, respectively, when compared to untreated groups. However, these changes in *HMOX1* resulted in increases in gene expression that did not statistically differ from control levels (Figure 27B). Lastly, *ASNS* was the only other gene to show significant changes between treated and untreated groups, with a 1.2-fold increase in expression in fibroblasts from patients with severe DCMA (Figure 27A). Both *TRIB3* and *XBP1* did not show any significant differences following treatment (Figure 27C & Figure 27D). Without the increase in *ATF4*, coupled with *HMOX1* levels approaching control values after treatment, increases in *ASNS* is insufficient to claim that the ISR is exacerbated following treatment with 3-MGC. These results would suggest that 3-MGC does not lead to increased expression of genes involved in the ISR and thus likely serves as a by-product of cellular stress not a causal agent.

3.16 Incubation with 3-MGC does not exacerbate UPRmt gene expression in DCMA patient fibroblasts

Control and patient fibroblasts were treated with 2.4 µM of 3-methylglutaconic acid (3-MGC) for 24 hours and activation of the UPRmt was measured. Compared to untreated fibroblasts, cells from patients with mild and severe DCMA that were treated with 3-MGC did not show significant changes in gene expression for *ATF4*, *ATF5*, *CHOP*, or *CLPP* (Figure 28 & Figure 29). However, *mtHsp70* resulted in a 2-fold increase in gene expression in fibroblasts from patients with mild DCMA when compared to untreated fibroblasts (Figure 28C). As for fibroblasts from patients with a severe DCMA, following treatment there was a 2-fold increase in *LONP1* expression and a 2.5-fold increase for *Hsp10* expression (Figure 28D & Figure 29D). Taken together, these results indicate that treatment with 3-MGC does not significantly increase expression of UPRmt genes beyond what is observed in untreated patient fibroblasts. These results suggest that elevated levels of 3-MGC are not responsible for the increased activation of the UPRmt observed in DCMA patient cells indicating that 3-MGC is likely not responsible for increased cellular dysfunction and stress.

3.17 Evaluation of apoptosis and cytotoxicity in patient cells

Prolonged activation of cellular stress responses can be maladaptive and suggests that the cell cannot effectively respond to the stress being faced (Kaspar et al., 2021). When activation of cellular stress responses stop being beneficial there is usually an increase in apoptosis and mitophagy (Anderson & Haynes, 2020; Eisner et al., 2018). Thus, cytotoxicity and apoptosis were used as measures for whether patient cells can adequately cope with the stress they are facing. Control and patient fibroblasts were assessed for increases in cytotoxicity using a lactate dehydrogenase (LDH) assay to quantify LDH released into the cell culture media, indicating damage to the plasma membrane and subsequently indicating cytotoxicity. Upon analysis, there

were no significant increases between control and DCMA patient fibroblasts (Figure 32). Furthermore, both control and patient cells were treated with 100 μM of tauroursodeoxycholic acid (TUDCA) for 24 hours and cytotoxicity was assessed again. Following treatment with TUDCA there were no significant difference in cytotoxicity between control and patient fibroblasts, nor between the untreated groups and the groups treated with TUDCA (Figure 32). These results indicate that there is no increase in cytotoxicity in patient cells, nor is there an increase following treatment with TUDCA.

Cells were then assessed for increased apoptosis using staining for DAP1 (4',6-diamindino-2-phenylindole) and TUNEL (terminal deoxynucleotidyl transferase dUTP nick end labeling). Staining with DAPI served to identify the total number of cells (Figure 33A), while TUNEL staining identified cells with fragmented DNA (Figure 33B). Colocalization of DAPI and TUNEL was used to identify cells that had undergone apoptosis (Figure 33C). Control and patient fibroblasts did not show any apoptosis upon analysis with TUNEL staining which indicates that patient cells can either cope with the stress they are facing or cellular stress is insufficient to warrant cell death (Figure 34).

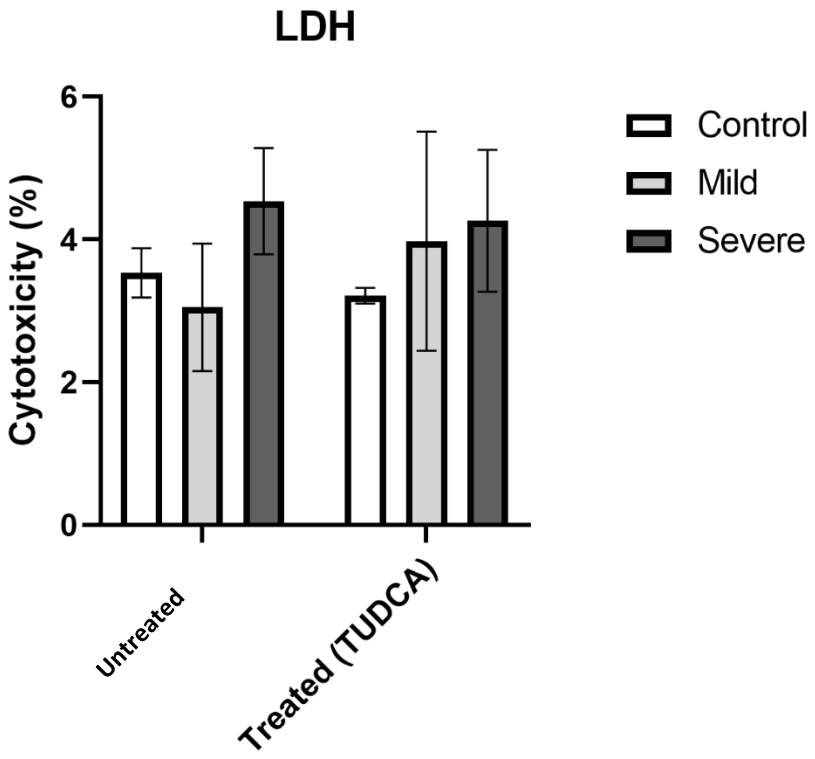

Figure 32. No increase in cytotoxicity in response to TUDCA determined in control and patient cells. Cytotoxicity was determined using a colorimetric assay for untreated control and patient cells and cells treated with 100 µM of TUDCA (tauroursodeoxycholic acid) for 24 hours (n = 3 for each group). No significant differences were detected within groups using a one-way ANOVA or between groups using a paired t-test. Bars represent the mean ± SEM.

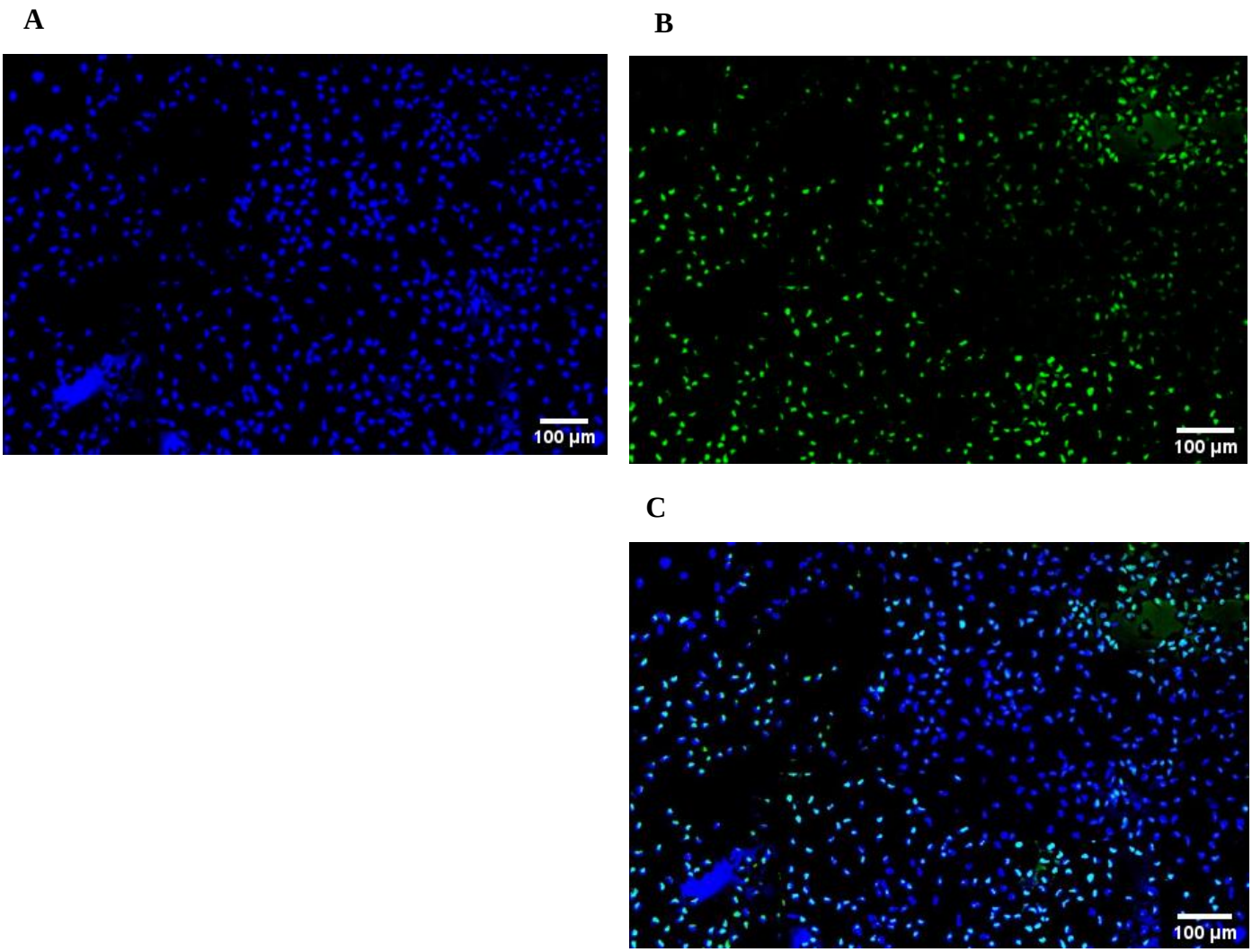

Figure 33. Example of positive control fibroblast staining for DAPI and TUNEL. (A) Positive control fibroblasts stained with 4',6-diamindino-2-phenylindole (DAPI). (B) Positive control fibroblasts stained with TUNEL (terminal deoxynucleotidyl transferase dUTP nick end labeling). (C) Colocalization of DAPI and TUNEL indicate the percentage of apoptotic cells. Positive control was generated by treating cells with DNase I. Images taken using the 20X objective of an Olympus VS110-S5 Slide Scanner. Scale bars represent 100 µm.

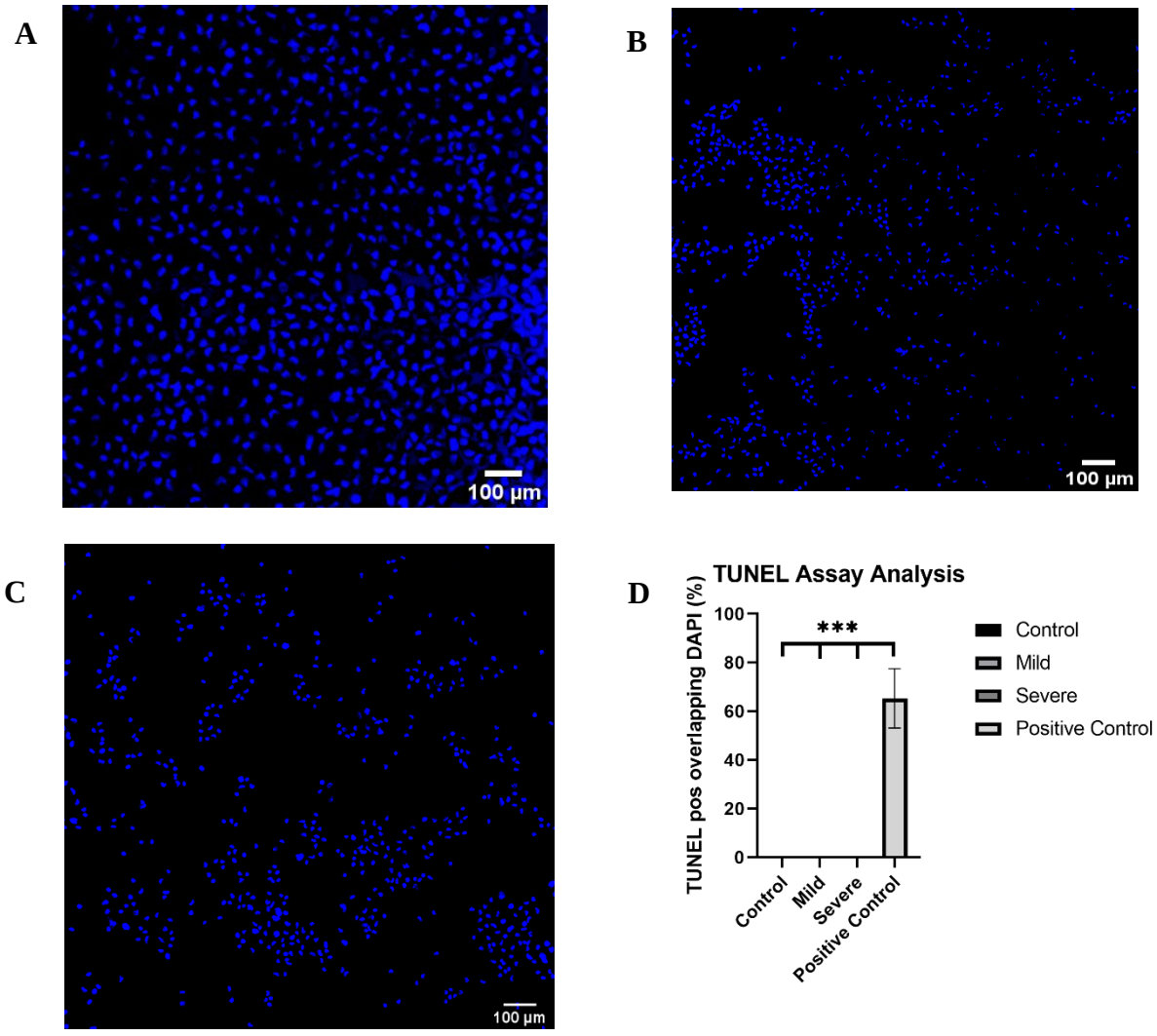

Figure 34. No increase in apoptosis in control or DCMA patient cells. (A) Control fibroblasts showing colocalization of DAPI (4',6-diamindino-2-phenylindole) and TUNEL (terminal deoxynucleotidyl transferase dUTP nick end labeling). (B) Mild patient fibroblast showing colocalization of DAPI and TUNEL. (C) Severe patient fibroblast showing colocalization of DAPI and TUNEL. (D) Object-based colocalization analysis using JACoP for TUNEL assay depicting % apoptosis. Positive control taken from Figure 33. Bars represent ± SEM. Images taken using the 20X objective of an Olympus VS110-S5 Slide Scanner (n = 3 per group). Scale bars represent 100 µm. P value was calculated using a paired t-test. *** $p < 0.001$.

Chapter 4: Discussion

4.1 Proteomic changes identified in DCMA patient cells

DCMA is a heterogenous disease, which complicates the understanding and treatment of this disorder. Furthermore, the gene implicated in DCMA, *DNAJC19*, is poorly characterized. I sought to analyze the mitochondrial proteome of patient cells to provide a better understanding of how deficiency of DNAJC19 leads to mitochondrial protein changes and to identify broader pathway changes that may help to elucidate the role of DNAJC19. To do so I used what I thought were pure mitochondrial isolates from patient fibroblasts. However, subsequent analysis revealed that the mitochondrial preparations were not as consistently pure as they could have been, as suggested by inconsistent VDAC1 abundance in the western blotting data and low mitochondrial enrichment (Figure 6 & Figure 8). In fact, the total number of proteins and mitochondrial proteins identified in the dataset was similar to the values seen in whole cell samples that were submitted for comparison (Figure 6). Thus, I concluded that the mitochondrial isolates were unsuccessful and the samples I had submitted more closely represented the entire proteome and not the mitochondrial proteome. As such, I considered the mitochondrial isolates to be total protein isolates. These isolates would provide insight into the total proteome of patient cells, rather than just the mitochondrial proteome. To avoid confusion with the whole cell lysate that was submitted, the samples that were thought to be mitochondrial isolates are termed total protein isolates. Thus, to perform proteome analysis, I utilized all proteins with a ±2-fold change within the dataset for downstream analyses, not limited to just mitochondrial proteins. It should also be noted that DNAJC19 was not detected within our dataset and thus, our cellular models are based on the assumption that DNAJC19 is deficient in patient cells but present in control cells. The inability to detect DNAJC19 may be partially explained by the poor mitochondrial

isolation, meaning that less abundant proteins could not be as readily identified due to the assay not be sensitive enough.

Despite not being able to generate pure mitochondrial isolates I was still able to note changes to mitochondrial membrane dynamics, particularly mitochondrial fission. Due to a previous study finding that DCMA patient cells showed increased mitochondrial fragmentation (Machiraju et al., 2019), I considered that mitochondrial dynamics and particularly mitochondrial fission and fusion may be impacted. I noted an increase in the pro-fission protein, DNM1L or dynamin-related protein 1 (Drp1) (Figure 15). Drp1 is predominantly found within the cytosol but is recruited to mitochondria during events associated with increased fission (Smirnova et al., 2001). Thus, increases in protein levels of Drp1 alone are suggested to be less important for increasing mitochondrial fission than the actual mitochondrial translocation and subsequent protein interactions (Chang & Blackstone, 2010). However, Drp1 was not the only protein where changes were observed. Coupling the increase in Drp1 with a significant decrease in OPA1 suggests changes to mitochondrial membrane fission in cells from patients with severe cardiac dysfunction (Figure 15). I validated these findings using western blotting wherein I confirmed an increase in Drp1 as well as a shift in the ratio of OPA1 isoforms towards increased abundance of S-OPA1 (Figure 30 & Figure 31). These results corroborate previous data suggesting DCMA patient cells have altered ratios of OPA1 isoforms and increased mitochondrial fragmentation (Machiraju et al., 2019).

OPA1 is a necessary protein responsible for mitochondrial fusion within the IMM and works alongside the mitofusin proteins (Mfn1 and Mfn2) on the OMM (Hu et al., 2017). OPA1 has also been shown to increase mitochondrial respiratory efficiency and aid in the reduction of mitochondrial dysfunction (Hu et al., 2017). Thus, OPA1 is a critical protein for mitochondrial

membrane dynamics and mitochondrial function. As we know, some patients with DCMA, even those from the same family present very differently (Ojala et al., 2012). Differences in the regulation of these pathways and processes could be linked to the heterogeneity we see in patients. More specifically, it is understood that mitochondrial stress can lead to increases in fission and apoptosis (Youle & van der Bliek, 2012). Thus, it is possible that cells from patients with a severe cardiac phenotype are faced with increased stress leading to increased fission.

The proteomic data also suggests that fibroblasts from patients with mild DCMA do not show similar upregulation or downregulation of cellular pathways when compared to control cells nor those from patients with severe DCMA (Figure 16). Thus, it appears that the mild phenotype is a more intermediate phenotype than the severe, wherein there is not as much dysfunction occurring. Further outlining the differences between cells from patients with mild and severe DCMA is the predicted downregulation of certain canonical pathways by IPA (Figure 16). Cells from patients with mild and severe DCMA showed upregulation of pathways to a similar degree, particularly the EIF2 signaling pathway which suggests increased cellular stress. However, there appears to be greater variability in the downregulation of pathways (Figure 16). Notably, the dilated cardiomyopathy pathway was predicted to be downregulated to a greater degree in cells from severely affected patients than cells from patients with mild DCMA (Figure 16). Specifically, IPA predicted that this pathway would lead to increased calcium leak and cardiomyocyte apoptosis with mitochondrial dysfunction. In addition, decreased contractility was also predicted by increases in MYH7, TNNT3 and TNNI2 which were identified in the dataset (Figure 18). These results would fit with the increased cardiac dysfunction noted in patients with severe DCMA, wherein the severe phenotype was characterized by left ventricular dysfunction, while patients with mild DCMA had no left ventricular dysfunction (Table 1).

Another potential pathway of interest was the pulmonary fibrosis idiopathic signaling pathway which was predicted by IPA to be increased in cells from patients with mild and severe DCMA (Figure 16). Notable predictions within this pathway were decreased mitochondrial function accompanied by increased mitochondrial dysfunction from a decrease in PINK1 (PTEN induced kinase 1) and PRKN (parkin RBR E3 ubiquitin protein ligase). These two proteins have been shown to be critically important in mediating mitochondrial quality control such as mitophagy (Ge et al., 2020). Thus, these changes were predicted by IPA to lead to decreased mitophagy which could prevent the clearing/removal of damaged mitochondria further exacerbating mitochondrial dysfunction and cellular stress (Ma et al., 2020). In fact, intermembrane lipid transfer protein VP13C was one of the top differentially expressed proteins in cells from patients with mild DCMA (Figure 10). This protein plays an important role in mitochondrial function and the maintenance of the mitochondrial membrane potential. In particular, this protein was found to be important in the regulation of PINK-PRKN-mediate mitophagy, wherein loss of this protein resulted in increased PINK-PRKN-mediated mitophagy (Lesage et al., 2016). Thus, overexpression of VP13C, as suggested in our proteomic data could lead to decreased PINK-PRKN interactions and mitophagy as predicted by IPA. Beyond these changes, increased ECM accumulation leading to lung fibrosis was also predicted. What is interesting with this is that idiopathic pulmonary fibrosis can be accompanied by cardiac dysfunction and heart failure (Papadopoulos et al., 2008). Thus, while patients with DCMA have not been shown to have pulmonary fibrosis as an accompanying clinical characteristic, respiratory issues have been identified in children with DCMA (Machiraju et al., 2022). Thus, further investigation into the cause of these respiratory issues and how they link to the cardiac

phenotype may provide insight into new therapeutics for the treatment of DCMA or to decrease morbidity for patients with respiratory issues.

While IPA noted numerous upregulated and downregulated pathways that should be explored in greater detail in the future, there was one pathway that was of particular interest. The top predicted canonical pathway for cells from patients with mild and severe DCMA was the EIF2 signaling pathway (Figure 16). This pathway is responsible for inhibition of global translation of proteins, which is a necessary response to numerous stressors, but critically important when discussing stress resulting from protein accumulation (Shrestha et al., 2012). How this occurs, is through phosphorylation of the α-subunit (eIF2α) which then prevents interactions with Met-$tRNA_i^{Met}$ and subsequently prevents binding to ribosomes (Park et al., 2018). Notably, phosphorylation of eIF2α is also necessary for activation of the ISR and the UPRmt (Pakos-Zebrucka et al., 2016).

Upregulation of EIF2 signaling is an initial indicator that there is cellular stress occurring within DCMA patient cells. Given the suggested role of DNAJC19 in mitochondrial protein import, one would expect that deficiency of DNAJC19 in patient cells could lead to errors in protein handling and processing and thus disrupt mitochondrial proteostasis. Should this be the case then we would anticipate upregulation of the UPRmt to address mitochondrial stress. Thus, it is possible that the upregulation in EIF2 signaling would activate the ISR to then subsequently upregulate the UPRmt to address perturbed mitochondrial proteostasis arising from the loss of DNAJC19. Considering the importance of EIF2 signaling in the regulation of the ISR and the UPRmt I looked towards this pathway generated by IPA based on the input data. Notably, TRIB3, ATF4, ATF5, and CHOP were all predicted to be upregulated (Figure 17b). Indeed, ATF4 and CHOP are involved in both the ISR and UPRmt, while ATF5 serves an important role

in the UPRmt and TRIB3 works within the ISR (Melber & Haynes, 2018). These data would suggest that cells from both mild and severe patient phenotypes are likely facing some stress that is sufficient to upregulate EIF2 signaling. Upregulation of this pathway would then suggest an attempt to restore cellular function to some degree. More specifically, upregulation of the UPRmt would suggest a loss of mitochondrial proteostasis. This could then mean that the changes to mitochondrial fission and mitochondrial membrane morphology observed in patient cells could be resultant from a loss of mitochondrial proteostasis and cellular stress.

Additionally, IPA predicted there to be increased cardioprotection, ER stress response, amino acid transport and biosynthesis, and decreased uptake of D-glucose as a result of EIF2 signaling (Figure 17a). In fact, the UPRmt is considered to be cardioprotective when initially activated (Svaguša et al., 2020; Wang et al., 2019). Thus, the increase in cardioprotection that was predicted from EIF2 signaling could be due to activation of the UPRmt. Additionally, the predicted decrease in glucose uptake was interesting as one study using DCMA patient fibroblasts indicated increased glutamine and glutamate metabolism (King et al., 2020). Thus, glutamine metabolism may be increased to compensate for decreased glucose uptake and metabolism in patient cells.

I then input the same proteins used in IPA into Metascape (Zhou et al., 2019) to see if similar pathways were predicted. While these pathways did not align greatly with those from IPA, it is important to note that within IPA I was interested in how the pathways changed and thus looked at those that were upregulated or downregulated based on fold change, log base 2 values, and p values. Nonetheless, the most confident prediction from Metascape for cells from patients with mild and severe DCMA was metabolism of RNA, which is a broad pathway encompassing the synthesis, modification, and processing of RNA (Figure 13 & Figure 14).

However, other notable predictions were heart contraction and glycogen metabolism when looking at statistically significant proteins in cells from patients with severe cardiac dysfunction (Figure 12). As well as regulation of catabolic processes, glycogen catabolism, cellular homeostasis, and membrane fission in cells from patients with mild and severe DCMA (Figure 13 & Figure 14). While IPA did not predict these exact pathways, there is overlap in some of the downstream consequences predicted by IPA and the pathways predicted by Metascape. For example, heart contraction and cardiomyocyte contraction were predicted to be decreased by IPA through DCM signaling which may have used some of the same proteins to predict heart contraction in Metascape (Figure 16 & Figure 12). Additionally, IPA predicted RHOGDI signaling to be decreased which involves Rho GTPases and may be similar to the Rho GTPase pathways predicted by Metascape (Figure 16 & Figure 14). Thus, while IPA and Metascape do not predict the same exact pathways, there does appear to be overlap in some functions.

Fitting with the top predicted pathways from Metascape, there were multiple differentially expressed proteins within my dataset that appear to be involved in processes that impact cardiac function and cellular metabolism. In patients with mild cardiac dysfunction, mitochondrial dicarboxylate carrier (DIC) was a top differentially expressed protein identified within the proteomic dataset (Figure 10). DIC is an important protein for catalyzing the import of metabolites across the IMM and is involved in FA metabolism and gluconeogenesis (Punzi et al., 2018). Upregulation of DIC could therefore being playing an important role in the maintenance of cardiac function as failing hearts shift away from FA oxidation and towards increased glycolysis (Bertero & Maack, 2018). In patients with severe cardiac dysfunction, one of the top differentially expressed proteins was glycogen phosphorylase (PYGM), which catalyzes the rate-limiting step in glycogen catabolism and is important for providing sufficient energy for muscle

contraction (Figure 11) (Migocka-Patrzałek & Elias, 2021). In fact, mutations in PYGM are associated with McArdle disease which presents with hypertrophic cardiomyopathy (Jones et al., 2019). Thus, overexpression of PYGM may also impact cardiac function. Titin was another protein that was overexpressed and related to cardiac muscle (Figure 11). Titin plays an important role in maintaining the passive and restorative force of cardiac sarcomeres (LeWinter & Granzier, 2010). Mutations in Titin are also associated with DCM, proving an important role for this protein in the maintenance of cardiac function (Tharp et al., 2019). From these data, we see multiple proteins that are differentially expressed and involved in cardiac function in DCMA patient cells. While these proteins seem to be involved in different processes from metabolic regulation to muscle contraction, alterations of these proteins still appear to impact the heart and their overexpression in DCMA patient cells may contribute to the cardiac phenotype observed making them potential candidates for further study.

Additionally, 4 differentially expressed proteins were identified as shared between cells from patients with mild and severe DCMA (Table 4 & Table 5). Looking into their functions in greater detail eukaryotic translation initiation factor 1A (IF1AX) is a eukaryotic translation initiation factor that is a component of the 43S pre-initiation complex and is responsible for locating the start codon on mRNA, thus serving an important role in translation (Majumdar et al., 2003). Increases in protein abundance for IF1AX could then suggest increased translation in patient cells. If DCMA patient cells are facing increased stress due to loss of DNAJC19 there would be an expected global decrease in translation followed by an increase in translation of important proteins used in response to cellular stress (Pakos-Zebrucka et al., 2016). Additionally, syntaxin-2 (STX2) is used in trafficking and fusion of vesicles to the plasma membrane. Recently, STX2 has been identified to inhibit exocytosis of insulin granules which could impact

insulin signaling and alter metabolism in the heart (Bertrand et al., 2008; Kang et al., 2022). As for complement decay-accelerating factor (DAF), it dissociates C3/C5 convertases to inhibit activation of the complement cascade used in innate immunity (Heeger et al., 2005). Meanwhile, nectin-2 (NECT2) serves a role in regulation of immune responses due to interactions with certain immune receptors on various immune cells like T cells and natural killer cells (Molfetta et al., 2019). Thus, changes in DAF and NECT2 could be related to possible alterations in immune function that is suspected in some patients with DCMA (Machiraju et al., 2022). Considering the function of these proteins and how they are shared between cells from patients with mild and severe cardiac phenotypes, they would also be compelling candidates for further validation.

I then sought to determine whether DNAJC19 deficiency impacted other DnaJ proteins or heat shock proteins. However, only DNAJB2 (Figure 23) was significantly downregulated. DNAJB2 serves to help degrade proteins through the ubiquitin-proteasome system through interactions with Hsp70 in the cytosol (Kampinga & Craig, 2010). My data also suggested that Hsp70, also known as HSP72, was slightly decreased in patient cells, although this was not statistically significant (Figure 25). This could indicate an inability to degrade misfolded proteins in the cytosol which could contribute to ER stress and activation of various stress responses likes the ISR. Other than DNAJB2, DNAJC3 was slightly increased in patient cells, however, this was not statistically significant. Nonetheless, this was interesting because DNAJC3 is a co-chaperone to BiP which is critical for regulating the UPR of the ER, a similar stress response to the UPRmt, and assists in protein folding within the cytosol (Frakes & Dillin, 2017). In addition, one study noted that increases in BiP protein levels corresponded with the terminal stage of a mouse model and represented prolonged activation of the UPRer (Kaspar et al., 2021). I, however, did not note

significant changes to protein levels for BiP (Figure 19). Alternatively, DNAJC3 itself is suggested to inhibit EIF2 signaling and allow attenuation of the stress response, preventing apoptosis (van Huizen et al., 2003). This would then suggest a beneficial role for DNAJC3 in preventing prolonged and maladaptive activation of cellular stress responses. While changes in these two DnaJ proteins could point towards alterations in cellular stress responses, they are insufficient to make any general conclusions about what is occurring in patient cells without further testing. In addition, there were no significant changes noted for any of the heat shock proteins identified in our dataset, despite HSP72 appearing to be greatly downregulated (Figure 25 & 25). These results would suggest that loss of DNAJC19 does not greatly affect other DnaJ proteins or heat shock proteins present in the cell. These results would also suggest that it is likely DNAJC19 that is responsible for the cellular changes that we observe in patient cells and not other DnaJ proteins nor heat shock proteins.

4.2 Activation of cellular stress responses within DCMA patient cells

Mitochondrial and ER stress have been known to impact cardiac function and have been implicated in the development of heart failure and cardiac dysfunction (Zhou & Tian, 2018). More specifically, within mitochondria, protein accumulation and misfolding can be detrimental to important mitochondrial functions such as formation and function of the electron transport chain (ETC) (Lévy et al., 2019). In turn, oxidative stress and perturbed ATP production are associated with heart failure and heart disease (Zhou & Tian, 2018). Unsurprisingly, multiple diseases that impact genes related to mitochondrial proteostasis present with cardiac involvement and cardiomyopathy (Wachoski-Dark et al., 2022). For example, combined oxidative phosphorylation deficiency 31 (COXPD31) presents with cardiomyopathy and results from

mutations impacting MIP which is involved in protein processing in mitochondria (Eldomery et al., 2016). When mitochondrial proteostasis is perturbed the cell activates certain stress responses like the UPRmt as a way to mitigate damage and restore mitochondrial function (Melber & Haynes, 2018). Thus, if deficiency of DNAJC19 impacts mitochondrial function, particularly through perturbed proteostasis, we would anticipate activation of the UPRmt.

As for the ER, it plays a pivotal role in protein synthesis, folding, and translocation. Thus, ER stress resulting from protein accumulation or misfolding can be detrimental to the cell and has been associated with heart failure (Wang et al., 2018). In addition, the ER is involved in transporting calcium to mitochondria which is involved in cardiomyocyte contractility, apoptosis, cell secretion, and cell migration (Sutanto et al., 2020). The ER also serves to synthesize most lipids including sterols, phosphatidylcholine, phosphatidylinositol, and phosphatidylserine, which are required to be imported into mitochondria (Flis & Daum, 2013). More recently, a study reported increased ER stress and increased sensitivity to apoptosis in a murine model of Barth Syndrome, a mitochondrial disease similar to DCMA (Sohn et al., 2022). They hypothesize that the accumulation of monolysocardiolipin and decrease in cardiolipin present in Barth Syndrome may be due to perturbed crosstalk between mitochondria and the ER (Sohn et al., 2022). This would disrupt mitochondrial import of phosphatidyl acid which is used to make cardiolipin. Thus, it is apparent that the ER and mitochondria are closely linked, wherein dysfunction in one organelle can greatly impact the other. This becomes important when we consider deficiency of DNAJC19 and how it may impact mitochondrial proteostasis and lead to upregulation of certain cellular stress responses like the ISR and UPRmt through EIF2 signaling.

The integrated stress response is a broad cellular response to numerous stressors (Pakos-Zebrucka et al., 2016). This means that there are numerous genes that can be activated depending

on the stress that the cell is facing. Considering predicted upregulation of EIF2 signaling and the suspected role of DNAJC19 in protein import, I wanted to investigate activation of the two stress responses mediated by this pathway: the ISR and the UPRmt. To do so, I used RT-qPCR to analyze gene expression levels for a subset of genes involved in either of these two stress responses. For the ISR, I chose a subset of genes that are activated by various conditions. The most important gene for analysis of the ISR became *ATF4* as it is the key regulator (Costa-Mattioli & Walter, 2020). Genes that assist during protein limitation or protein accumulation are *ASNS* and *CHOP* (Balasubramanian et al., 2013). *HMOX1* is an antioxidase that assists during oxidative stress (Dey et al., 2015). More broadly, *XBP1* is similar to *ATF4* in that it will regulate a number of other downstream targets, particularly various chaperones and proteases (Pakos-Zebrucka et al., 2016; Park et al., 2021). Lastly, *TRIB3* encodes a downstream product that inhibits activation of *ATF4* through a negative feedback loop, thereby terminating the ISR (Pakos-Zebrucka et al., 2016).

The integrated stress response is believed to be necessary for activation of the UPRmt (Melber & Haynes, 2018). Within the UPRmt, *CHOP*, *ATF4*, and *ATF5* are key regulators and are required for regulation of other downstream genes (Melber & Haynes, 2018). Thus, when choosing which genes to assess for activation of the UPRmt it became important to include notable genes used in both the ATF5 and the CHOP branches. ATF5 regulates *LONP1* which encodes the well-known LONP1 protease, and, *mtHsp70*, which encodes mtHsp70, a subunit that is involved in protein refolding but also serves a role in protein import via the TIM23 complex which includes DNAJC19 (Fiorese et al., 2016). For the CHOP branch both *Hsp10* and *Hsp60* are key genes that encode subunits of the HSP60 complex which serves as a chaperone to refold proteins (Horibe & Hoogenraad, 2007). Meanwhile, *CLPP*, also regulated by CHOP, serves

protease functions (Zhao et al., 2002). Understanding what upregulation of the UPRmt looked like in terms of expression levels for these genes was important to then understanding whether the UPRmt was activated in patient cells.

DNP serves as a direct mitochondrial membrane uncoupler by promoting the leaking of protons across the IMM, dissipating the mitochondrial membrane potential (Yoneda et al., 2004). While a direct link between mitochondrial membrane potential and the UPRmt is not explicitly clear, the UPRmt is known to be activated under a myriad of conditions, such as, accumulation of misfolded proteins, impaired OXPHOS, and increases in ROS (Lin & Haynes, 2016). Notably, many of these conditions can deplete the mitochondrial membrane potential but are not associated with complete depolarization. In addition, it has been shown that mitochondrial membrane depolarization is not necessary for activation of the UPRmt as one study found that PINK1 accumulation independent of changes in the mitochondrial membrane potential resulted in activation of the UPRmt (Jin & Youle, 2013). Alternatively, one study noted that dissipation of the mitochondrial membrane potential resulted in increases in *LONP1* expression in an ATF5-dependent manner (Fiorese et al., 2016). Thus, while not considered necessary for activation, changes in the mitochondrial membrane potential can impair mitochondrial function and activate the UPRmt. Other laboratories have noted increases in expression of genes involved in the UPRmt following treatment with 500 µM of DNP (personal communication). Similarly, treating healthy control fibroblasts with 500 µM of DNP increased gene expression for most genes involved in the UPRmt for both the ATF5 branch and the CHOP branch, suggesting DNP can be used as a positive control for the UPRmt in mammalian cells (Figure 28 & Figure 29). As we expect that UPRmt activation follows activation of the ISR, treating health control cells with

DNP also resulted in the activation of certain ISR genes (Figure 27). Overall, our results indicate that DNP works as a positive control for both activation of the UPRmt and the ISR in fibroblasts.

Notably, DNP also serves to cause upregulation of the heat shock response, a stress response that increases molecular chaperones, preventing protein aggregation and assisting in refolding (Jolly & Morimoto, 2000). This response is similar to the UPRmt and the ISR, but differs as it is activated upon numerous insults that are nonspecific to locations within the cell, such as temperature changes, infections, respiratory chain uncoupling, and more (Richter et al., 2010). Indeed, upon addition of DNP to control cells, as mentioned previously, we saw significant upregulation of genes involved in the UPRmt and the ISR (Figure 27, 27, 28). However, addition of DNP at the same concentration to patient cells did not elicit a greater increase than what was already observed in untreated patient cells (Figure 27, 27, 28). Notably only *LONP1*, *HMOX1* and *CLPP* showed significant increases in gene expression following treatment (Figure 27, 27, 28). Interestingly, both *LONP1* and *HMOX1* did not show significant increases prior to treatment. The fact that these two genes are still able to be upregulated in patient cells would suggest that they are still capable of serving a functional role. However, these genes may be less important in the maintenance of the mitochondrial proteome following DNAJC19 deficiency and more important when addressing the stress caused by addition of DNP. Nonetheless, while most genes do not show increases in expression following treatment, this would suggest that patient cells are already at the maximum stress response. Due to mitochondria already facing stress, it is possible that addition of DNP does not further increase mitochondrial stress and thus does not result in a greater increase like what is seen in control cells.

The concept of a maximum response to stress is not foreign, as studies have shown that increasing the dose of DNP in yeast above a certain threshold resulted in a decrease in the heat

shock response which they postulate to be due to severe damage preventing all metabolic processes including protein synthesis (Weitzel et al., 1985). Alternatively, there have been studies that show cross-tolerance in stress responses (Wheeler & Wong, 2007). Particularly, cross-tolerance has been observed wherein primary exposure to stress, could then lead to resistance to subsequent stress that is different from the primary. In the case of what has been observed with the heat shock response, initial induction of this response has conferred protection against nitric oxide, hydrogen peroxide, and IR injury (Wheeler & Wong, 2007). Thus, the reverse could be happening in patient cells with DCMA, wherein their genetic mutation resulting in mitochondrial stress has allowed for cross-tolerance to the heat shock response following addition of DNP. Thus, while the exact reason as to why addition of DNP to patient cells does not result in the same increase in gene expression for control cells is unknown, it is likely in part due to patient cells already facing cellular stress.

When looking at activation of the UPRmt and the ISR in cells from patients with mild DCMA, there were no significant changes in gene expression for the key regulators *CHOP* or *ATF4* (Figure 28 & Figure 29). The only genes to show significant changes in expression were *Hsp60* and *CLPP* (Figure 29). Despite most genes not changing significantly, there did appear to be a step-wise increase in expression for the majority of genes, including the three key regulators. Nonetheless, these results suggest that cells taken from patients with mild DCMA are not undergoing significant protein stress or accumulation to warrant activation of the ISR and the UPRmt. While this does not necessarily mean that mitochondrial proteostasis is not perturbed due to deficiency of DNAJC19 in mild patient phenotypes, it suggests that any protein accumulation is insufficient to cause activation of the UPRmt or the ISR. This could be due to the aggregation of misfolded proteins being low enough to be addressed by the necessary cellular

machinery, or other compensatory mechanisms at work, such as DNAJC15 (Sinha et al., 2016). DNAJC15 is similar to DNAJC19, in that they both interact with mtHsp70, but form independent complexes (Sinha et al., 2016). However, loss of DNAJC19 results in increased cell mortality, while loss of DNAJC15 had minimal impacts on cell viability, suggesting a dispensable role (Sinha et al., 2016). While DNAJC15 is considered to have a non-essential role for cell survival, it could still compensate for deficiency of DNAJC19 in patient cells.

Using cells from patients with severe DCMA, there was significant upregulation of *ATF4*, *XBP1*, *CHOP* and *ASNS* within the ISR (Figure 27). From these results we can conclude that the severe patient phenotype results in sufficient stress to elicit the broad response of the ISR. In addition, I was able to identify some of the proteins encoded by these genes in the proteomic data, such as HMOX1 and ASNS (Figure 21). However, these proteins did not show changes like observed with gene expression. It is important to note that these are only two out of a larger set of genes that were investigated, and protein abundance does not always follow gene expression due to a variety of reasons. Unlike the gene expression data that suggested *HMOX1* decreased, albeit this was not statistically significant, proteomic data showed a slight increase in HMOX1 (Figure 21). A loss or downregulation in *HMOX1* could mean a cellular inability to respond to oxidative stress. However, considering that we see upregulation of this gene following DNP treatment, this would suggest that the cell would still be able to respond via upregulation of *HMOX1* if needed (Yachie, 2021). Meanwhile ASNS was slightly increased in our proteomic data, but it was not considered significant like the increase in gene expression data (Figure 21). Despite two proteins in our proteomic data not perfectly matching our gene expression data, the number of genes identified along with the consistent changes observed in cells from patients with severe DCMA suggests activation of the ISR.

Further investigation into why the ISR is activated and specifically what subsequent genes are upregulated is important to better understanding the role of DNAJC19. For example, *XBP1* upregulates other genes involved in protein folding and vesicular trafficking (Byrd et al., 2012). In addition, *ASNS* is involved in protein limitation and known to be upregulated during protein accumulation (Balasubramanian et al., 2013). Thus, increases in *ASNS* and *XBP1* in our dataset points towards errors in protein handling as being one possible reason for activation of the ISR. However, we must consider that these genes serve a role in ER stress rather than mitochondrial stress. Thus, it is likely that deficiency of DNAJC19 impacts more than mitochondria, or that mitochondrial stress is sufficient to signal to various kinases to activate the ISR, such as GCN2, PERK or HRI (Mick et al., 2020).

One study found that inhibition of complex I of the ETC was sufficient to trigger the ISR through the GCN2 kinase in response to asparagine deficiency, indicating that mitochondrial events can result in broad activation of the ISR (Mick et al., 2020). Further outlining the unique connection between mitochondria and the ISR is the fact that under mitochondrial stress, GCN2 again, serves to regulate protein synthesis within the cytosol, limiting the import of proteins into mitochondria (Melber & Haynes, 2018). This allows mitochondrial machinery to focus on addressing misfolded and aggregated proteins. While I did not identify GCN2, when investigating the proteomic data, I did identify PKR as one kinase present in the dataset. As anticipated, levels of PKR were stable between control and patient cells (Figure 21). PKR is an activating kinase of the ISR that is activated following viral infection, and as we anticipate loss of DNAJC19 to impact proteostasis, I would not expect PKR to be responsible for the activation of the ISR (Pakos-Zebrucka et al., 2016). Instead, I would expect GCN2 for reasons previously mentioned. Alternatively, PERK responds to unfolded proteins in the ER and thus could be an

activating kinase for the ISR during DNAJC19 deficiency (Costa-Mattioli & Walter, 2020). Though another likely candidate would be HRI as it has been shown to relay mitochondrial stress to the cytosol to trigger the ISR (Girardin et al., 2021). However, further studies would need to be done to determine which kinases are at work within the ISR following deficiency of DNAJC19.

From this, I then looked towards the UPRmt in cells collected from patients with severe DCMA. There was upregulation of *ATF4*, *ATF5*, *CHOP*, *mtHsp70* and *CLPP* (Figure 28 & Figure 29). While there were no significant increases in gene expression for *LONP1*, *Hsp10*, or *Hsp60*, these are downstream targets of the UPRmt and only a small subset of potential genes that are regulated by ATF5 and CHOP. In addition, the proteomic data did not identify significant changes in LONP1 or Hsp60 protein abundance (Figure 20). While LONP1 is understood to be critically important for cell survival, overexpression is also considered detrimental leading to poor mitochondrial respiration and excessive degradation of ETC complexes (Venkatesh et al., 2019; Zurita Rendón & Shoubridge, 2018). Thus, while it is unclear why *LONP1* does not increase like the other genes, one possible reason could be that preventing overexpression of *LONP1* serves to maintain mitochondrial energetics during deficiency of DNAJC19. Beyond this, upregulation of *Hsp60* has been noted to be detrimental in human neuroblastoma cells from patients with Alzheimer's disease, meanwhile a loss of Hsp60 resulted in a loss of mitochondrial proteostasis and heart failure in a mouse model (Fan et al., 2020; Veereshwarayya et al., 2006). Thus, maintenance of Hsp60 protein and gene expression levels appear to be important for mitochondrial proteostasis. However, we do not see any significant changes in gene expression, nor protein abundance for Hsp60, which could indicate that it is being maintained and is simply not a necessary chaperone for the type of mitochondrial

dysfunction caused by DNAJC19 deficiency. In addition, following treatment with DNP, control cells show increased gene expression for both *LONP1* and *Hsp60*, which could indicate that their upregulation is more important for a different type of mitochondrial stress, such as that caused by direct mitochondrial membrane uncoupling (Figure 28 & 28). *LONP1* also increased in patient cells following treatment with DNP (Figure 28D), thus, perhaps untreated patient cells are not faced with sufficient stress to warrant upregulation of *LONP1*. While not every gene that was investigated was upregulated, the upregulation we see in *ATF5*, *CHOP*, and *ATF4*, coupled with the upregulation of some of the downstream targets is sufficient to say that the UPRmt is indeed activated within cells from patients with severe DCMA.

The UPRmt is upregulated to respond to a very specific type of stress that is due to errors in protein handling compromising mitochondrial proteostasis. These errors in protein handling can encompasses processes related to protein import, localization, or folding (Anderson & Haynes, 2020). Therefore, activation of the UPRmt would suggest that cells from patients with severe DCMA are facing difficulty with maintenance of mitochondrial proteostasis. Our results indicating activation of the UPRmt in cells from patients with a severe phenotype point to a more specific role for DNAJC19 in mitochondrial proteostasis, wherein loss of this protein is sufficient to trigger the UPRmt. Thus, activation of the UPRmt in patient cells would support classifying DCMA as a disease of mitochondrial proteostasis. However, further work would need to be done to elicit the specific role of DNAJC19 in mitochondrial proteostasis, whether that role be in protein import like previously suggested (Davey et al., 2006) or in other processes.

While activation of the UPRmt and the ISR are generally considered to be beneficial, prolonged activation can become maladaptive (Fulda et al., 2010). In fact, aspects of the UPRmt and the ISR have been implicated in heart failure and other diseases that present with cardiac

dysfunction. However, these two stress responses have also been shown to be cardioprotective, indicating that they can serve a dual role in the progression and amelioration of cardiac dysfunction depending on circumstances. For example, pharmacological intervention with the tyrosine kinase inhibitor, sunitinib, leads to activation of *XBP1*, which has been shown to alleviate ER stress (Korennykh et al., 2009). ER stress is associated with hypertension and different forms of cardiomyopathy, such as congenital dilated cardiomyopathy, and heart failure (Hamada et al., 2004; Okada et al., 2004). Additionally, TUDCA, a compound that has been shown to refold proteins and reduce ER stress, has been shown to improve cardiomyocyte contractility in a mouse model wherein ER stress was induced following oxidative stress (Guo et al., 2009). From this, it is evident that the ISR and subsequent reduction of ER stress, serves a cardioprotective role. However, aspects of the ISR have also been considered maladaptive, such as increases in PERK leading to increased susceptibility to arrhythmias and causing abnormal increases in intracellular calcium (Liu et al., 2014). Similarly, knockdown of various ISR kinases, such as PKR reduced myocardial fibrosis and proapoptotic factors while maintaining left ventricular function, protecting against heart failure (Wang et al., 2014).

As for the UPRmt, enhanced induction of this stress response using the chemical compound isoproterenol reduced mitochondrial dysfunction and preserved cardiomyocyte viability in a murine model subject to chronic pressure overload (Smyrnias et al., 2019). Similarly, LONP1 was considered to be protective in a murine model of cardiac ischemia-reperfusion injury (Venkatesh et al., 2019). Despite some studies showing that the UPRmt can be beneficial against cardiac dysfunction, there are multiple studies showing harmful effects of UPRmt components on the heart. One such study found that deletion of CLPP, actually reduced mitochondrial cardiomyopathy in a murine model facing proteostatic stress (Seiferling et al.,

2016). However, this same study noted that loss of CLPP did not impact the rest of the UPRmt signaling, indicating that while CLPP plays a role in the UPRmt, it is not required for UPRmt signaling (Seiferling et al., 2016). Another study found that increased localization of Hsp60 to the cell surface corresponded with the progression of heart failure in both a murine model and in human explanted failing hearts. This increase in cell surface localization correlated with increased apoptosis. Thus, the authors of this study suggest that abnormal distribution of Hsp60 may aid in the progression of heart failure (Lin et al., 2007).

From this, it is apparent that the type of stress the cell is facing, as well as which components of the ISR and UPRmt are activated, may impact whether these stress responses are serving adaptive or maladaptive roles. Nonetheless, it is apparent that the ISR and the UPRmt are closely linked to cardiac disease, heart failure, and cardiomyopathy, making them important cellular responses to study in the context of both mitochondrial disease and diseases with heavy cardiac involvement.

4.3 Testing of potential therapeutics

Next, I looked to see if the stress response in patient fibroblasts could be ameliorated or exacerbated using various toxins or therapeutics. SS-31 is a therapeutic that has been shown to ameliorate mitochondrial dysfunction through reduction of ROS, prevention of apoptosis, and prevention of lipid peroxidation (Szeto, 2014). In addition, SS-31 has been shown to attenuate oxidative stress in a number of studies (Escribano-López et al., 2019; Hou et al., 2016; Lightfoot et al., 2015). One study found that SS-31 was able to normalize total cardiolipin and improve left ventricular function in canines with microembolization-induced heart failure (Sabbah et al., 2016). Meanwhile, SS-31 administered to a porcine model of renovascular hypertension found

that following treatment, cardiomyocyte hypertrophy was reduced, ROS production decreased, and mitochondrial respiration increased (Eirin et al., 2016).

Given the ability of SS-31 to restore mitochondrial function and improve the CL profile, it has been suggested to be a potential therapeutic for the treatment of Barth syndrome, a disorder that presents similarly to DCMA (Sabbah, 2022). In fact, a murine model of Barth syndrome was recently treated with SS-31 wherein mitochondrial respiratory capacity and supercomplex formation was increased (Russo et al., 2022). However, the ratio of MLCL/CL did not change, suggesting that SS-31 does not directly impact CL, rather it likely influences the respiratory chain (Russo et al., 2022). Of particular interest to us, SS-31 has been used to treat DCMA patient cells and proven beneficial to reduce mitochondrial fragmentation and restore the OPA1 isoform ratio necessary for maintenance of mitochondrial fusion (Machiraju et al., 2019; Rohani et al., 2020). As mitochondrial morphology is closely tied to mitochondrial function and dysfunction (Karbowski & Youle, 2003), SS-31 may be useful to reduce cellular stress responses like the UPRmt and the ISR. In addition, SS-31 has been shown to reduce ER stress which is closely linked to mitochondrial stress as well as the ISR (Escribano-López et al., 2019).

Following treatment with 100 µM of SS-31, gene expression levels in patient cells for the ISR and the UPRmt were reduced close to control levels. *ATF4* and *XBP1* were the only genes for the ISR that showed significant reduction in expression between treated and untreated fibroblasts from patients with severe DCMA, however, all other genes did return close to control levels (Figure 27C & Figure 28A). For example, *ASNS* did not show significant changes between treated and untreated groups; however, when compared to controls there were no significant difference in treated patient fibroblasts (Figure 27A). As for *TRIB3*, gene expression was not significantly increased in untreated cells, and following treatment there was still no increase

(Figure 27D). These results suggest that SS-31 can attenuate gene expression of the ISR. However, it is apparent that SS-31 was not as effective for attenuation of the ISR as it was for the UPRmt (Figure 27, 27 & 28). This could perhaps be explained by the localization of SS-31 to the IMM. If there is stress outside of mitochondria that contributes to ISR activation, then SS-31 is likely unable to mitigate such stress and thus is less effective for the ISR.

Following treatment with SS-31 cells from both mild and severe patient phenotypes showed significant changes in gene expression (Figure 28 & Figure 29). Both regulators, *ATF5* and *CHOP* showed significant reductions in gene expression in cells from patients with severe DCMA, along with *CLPP* and *mtHsp70* (Figure 28 & Figure 29). As for cells from patients with mild DCMA, there was a decrease in expression of *ATF5* and *CLPP*. These results show that through addressing oxidative stress and mitochondrial dysfunction using SS-31 there is downregulation in the activation of genes involved in the UPRmt (Figure 35). Our results have been supported in part by previous work that shows SS-31 attenuates *CHOP* gene expression levels (Escribano-López et al., 2019). However, further work on SS-31 as a potential therapeutic to reduce mitochondrial stress in DCMA will be required.

Tauroursodeoxycholic acid (TUDCA) is a taurine conjugate of ursodeoxycholic acid (UDCA). UDCA has been approved by the Food and Drug Administration in the United States for the treatment of certain cholestatic liver diseases as it can protect hepatocytes from hydrophobic bile acids (Kumar & Tandon, 2001). While TUDCA has also been shown to be protective against hydrophobic bile acids, more recently it has been investigated as a potential therapeutic for numerous non-liver diseases (Vang et al., 2014). This is due to TUDCA being shown to prevent UPR activation and ER stress by increasing protein folding and preventing apoptosis through interactions with mitochondria (Omura et al., 2013; Paridaens et al., 2017).

For example, treating mouse models of Alzheimer's disease with TUDCA reduced amyloid-β deposits in the brain and neuronal apoptosis (Lo et al., 2013; Nunes et al., 2012). TUDCA has also been shown to limit ROS production and protect against mitochondrial dysfunction in animal models of Parkinson's disease (Moreira et al., 2017; Rosa et al., 2017). Specifically, TUDCA has been shown to prevent increases in CHOP protein during ER stress activation (Memme et al., 2016), but has also reduced mRNA levels of pro-apoptotic genes, serving as a preventative to apoptosis (Paridaens et al., 2017). In addition, TUDCA treatment reduced gene expression levels for *XBP1,* used in both the UPR of the ER and the ISR (Groenendyk et al., 2016). This compound also inhibits phosphorylation of eIF2α, which is necessary for activation of the ISR and subsequently necessary for activation of the UPRmt (Omura et al., 2013). As for mitochondria, treating rats with TUDCA, was shown to increase mitochondrial biogenesis and assist with ROS production through enhanced antioxidant responses (Soares et al., 2018). Other studies have also shown that TUDCA works to prevent apoptosis through inhibiting the swelling of mitochondria and the release of cytochrome *c* (Rodrigues et al., 2000). Thus, if TUDCA can inhibit the ISR and serve to ameliorate mitochondrial function, then it may also work to prevent activation of the UPRmt.

Following treatment with 100 µM of TUDCA, all genes investigated in the ISR were shown to be affected. There was a significant reduction in gene expression for *ATF4*, *ASNS,* and *XBP1*, which TUDCA is known to affect (Groenendyk et al., 2016), in cells from patients with severe DCMA (Figure 27). In addition, *HMOX1* which was found to be slightly decreased in untreated patient fibroblasts was increased back to control levels following treatment (Figure 27). These results show that TUDCA is quite effective for attenuating the expression of genes involved in the ISR and more effective than SS-31 at blocking ISR activation. This could be

explained by TUDCA working primarily in the cytosol, while SS-31 directly targets mitochondria (Figure 35). Thus, it is likely that changes in gene expression for the ISR following treatment with SS-31 are a result of feedback from mitochondrial stress being addressed rather than direct cytosolic interactions like TUDCA.

Beyond attenuation of the ISR, TUDCA was also effective in addressing the UPRmt. Following treatment with TUDCA gene expression was reduced close to control levels for all three regulators of the UPRmt and their downstream targets, *CLPP* and *mtHsp70*, in cells from patients with severe DCMA (Figure 28 & Figure 29). Thus, not only does TUDCA work to address ISR activation, but it also serves to mitigate upregulation of genes involved in the UPRmt. Considering that TUDCA primarily works through refolding proteins within the cytosol, this would suggest that targeting of misfolded proteins can then lead to downregulation of the ISR and subsequently the UPRmt (Figure 35). Together, these results support the classification of DCMA as a disease of mitochondrial proteostasis and identify TUDCA as a potential therapeutic for the treatment of this disease.

TUDCA served as a more likely candidate to attenuate activation of the ISR, while SS-31 was thought to be more likely to attenuate UPRmt activation as it is a mitochondrial targeting peptide. Targeting of mitochondrial dynamics including addressing mitochondrial fission has been a method of treating cardiac dysfunction and more specifically mitochondrial dysfunction (Huang et al., 2022). This is partially why SS-31 has been gaining traction as a potential therapeutic for the treatment of mitochondrial disease as it effectively targets mitochondria and ameliorates mitochondrial dynamics by restoring fragmentation (Rohani et al., 2020). However, we show that TUDCA may also serve as a novel therapeutic for the treatment of DCMA and other mitochondrial diseases.

Following treatment with TUDCA we saw reductions in proteins involved in mitochondrial fission in cells from patients with severe DCMA. Western blotting analysis revealed a significant increase in the pro-fission protein, Drp1, and a decrease in the ratio of L-OPA1:S-OPA1 isoforms which verified changes observed in the proteomic data (Figure 30). Following addition of TUDCA, Drp1 was reduced back to control levels and the isoform ratio of OPA1 was restored (Figure 30 & Figure 31). OPA1 has both a short and long isoform and alterations to the ratio of these isoforms is associated with increased mitochondrial fission or fusion (Anand et al., 2014). An increase in the long isoform is associated with mitochondrial fusion, while an increase in the short isoform leads to mitochondrial fission and has been associated with mitochondrial fragmentation (Wai et al., 2015). Upon western blotting analysis, indeed, the ratio of L-OPA1:S-OPA1 was altered in fibroblasts from patients with severe DCMA, showing a decrease in L-OPA1, confirming our proteomic data (Figure 31). Previous studies have shown that DCMA patient cells have an increased amount of S-OPA1 relative to L-OPA1, suggesting increased mitochondrial fission (Machiraju et al., 2019; Rohani et al., 2020). This imbalance in the OPA1 isoform ratio was then restored following addition of SS-31 (Machiraju et al., 2019; Rohani et al., 2020). In this study, I confirm the imbalance of the OPA1 isoform ratio with western blotting (Figure 31). However, I also show that TUDCA works to restore the balance of OPA1 isoforms (Figure 31). SS-31 likely restores changes to mitochondrial fission as it works to target mitochondrial dysfunction through harvesting ROS and addressing oxidative stress (Szeto & Schiller, 2011). TUDCA, however, likely impacts these proteins through indirect interactions with mitochondria, such as regulating upstream signaling. It is suggested that TUDCA works to upregulate numerous cytoprotective pathways, however, the exact mechanism behind this is still unclear (Rosa et al., 2017). Thus, it is possible that

through mitigation of cellular stress, through the addition of TUDCA, is sufficient to restore changes observed in proteins involved in mitochondrial membrane dynamics.

Next, I sought to exacerbate the cellular stress responses using 3-methylglutaconic acid (3-MGC). 3-MGC is an intermediate in the catabolism of mitochondrial leucine (Wortmann, Kluijtmans, et al., 2012). There are a variety of disorders called 3-methylglutaconic acidurias (3-MGA) which are characterized by elevated levels of 3-MGC in bodily fluids, and particularly the urine. Accumulation of this metabolite occurs in what is called primary 3-methylglutaconic acidurias (3-MGA) which disrupts leucine catabolism through defects in the 3-methylglutaconyl-CoA hydratase which converts 3-methylglutaconyl-CoA to 3-hydroxy-3-methylglutaryl-CoA (Wortmann et al., 2013; Wortmann, Kluijtmans, et al., 2012). However, secondary 3-MGAs do not arise due to errors in leucine catabolism. Rather it is suspected that perturbed phospholipid remodelling, such as in Barth syndrome, or defective OXPHOS and mitochondrial membrane organization are the cause for elevated levels of 3-MGC (Wortmann et al., 2013).

DCMA is a disorder of 3-MGA and as such a defining clinical characteristic is elevated levels of 3-MGC in bodily fluids (Wortmann, Vaz, et al., 2012). I considered that accumulation of 3-MGC may be detrimental to cellular functions and in part responsible for the elevated stress responses observed in patient cells. Interestingly, treatment of patient cells with 2.4μM of 3-MGC did not result in sufficient significant changes to gene expression for the ISR nor the UPRmt (Figure 27, 27 & 28). For example, *ASNS* showed a significant upregulation in fibroblasts from patients with severe DCMA following treatment with 3-MGC relative to untreated cells (Figure 27A). In addition, following treatment *HMOX1* expression significantly increased in cells from patients with mild and severe DCMA relative to untreated groups, however, this increase was not significant relative to control levels (Figure 27B). These results

coupled with no changes to *ATF4* after treatment suggest that the ISR is not upregulated beyond what was initially observed within untreated patient cells (Figure 28A). As for the UPRmt, *mtHsp70* showed an increase following treatment relative to untreated cells from patients with mild DCMA, while *LONP1* and *Hsp10* expression increased in treated cells from patients with severe DCMA (Figure 28 & Figure 29). However, without an increase in *ATF5* or *CHOP* and without consistent upregulation in cells from patients with either severe or mild DCMA, we cannot confidently suggest that 3-MGC exacerbates the UPRmt. Thus, these results indicate that elevated levels of 3-MGC are likely a by-product of cellular stress rather than a causal agent of cellular stress.

Understanding the importance of activation and attenuation of these stress responses could suggest another reason why some patients with DCMA have a much more severe phenotype. It is possible that cells from patients with severe DCMA are facing a greater deal of stress which cannot be as effectively addressed through upregulation of these stress response pathways. However, it is important to recognize that prolonged activation of these stress responses can be maladaptive and detrimental for the cell (Eisner et al., 2018). When cellular stress responses can no longer effectively respond to the stress either due to increased severity or prolonged activation, this results in cell death (Fulda et al., 2010). Thus, if patient cells are unable to offset the stress that has caused upregulation of the ISR or UPRmt, then there would be decreased energetics and a shift towards apoptosis (Anderson & Haynes, 2020).

Upon analysis of cytotoxicity and apoptosis, there were no significant changes observed in patient cells (Figure 32 & Figure 34). This would suggest that DCMA patient cells are not facing sufficient stress to cause upregulation of apoptosis, or they are able to address the stress in a timely manner with activation of the ISR and UPRmt. Nonetheless, it is likely that despite

upregulation of protective responses, there is still sufficient stress to cause changes to mitochondrial dynamics. This is evident through alterations in mitochondrial fission, and the identification of mitochondrial fragmentation noted in previous studies (Machiraju et al., 2019; Rohani et al., 2020). However, future work would need to be done to verify adaptive or maladaptive upregulation. I have shown two therapeutics that serve to attenuate activation of these stress responses but cannot say for certain whether these therapeutics act directly on the stress responses, or whether they first mitigate mitochondrial and ER dysfunction which subsequently downregulates the ISR and UPRmt.

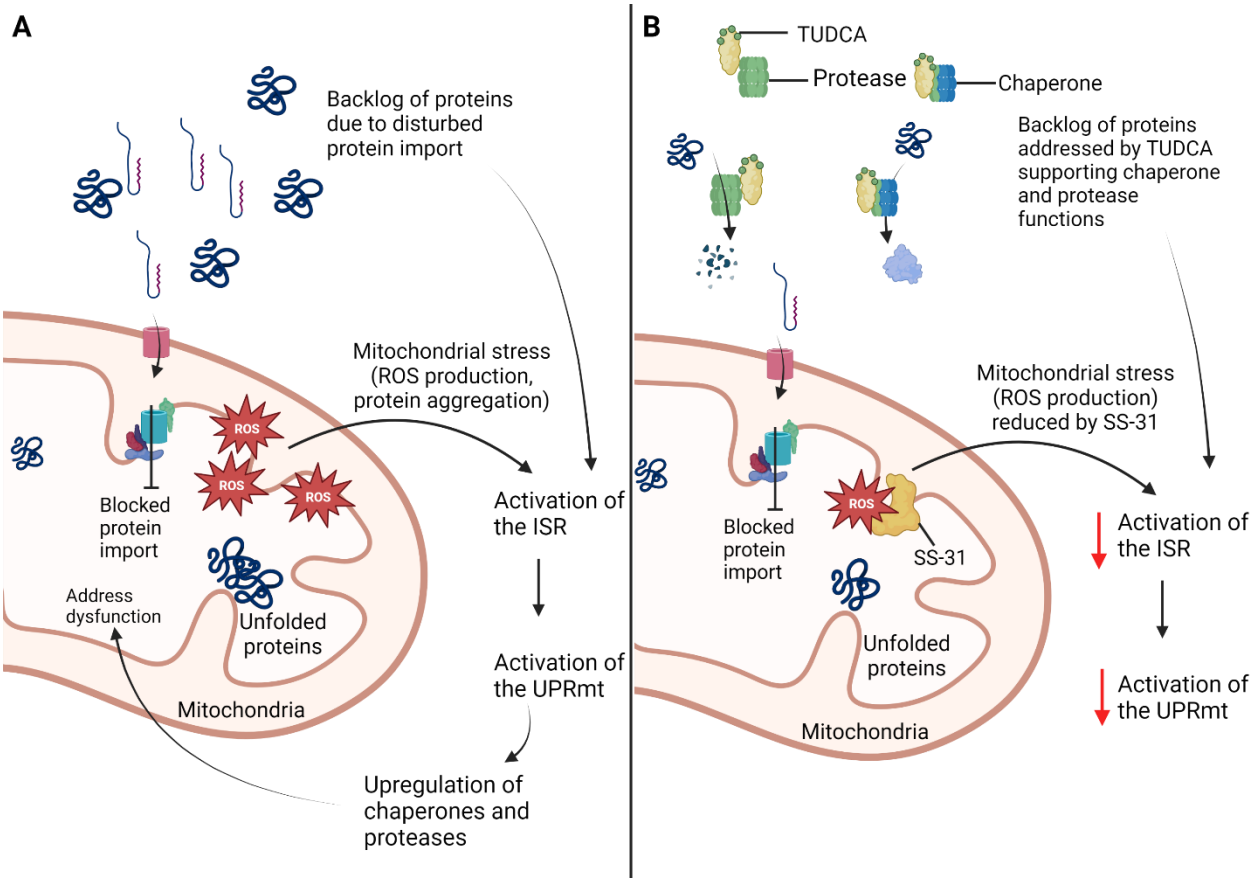

Figure 35. Potential interactions of SS-31 and tauroursodeoxycholic acid that alleviate mitochondrial dysfunction in DCMA patient cells. (A) Potential impacts to mitochondrial and cytosolic functions if DNAJC19 deficiency impairs mitochondrial protein import. (B) Mitigation of cytosolic and mitochondrial stress by addition of SS-31 and TUDCA. Created in BioRender.

4.4 Limitations

The major limitation to this project was the use of fibroblasts as a cellular model. Considering that DCMA greatly impacts the heart and other organs with high energy requirements, using a tissue specific cell-type such as cardiomyocytes would have been more useful. While the fibroblasts are patient-derived and thus recapitulate the patient's cellular phenotype, they have a low number of mitochondria per cell. This resulted in difficulties when trying to analyze the mitochondrial proteome. Due to the low number of mitochondria present per fibroblast the mitochondrial isolation was not as pure as it could have been. This resulted in terming the samples total protein isolates. However, without testing for enrichment of other organelles it cannot be stated with certainty that these isolates were total protein or enriched for other components rather than mitochondria. Nonetheless, the abundance of VDAC1 identified using 1D LC-MS/MS in total protein isolates along with low mitochondrial enrichment was indicative of poor mitochondrial purity. In addition, the western blotting data for VDAC1 in total protein isolates suggests varying success in how much mitochondria were isolated from each sample. This could contribute to the overall lower number of mitochondrial proteins present in the isolates. However, it is important to note that the samples submitted for 1D LC-MS/MS and those used for western blotting of VDAC1 were isolated over a year apart and were not the same samples. Thus, I cannot confirm whether the samples submitted for 1D LC-MS/MS would yield similar results if western blotting was performed for VDAC1. Nonetheless, these limitations meant that the data was representative of the total proteome and not the mitochondrial proteome. This meant that I could not accurately predict changes to the mitochondrial proteome and subsequent mitochondrial pathways due to the low number of mitochondrial proteins. In

addition, this also meant that less abundant mitochondrial proteins were difficult to identify in the dataset.

It was also assumed within this study that DNAJC19 was present in healthy control cells but deficient in patient cells; however, this was not confirmed. The inability to detect DNAJC19 within the dataset was likely due to fibroblasts having a low number of mitochondria, which when coupled with the variable success of mitochondrial isolation, made it difficult to detect. In addition, DNAJC19 is a protein in relatively low abundance, thus, the 1D LC-MS/MS performed with the samples submitted was likely not sensitive enough for small mitochondrial proteins. Future experiments should seek to improve the mitochondrial enrichment for samples that would be submitted for 1D LC-MS/MS. This could in part be done by verifying mitochondrial enrichment with western blotting prior to the submission of samples, to ensure amounts of mitochondrial proteins would be relatively consistent between samples and would provide the option to remove outliers with poor mitochondrial enrichment. This would provide better insight into the mitochondrial proteome rather than the entire proteome. This would also likely allow for better detection of smaller and less abundant mitochondrial proteins, such as DNAJC19. Thus, smaller changes would be detected which could be altering mitochondrial pathways that may have been missed using total protein. There are also alternative quantitative proteomic techniques which could be used such as DIA or TMT labelling along with true 2D-LC.

Another limitation for the analysis of the proteome of control and patient cells was the sample size used. We had a total of three biological replicates that were submitted in triplicate technical replicates for analysis. However, there was substantial variation between samples which likely resulted in many changes not being statistically significant. If the sample size were

to be increased, then standard error could have been decreased and some of the changes observed may have been more pronounced.

As for our gene expression analysis for determining upregulation of the ISR and UPRmt, this was an indirect measure. Coupling gene expression with RNA sequencing would provide further validation of my data and could identify additional genes of interest within each pathway. Similarly, I only analyzed a small subset of genes involved in the two stress responses, thus, increasing the number of genes analyzed would increase the confidence of my claims. However, while gene expression is one of the most common ways to determine activation of stress responses, there are other methods that could be used. For example, analysis of protein abundance for proteins encoded by various genes within these stress responses has been used to identify activation. Specifically, looking at phosphorylation of eIF2α has been a good measure of initial activation of the ISR. Meanwhile, investigation of translational attenuation and protein refolding/stability have also been used. However, it is important to note that I did assess multiple genes and the genes of interest within my study have been used in numerous other studies to show activation of these two pathways.

In addition, the control cell lines used within this study were from non-Hutterites, and thus may have differing genetics to cell lines isolated from healthy individuals within the Hutterite community. The DCMA patient and control cells also vary greatly in age and are comprised of cells from both male and female patients. Thus, I cannot conclude as to if any of the changes observed are due to differences in sex and/or age. Future work should therefore seek to determine whether there are age-related or sex-related differences between patient cells. Better understanding of age- and sex-related differences in DCMA could aid in formulating more

specific diagnostic criteria and therapeutic options which would allow for better diagnosis and treatment of this heterogenous disease.

4.5 Future Directions

Future experiments should seek to understand the roles that the ISR and UPRmt play in the progression of DCMA. It is well understood that prolonged activation of stress responses can be maladaptive and lead to further cellular dysfunction. Understanding whether these stress responses are serving an adaptive or maladaptive role could indicate whether targeting of these responses could be beneficial for patient care and longevity. For example, performing knockdown experiments in patient cells using *ATF4* or other key regulators of the ISR and UPRmt could indicate whether these stress responses are beneficial or maladaptive. In addition, determining which kinase is activated within DCMA patient cells would provide better insight into what is causing activation of the ISR and UPRmt. This could be done through knockdown experiments of each kinase and measuring eIF2α phosphorylation. These future experiments will increase our understandings of these stress responses could further elucidate the role of DNAJC19.

Understanding why these stress responses, and particularly a protein-based stress response, would be activated will help us to better understand and treat this disorder. Activation of the UPRmt suggests that there is mitochondrial dysfunction arising from perturbed mitochondrial proteostasis. Thus, looking at protein import and important proteins involved in preprotein processing and handling, such as other components of the TIM23 complex, will help to clarify the precise role of DNAJC19. This could be done using a direct protein import assay with radiolabeled proteins targeted to mitochondria. In addition, looking at what other proteins

DNAJC19 interacts with and confirming potential interacting partners of DNAJC19 in DCMA patient cells, such as PHB2 or mtHsp70 using co-immunoprecipitation assays would be beneficial as previous studies did not use patient cells.

In addition, considering that diseases impacting the heart often manifest differently for males and females, it is important that future studies look at sex differences in DCMA. Our study had an uneven distribution of sexes across patient and control cells, making it impossible to determine whether changes were related to patient sex. In addition, that majority of the patient cells were from infants, while two of the three control lines were taken from adults. This means that I could not determine any age-related changes between or within groups, nor rule out if the changes observed were resultant from differences in sex and/or age. Considering that patients have varying longevity, it will be important to understand what cellular changes are occurring that enable some patients to live longer than others. Thus, performing the same experiments but using cell lines from patients with the same sex and/or age will be beneficial in outlining whether the differences observed are consistent between age and sex, or whether there are changes.

To build from the experiments performed in this study, RT-qPCR was used to analyze gene expression for a subset of genes involved in the ISR or UPRmt. RNA sequencing would be beneficial to confirm the gene expression data and look for other genes involved in both the ISR and UPRmt. This would provide an additional method of verification and likely elicit new genes of interest that could be impacting the cellular ability to mitigate stress and the downstream consequences. Coupling this data with protein analysis to determine accumulation of ATF4 or other proteins encoded by the genes of interest would provide further validation. In addition, looking into abundance of the kinases involved in the ISR would provide insight into what type of stress is triggering activation of these stress responses. Beyond this, phosphorylation of eIF2α

has been shown to be a good indicator of cellular stress and ISR activation. Thus, performing western blotting for the phosphorylated subunit of eIF2α would be an additional indicator of activation of the ISR and would help verify if EIF2 signaling is indeed upregulated as predicted within the proteomic data.

Additionally, the proteomic data identified numerous pathways that could be investigated in greater detail to better understand the heterogeneity of the disease and to potentially identify new targets for therapeutic intervention. I identified 10 upregulated and 10 downregulated pathways using IPA. While EIF2 signaling was of the most interest in relation to activation of cellular stress responses, other pathways like DCM signaling or idiopathic pulmonary fibrosis signaling could be of interest. Particularly, further investigation into DCM signaling would provide insight into what proteins changes are impacting cardiac function and could identify individual proteins of interest for therapeutic treatment. Patients with DCMA have also been known to have respiratory issues. IPA identified idiopathic pulmonary fibrosis signaling as an impacted pathway that would lead to mitochondrial dysfunction and pulmonary fibrosis. While patients are not known to have pulmonary fibrosis, this signaling pathway may help elucidate what is causing respiratory issues within patients. Better understanding of pathways that are activated and affecting other organs beyond the heart becomes important when we seek to reduce patient morbidity and increase our understanding of systemic consequences that DNAJC19 deficiency has on the body. In addition, EIF2 signaling was predicted to impact glucose uptake which could be related to metabolic changes observed in DCMA patient cells. Thus, further investigation into the proteins involved in this pathway that suggested impaired glucose uptake may be useful for furthering our understanding of metabolic changes occurring within DCMA patient cells.

It should also be noted that because we assumed deficiency of DNAJC19, this should be validated to confirm our cellular models. While it is suggested that the mutations causing DCMA lead to truncation of the protein, there is the possibility that there is complete depletion of DNAJC19 in DCMA patient cells and this should be confirmed. To do so, performing western blotting for DNAJC19 could be done with a working antibody, or PCR could be another method of validation. In addition, looking at abundance of DNAJC15 and other import machinery may provide further validation of our experimental model.

Lastly, our findings of increased protein abundance related to mitochondrial membrane fission could be further validated by looking at a broader subset of proteins involved in the fission and fusion processes. In addition, testing TUDCA to see if it ameliorates mitochondrial fragmentation, like previous studies have shown with SS-31, would provide more conclusive findings for the role of TUDCA in mitochondrial morphology. It would also be interesting to see if there is a dose-dependent response for both TUDCA and SS-31, or if there is an optimal dose that is able to attenuate activation of the stress responses and address mitochondrial fission and fragmentation.

4.6 Conclusions

For the first time, I have shown that there are changes to the proteome of dermal fibroblasts isolated from patients with DCMA. I identify numerous pathways that are predicted to be altered from patients with severe and mild cardiac phenotypes. There are distinct differences between control and patient cells wherein the mild phenotype does not perfectly recapitulate either the control or the severe phenotype, suggesting that it is facing some of the same challenges that cells from the severe phenotype are but not to the same degree.

From analysis of the proteome, I identified several pathways classified as being involved in RNA processing, metabolism, and cellular stress. Upon closer analysis IPA predicted upregulation of EIF2 signaling indicating increased cellular stress in patient cells, along with decreased activation of DCM signaling suggesting cardiac dysfunction. Many pathways varied in the degree to which they were up- or down-regulated, suggesting differences between cells collected from patients with a mild or severe phenotype. These results suggest that while both cells from patients with mild and severe DCMA seem to be facing increased stress, they likely vary in the degree to which they experience stress and the resulting downstream consequences.

Looking at individually identified proteins, there was an increase in Drp1, while the ratio of OPA1 isoforms was decreased, suggesting a loss of fusion and a shift towards fission in cells from patients with severe DCMA. The changes observed in mitochondrial membrane dynamics do appear to be related to DNAJC19 deficiency and could be linked to increased cellular stress and could contribute to mitochondrial dysfunction leading to the patient phenotype.

Building on these observations which support previous work, I have identified novel increases in the expression of genes involved in two key cellular stress responses. The broad stress response of the ISR indicates that patient cells are facing some deal of stress, while upregulation of the UPRmt suggests that there is more specific protein-based stress within mitochondria. This suggests a role for DNAJC19 in mitochondrial proteostasis, as deficiency of this protein is sufficient to cause upregulation of the UPRmt. Previous work has identified increased mitochondrial fragmentation and fission, suggesting mitochondrial dysfunction. I show that the cause of that dysfunction may be related to maintenance of the mitochondrial proteome, hence upregulation of the UPRmt. Despite activation of these stress responses, it is apparent that

there is no apoptosis or cytotoxicity, suggesting these stress responses are serving their intended role to mitigate cellular stress in a timely manner.

In addition, I show that both the UPRmt and the ISR can be blocked using two therapeutics, TUDCA and SS-31. These are two therapeutics that work in different subcellular locations and their mechanisms of action vary greatly. Nonetheless, I show that targeting of the ISR with TUDCA is sufficient to cause reduction in activation of the UPRmt, identifying TUDCA as a potentially novel therapeutic for DCMA. Additionally, targeting of the UPRmt with SS-31 also works to cause reduction in activation of the ISR but not to the same degree. While SS-31 was previously shown to ameliorate mitochondrial morphology in DCMA patient cells, I show that TUDCA also works to address increased mitochondrial fission. Thus, I show that one can rescue the phenotype of cellular stress and mitochondrial fission with either TUDCA or SS-31. Better understanding of the mechanism of this disease and potential treatment options is necessary for improving the mortality and morbidity that those patients with DCMA experience.

References

Acehan, D., Vaz, F., Houtkooper, R. H., James, J., Moore, V., Tokunaga, C., Kulik, W., Wansapura, J., Toth, M. J., Strauss, A., & Khuchua, Z. (2011). Cardiac and skeletal muscle defects in a mouse model of human Barth syndrome. *The Journal of Biological Chemistry*, *286*(2), 899–908. https://doi.org/10.1074/jbc.M110.171439

Acehan, D., Xu, Y., Stokes, D. L., & Schlame, M. (2007). Comparison of lymphoblast mitochondria from normal subjects and patients with Barth syndrome using electron microscopic tomography. *Laboratory Investigation*, *87*(1), Article 1. https://doi.org/10.1038/labinvest.3700480

Adès, L. C., Gedeon, A. K., Wilson, M. J., Latham, M., Partington, M. W., Mulley, J. C., Nelson, J., Lui, K., & Sillence, D. O. (1993). Barth syndrome: Clinical features and confirmation of gene localisation to distal Xq28. *American Journal of Medical Genetics*, *45*(3), 327–334. https://doi.org/10.1002/ajmg.1320450309

Al Teneiji, A., Siriwardena, K., George, K., Mital, S., & Mercimek-Mahmutoglu, S. (2016). Progressive Cerebellar Atrophy and a Novel Homozygous Pathogenic DNAJC19 Variant as a Cause of Dilated Cardiomyopathy Ataxia Syndrome. *Pediatric Neurology*, *62*, 58–61. https://doi.org/10.1016/j.pediatrneurol.2016.03.020

Al Tuwaijri, A., Alyafee, Y., Alharbi, M., Ballow, M., Aldrees, M., Alam, Q., Sleiman, R. A., Umair, M., & Alfadhel, M. (2022). Novel homozygous pathogenic mitochondrial DNAJC19 variant in a patient with dilated cardiomyopathy and global developmental delay. *Molecular Genetics & Genomic Medicine*, *10*(8), e1969. https://doi.org/10.1002/mgg3.1969

Anand, R., Wai, T., Baker, M. J., Kladt, N., Schauss, A. C., Rugarli, E., & Langer, T. (2014). The i-AAA protease YME1L and OMA1 cleave OPA1 to balance mitochondrial fusion and fission. *The Journal of Cell Biology*, *204*(6), 919–929. https://doi.org/10.1083/jcb.201308006

Anderson, N., & Haynes, C. M. (2020). Folding the Mitochondrial UPR into the Integrated Stress Response. *Trends in Cell Biology*, *30*(6), 428–439. https://doi.org/10.1016/j.tcb.2020.03.001

Arrieta, A., Blackwood, E. A., Stauffer, W. T., & Glembotski, C. C. (2019). Integrating ER and Mitochondrial Proteostasis in the Healthy and Diseased Heart. *Frontiers in Cardiovascular Medicine*, *6*, 193. https://doi.org/10.3389/fcvm.2019.00193

Baker, M. J., Lampe, P. A., Stojanovski, D., Korwitz, A., Anand, R., Tatsuta, T., & Langer, T. (2014). Stress-induced OMA1 activation and autocatalytic turnover regulate OPA1-dependent mitochondrial dynamics. *The EMBO Journal*, *33*(6), 578–593. https://doi.org/10.1002/embj.201386474

Balasubramanian, M. N., Butterworth, E. A., & Kilberg, M. S. (2013). Asparagine synthetase: Regulation by cell stress and involvement in tumor biology. *American Journal of Physiology - Endocrinology and Metabolism*, *304*(8), E789–E799. https://doi.org/10.1152/ajpendo.00015.2013

Barth, P. G., Scholte, H. R., Berden, J. A., Van der Klei-Van Moorsel, J. M., Luyt-Houwen, I. E., Van 't Veer-Korthof, E. T., Van der Harten, J. J., & Sobotka-Plojhar, M. A. (1983). An X-linked mitochondrial disease affecting cardiac muscle, skeletal muscle and neutrophil leucocytes. *Journal of the Neurological Sciences*, *62*(1–3), 327–355. https://doi.org/10.1016/0022-510x(83)90209-5

Barth, P. G., Valianpour, F., Bowen, V. M., Lam, J., Duran, M., Vaz, F. M., & Wanders, R. J. A. (2004). X-linked cardioskeletal myopathy and neutropenia (Barth syndrome): An update. *American Journal of Medical Genetics. Part A*, *126A*(4), 349–354. https://doi.org/10.1002/ajmg.a.20660

Barth, P. G., Wanders, R. J., Vreken, P., Janssen, E. A., Lam, J., & Baas, F. (1999). X-linked cardioskeletal myopathy and neutropenia (Barth syndrome) (MIM 302060). *Journal of Inherited Metabolic Disease*, *22*(4), 555–567. https://doi.org/10.1023/a:1005568609936

Bauer, T. M., & Murphy, E. (2020). Role of Mitochondrial Calcium and the Permeability Transition Pore in Regulating Cell Death. *Circulation Research*, *126*(2), 280–293. https://doi.org/10.1161/CIRCRESAHA.119.316306

Becker, T., Guiard, B., Thornton, N., Zufall, N., Stroud, D. A., Wiedemann, N., & Pfanner, N. (2010). Assembly of the Mitochondrial Protein Import Channel. *Molecular Biology of the Cell*, *21*(18), 3106–3113. https://doi.org/10.1091/mbc.e10-06-0518

Becker, T., Vögtle, F.-N., Stojanovski, D., & Meisinger, C. (2008). Sorting and assembly of mitochondrial outer membrane proteins. *Biochimica et Biophysica Acta (BBA) - Bioenergetics*, *1777*(7), 557–563. https://doi.org/10.1016/j.bbabio.2008.03.017

Benson, M. D., Ferreira, P., & MacDonald, I. M. (2017). Oculomotor apraxia and dilated cardiomyopathy with ataxia syndrome: A case report. *Ophthalmic Genetics*, *38*(1), Article 1. https://doi.org/10.3109/13816810.2015.1137327

Bertero, E., & Maack, C. (2018). Metabolic remodelling in heart failure. *Nature Reviews. Cardiology*, *15*(8), 457–470. https://doi.org/10.1038/s41569-018-0044-6

Bertrand, L., Horman, S., Beauloye, C., & Vanoverschelde, J.-L. (2008). Insulin signalling in the heart. *Cardiovascular Research*, *79*(2), 238–248. https://doi.org/10.1093/cvr/cvn093

Birk, A. V., Chao, W. M., Bracken, C., Warren, J. D., & Szeto, H. H. (2014). Targeting mitochondrial cardiolipin and the cytochrome c/cardiolipin complex to promote electron transport and optimize mitochondrial ATP synthesis. *British Journal of Pharmacology*, *171*(8), Article 8. https://doi.org/10.1111/bph.12468

Birk, A. V., Liu, S., Soong, Y., Mills, W., Singh, P., Warren, J. D., Seshan, S. V., Pardee, J. D., & Szeto, H. H. (2013). The Mitochondrial-Targeted Compound SS-31 Re-Energizes Ischemic Mitochondria by Interacting with Cardiolipin. *Journal of the American Society of Nephrology : JASN*, *24*(8), Article 8. https://doi.org/10.1681/ASN.2012121216

Bolender, N., Sickmann, A., Wagner, R., Meisinger, C., & Pfanner, N. (2008). Multiple pathways for sorting mitochondrial precursor proteins. *EMBO Reports*, *9*(1), 42–49. https://doi.org/10.1038/sj.embor.7401126

Bonora, M., & Pinton, P. (2014). The Mitochondrial Permeability Transition Pore and Cancer: Molecular Mechanisms Involved in Cell Death. *Frontiers in Oncology*, *4*. https://www.frontiersin.org/article/10.3389/fonc.2014.00302

Byrd, A. E., Aragon, I. V., & Brewer, J. W. (2012). MicroRNA-30c-2* limits expression of proadaptive factor XBP1 in the unfolded protein response. *Journal of Cell Biology*, *196*(6), 689–698. https://doi.org/10.1083/jcb.201201077

Calkins, M. J., Manczak, M., Mao, P., Shirendeb, U., & Reddy, P. H. (2011). Impaired mitochondrial biogenesis, defective axonal transport of mitochondria, abnormal mitochondrial dynamics and synaptic degeneration in a mouse model of Alzheimer's disease. *Human Molecular Genetics*, *20*(23), 4515–4529. https://doi.org/10.1093/hmg/ddr381

Cao, Y.-L., Meng, S., Chen, Y., Feng, J.-X., Gu, D.-D., Yu, B., Li, Y.-J., Yang, J.-Y., Liao, S., Chan, D. C., & Gao, S. (2017). Mfn1 structures reveal nucleotide-triggered dimerization critical for mitochondrial fusion. *Nature*, *542*(7641), 372–376. https://doi.org/10.1038/nature21077

Chacinska, A., Koehler, C. M., Milenkovic, D., Lithgow, T., & Pfanner, N. (2009). Importing Mitochondrial Proteins: Machineries and Mechanisms. *Cell*, *138*(4), 628–644. https://doi.org/10.1016/j.cell.2009.08.005

Chang, C.-R., & Blackstone, C. (2010). Dynamic regulation of mitochondrial fission through modification of the dynamin-related protein Drp1. *Annals of the New York Academy of Sciences*, *1201*, 34–39. https://doi.org/10.1111/j.1749-6632.2010.05629.x

Chavez, J. D., Tang, X., Campbell, M. D., Reyes, G., Kramer, P. A., Stuppard, R., Keller, A., Zhang, H., Rabinovitch, P. S., Marcinek, D. J., & Bruce, J. E. (2020). Mitochondrial protein interaction

landscape of SS-31. *Proceedings of the National Academy of Sciences*. https://doi.org/10.1073/pnas.2002250117

Consolato, F., Maltecca, F., Tulli, S., Sambri, I., & Casari, G. (2018). M-AAA and i-AAA complexes coordinate to regulate OMA1, the stress-activated supervisor of mitochondrial dynamics. *Journal of Cell Science*, *131*(7), Article 7. https://doi.org/10.1242/jcs.213546

Costa-Mattioli, M., & Walter, P. (2020). The integrated stress response: From mechanism to disease. *Science (New York, N.Y.)*, *368*(6489), eaat5314. https://doi.org/10.1126/science.aat5314

Davey, K. M., Parboosingh, J. S., McLeod, D. R., Chan, A., Casey, R., Ferreira, P., Snyder, F. F., Bridge, P. J., & Bernier, F. P. (2006). Mutation of DNAJC19, a human homologue of yeast inner mitochondrial membrane co-chaperones, causes DCMA syndrome, a novel autosomal recessive Barth syndrome-like condition. *Journal of Medical Genetics*, *43*(5), Article 5. https://doi.org/10.1136/jmg.2005.036657

Dedkova, E. N., & Blatter, L. A. (2013). Calcium signaling in cardiac mitochondria. *Journal of Molecular and Cellular Cardiology*, *58*, 125–133. https://doi.org/10.1016/j.yjmcc.2012.12.021

Del Dotto, V., Mishra, P., Vidoni, S., Fogazza, M., Maresca, A., Caporali, L., McCaffery, J. M., Cappelletti, M., Baruffini, E., Lenaers, G., Chan, D., Rugolo, M., Carelli, V., & Zanna, C. (2017). OPA1 Isoforms in the Hierarchical Organization of Mitochondrial Functions. *Cell Reports*, *19*(12), 2557–2571. https://doi.org/10.1016/j.celrep.2017.05.073

Dey, S., Sayers, C. M., Verginadis, I. I., Lehman, S. L., Cheng, Y., Cerniglia, G. J., Tuttle, S. W., Feldman, M. D., Zhang, P. J. L., Fuchs, S. Y., Diehl, J. A., & Koumenis, C. (2015). ATF4-dependent induction of heme oxygenase 1 prevents anoikis and promotes metastasis. *The Journal of Clinical Investigation*, *125*(7), 2592–2608. https://doi.org/10.1172/JCI78031

Dietl, A., & Maack, C. (2017). Targeting Mitochondrial Calcium Handling and Reactive Oxygen Species in Heart Failure. *Current Heart Failure Reports*, *14*(4), 338–349. https://doi.org/10.1007/s11897-017-0347-7

Doan, K. N., Grevel, A., Mårtensson, C. U., Ellenrieder, L., Thornton, N., Wenz, L.-S., Opaliński, Ł., Guiard, B., Pfanner, N., & Becker, T. (2020). The Mitochondrial Import Complex MIM Functions as Main Translocase for α-Helical Outer Membrane Proteins. *Cell Reports*, *31*(4), 107567. https://doi.org/10.1016/j.celrep.2020.107567

Dudek, J., Hartmann, M., & Rehling, P. (2019). The role of mitochondrial cardiolipin in heart function and its implication in cardiac disease. *Biochimica et Biophysica Acta (BBA) - Molecular Basis of Disease*, *1865*(4), 810–821. https://doi.org/10.1016/j.bbadis.2018.08.025

Dudek, J., Rehling, P., & van der Laan, M. (2013). Mitochondrial protein import: Common principles and physiological networks. *Biochimica et Biophysica Acta (BBA) - Molecular Cell Research*, *1833*(2), 274–285. https://doi.org/10.1016/j.bbamcr.2012.05.028

Duncan, A. L. (2020). Monolysocardiolipin (MLCL) interactions with mitochondrial membrane proteins. *Biochemical Society Transactions*, *48*(3), 993–1004. https://doi.org/10.1042/BST20190932

Ehses, S., Raschke, I., Mancuso, G., Bernacchia, A., Geimer, S., Tondera, D., Martinou, J.-C., Westermann, B., Rugarli, E. I., & Langer, T. (2009). Regulation of OPA1 processing and mitochondrial fusion by m-AAA protease isoenzymes and OMA1. *The Journal of Cell Biology*, *187*(7), Article 7. https://doi.org/10.1083/jcb.200906084

Eirin, A., Ebrahimi, B., Kwon, S. H., Fiala, J. A., Williams, B. J., Woollard, J. R., He, Q., Gupta, R. C., Sabbah, H. N., Prakash, Y. S., Textor, S. C., Lerman, A., & Lerman, L. O. (2016). Restoration of Mitochondrial Cardiolipin Attenuates Cardiac Damage in Swine Renovascular Hypertension. *Journal of the American Heart Association*, *5*(6), e003118. https://doi.org/10.1161/JAHA.115.003118

Eisner, V., Picard, M., & Hajnóczky, G. (2018). Mitochondrial dynamics in adaptive and maladaptive cellular stress responses. *Nature Cell Biology*, *20*(7), Article 7. https://doi.org/10.1038/s41556-018-0133-0

Eldomery, M. K., Akdemir, Z. C., Vögtle, F.-N., Charng, W.-L., Mulica, P., Rosenfeld, J. A., Gambin, T., Gu, S., Burrage, L. C., Al Shamsi, A., Penney, S., Jhangiani, S. N., Zimmerman, H. H., Muzny, D. M., Wang, X., Tang, J., Medikonda, R., Ramachandran, P. V., Wong, L.-J., … Sutton, V. R. (2016). MIPEP recessive variants cause a syndrome of left ventricular non-compaction, hypotonia, and infantile death. *Genome Medicine*, *8*, 106. https://doi.org/10.1186/s13073-016-0360-6

El-Hattab, A. W., & Scaglia, F. (2016). Mitochondrial Cardiomyopathies. *Frontiers in Cardiovascular Medicine*, *3*. https://www.frontiersin.org/article/10.3389/fcvm.2016.00025

Elouil, H., Bensellam, M., Guiot, Y., Vander Mierde, D., Pascal, S. M. A., Schuit, F. C., & Jonas, J. C. (2007). Acute nutrient regulation of the unfolded protein response and integrated stress response in cultured rat pancreatic islets. *Diabetologia*, *50*(7), 1442–1452. https://doi.org/10.1007/s00125-007-0674-4

Escribano-López, I., de Marañon, A. M., Iannantuoni, F., López-Domènech, S., Abad-Jiménez, Z., Díaz, P., Solá, E., Apostolova, N., Rocha, M., & Víctor, V. M. (2019). The Mitochondrial Antioxidant SS-31 Modulates Oxidative Stress, Endoplasmic Reticulum Stress, and Autophagy in Type 2 Diabetes. *Journal of Clinical Medicine*, *8*(9), 1322. https://doi.org/10.3390/jcm8091322

Fan, F., Duan, Y., Yang, F., Trexler, C., Wang, H., Huang, L., Li, Y., Tang, H., Wang, G., Fang, X., Liu, J., Jia, N., Chen, J., & Ouyang, K. (2020). Deletion of heat shock protein 60 in adult mouse cardiomyocytes perturbs mitochondrial protein homeostasis and causes heart failure. *Cell Death & Differentiation*, *27*(2), 587–600. https://doi.org/10.1038/s41418-019-0374-x

Fiorese, C. J., Schulz, A. M., Lin, Y.-F., Rosin, N., Pellegrino, M. W., & Haynes, C. M. (2016). The transcription factor ATF5 mediates a mammalian mitochondrial UPR. *Current Biology : CB*, *26*(15), 2037–2043. https://doi.org/10.1016/j.cub.2016.06.002

Flis, V. V., & Daum, G. (2013). Lipid Transport between the Endoplasmic Reticulum and Mitochondria. *Cold Spring Harbor Perspectives in Biology*, *5*(6), a013235. https://doi.org/10.1101/cshperspect.a013235

Frakes, A. E., & Dillin, A. (2017). The UPRER: Sensor and Coordinator of Organismal Homeostasis. *Molecular Cell*, *66*(6), 761–771. https://doi.org/10.1016/j.molcel.2017.05.031

Fulda, S., Gorman, A. M., Hori, O., & Samali, A. (2010). Cellular Stress Responses: Cell Survival and Cell Death. *International Journal of Cell Biology*, *2010*, 214074. https://doi.org/10.1155/2010/214074

Gakh, O., Cavadini, P., & Isaya, G. (2002). Mitochondrial processing peptidases. *Biochimica et Biophysica Acta (BBA) - Molecular Cell Research*, *1592*(1), 63–77. https://doi.org/10.1016/S0167-4889(02)00265-3

Ge, P., Dawson, V. L., & Dawson, T. M. (2020). PINK1 and Parkin mitochondrial quality control: A source of regional vulnerability in Parkinson's disease. *Molecular Neurodegeneration*, *15*(1), 20. https://doi.org/10.1186/s13024-020-00367-7

Giacomello, M., Pyakurel, A., Glytsou, C., & Scorrano, L. (2020). The cell biology of mitochondrial membrane dynamics. *Nature Reviews Molecular Cell Biology*, *21*(4), 204–225. https://doi.org/10.1038/s41580-020-0210-7

Gilkerson, R., De La Torre, P., & St. Vallier, S. (2021). Mitochondrial OMA1 and OPA1 as Gatekeepers of Organellar Structure/Function and Cellular Stress Response. *Frontiers in Cell and Developmental Biology*, *9*. https://www.frontiersin.org/articles/10.3389/fcell.2021.626117

Girardin, S. E., Cuziol, C., Philpott, D. J., & Arnoult, D. (2021). The eIF2α kinase HRI in innate immunity, proteostasis, and mitochondrial stress. *The FEBS Journal*, *288*(10), 3094–3107. https://doi.org/10.1111/febs.15553

Groenendyk, J., Lee, D., Jung, J., Dyck, J. R. B., Lopaschuk, G. D., Agellon, L. B., & Michalak, M. (2016). Inhibition of the Unfolded Protein Response Mechanism Prevents Cardiac Fibrosis. *PLOS ONE*, *11*(7), e0159682. https://doi.org/10.1371/journal.pone.0159682

Guo, R., Ma, H., Gao, F., Zhong, L., & Ren, J. (2009). Metallothionein alleviates oxidative stress-induced endoplasmic reticulum stress and myocardial dysfunction. *Journal of Molecular and Cellular Cardiology*, *47*(2), 228–237. https://doi.org/10.1016/j.yjmcc.2009.03.018

Hamada, H., Suzuki, M., Yuasa, S., Mimura, N., Shinozuka, N., Takada, Y., Suzuki, M., Nishino, T., Nakaya, H., Koseki, H., & Aoe, T. (2004). Dilated cardiomyopathy caused by aberrant endoplasmic reticulum quality control in mutant KDEL receptor transgenic mice. *Molecular and Cellular Biology*, *24*(18), 8007–8017. https://doi.org/10.1128/MCB.24.18.8007-8017.2004

Hamilton, K. L., & Miller, B. F. (2017). Mitochondrial proteostasis as a shared characteristic of slowed aging: The importance of considering cell proliferation. *The Journal of Physiology*, *595*(20), Article 20. https://doi.org/10.1113/JP274335

Hampton, R. Y. (2002). ER-associated degradation in protein quality control and cellular regulation. *Current Opinion in Cell Biology*, *14*(4), 476–482. https://doi.org/10.1016/S0955-0674(02)00358-7

Heeger, P. S., Lalli, P. N., Lin, F., Valujskikh, A., Liu, J., Muqim, N., Xu, Y., & Medof, M. E. (2005). Decay-accelerating factor modulates induction of T cell immunity. *Journal of Experimental Medicine*, *201*(10), 1523–1530. https://doi.org/10.1084/jem.20041967

Hernando-Rodríguez, B., & Artal-Sanz, M. (2018). Mitochondrial Quality Control Mechanisms and the PHB (Prohibitin) Complex. *Cells*, *7*(12), Article 12. https://doi.org/10.3390/cells7120238

Hoch, F. L. (1992). Cardiolipins and biomembrane function. *Biochimica Et Biophysica Acta*, *1113*(1), 71–133. https://doi.org/10.1016/0304-4157(92)90035-9

Horibe, T., & Hoogenraad, N. J. (2007). The chop gene contains an element for the positive regulation of the mitochondrial unfolded protein response. *PloS One*, *2*(9), e835. https://doi.org/10.1371/journal.pone.0000835

Hou, Y., Li, S., Wu, M., Wei, J., Ren, Y., Du, C., Wu, H., Han, C., Duan, H., & Shi, Y. (2016). Mitochondria-targeted peptide SS-31 attenuates renal injury via an antioxidant effect in diabetic nephropathy. *American Journal of Physiology. Renal Physiology*, *310*(6), Article 6. https://doi.org/10.1152/ajprenal.00574.2014

Houtkooper, R. H., Turkenburg, M., Poll-The, B. T., Karall, D., Pérez-Cerdá, C., Morrone, A., Malvagia, S., Wanders, R. J., Kulik, W., & Vaz, F. M. (2009). The enigmatic role of tafazzin in cardiolipin metabolism. *Biochimica et Biophysica Acta (BBA) - Biomembranes*, *1788*(10), 2003–2014. https://doi.org/10.1016/j.bbamem.2009.07.009

Hu, C., Huang, Y., & Li, L. (2017). Drp1-Dependent Mitochondrial Fission Plays Critical Roles in Physiological and Pathological Progresses in Mammals. *International Journal of Molecular Sciences*, *18*(1), 144. https://doi.org/10.3390/ijms18010144

Huang, X., Zeng, Z., Li, S., Xie, Y., & Tong, X. (2022). The Therapeutic Strategies Targeting Mitochondrial Metabolism in Cardiovascular Disease. *Pharmaceutics*, *14*(12), Article 12. https://doi.org/10.3390/pharmaceutics14122760

Ikon, N., & Ryan, R. O. (2017). Barth Syndrome: Connecting Cardiolipin to Cardiomyopathy. *Lipids*, *52*(2), 99–108. https://doi.org/10.1007/s11745-016-4229-7

Ishizawa, J., Zarabi, S. F., Davis, R. E., Halgas, O., Nii, T., Jitkova, Y., Zhao, R., St-Germain, J., Heese, L. E., Egan, G., Ruvolo, V. R., Barghout, S. H., Nishida, Y., Hurren, R., Ma, W., Gronda, M., Link, T., Wong, K., Mabanglo, M., … Andreeff, M. (2019). Mitochondrial ClpP-Mediated Proteolysis

Induces Selective Cancer Cell Lethality. *Cancer Cell*, *35*(5), 721-737.e9. https://doi.org/10.1016/j.ccell.2019.03.014

Jensen, R. E., & Dunn, C. D. (2002). Protein import into and across the mitochondrial inner membrane: Role of the TIM23 and TIM22 translocons. *Biochimica et Biophysica Acta (BBA) - Molecular Cell Research*, *1592*(1), 25–34. https://doi.org/10.1016/S0167-4889(02)00261-6

Jin, S. M., & Youle, R. J. (2013). The accumulation of misfolded proteins in the mitochondrial matrix is sensed by PINK1 to induce PARK2/Parkin-mediated mitophagy of polarized mitochondria. *Autophagy*, *9*(11), 1750–1757. https://doi.org/10.4161/auto.26122

Jolly, C., & Morimoto, R. I. (2000). Role of the Heat Shock Response and Molecular Chaperones in Oncogenesis and Cell Death. *JNCI: Journal of the National Cancer Institute*, *92*(19), 1564–1572. https://doi.org/10.1093/jnci/92.19.1564

Jones, D. M., Lopes, L., Quinlivan, R., Elliott, P. M., & Khanji, M. Y. (2019). Cardiac manifestations of McArdle disease. *European Heart Journal*, *40*(4), 397–398. https://doi.org/10.1093/eurheartj/ehy783

Jousse, C., Deval, C., Maurin, A.-C., Parry, L., Chérasse, Y., Chaveroux, C., Lefloch, R., Lenormand, P., Bruhat, A., & Fafournoux, P. (2007). TRB3 inhibits the transcriptional activation of stress-regulated genes by a negative feedback on the ATF4 pathway. *The Journal of Biological Chemistry*, *282*(21), 15851–15861. https://doi.org/10.1074/jbc.M611723200

Jung, J. G., Yi, S.-A., Choi, S.-E., Kang, Y., Kim, T. H., Jeon, J. Y., Bae, M. A., Ahn, J. H., Jeong, H., Hwang, E. S., & Lee, K.-W. (2015). TM-25659-Induced Activation of FGF21 Level Decreases Insulin Resistance and Inflammation in Skeletal Muscle via GCN2 Pathways. *Molecules and Cells*, *38*(12), 1037–1043. https://doi.org/10.14348/molcells.2015.0100

Kagan, V. E., Bayir, H. A., Belikova, N. A., Kapralov, O., Tyurina, Y. Y., Tyurin, V. A., Jiang, J., Stoyanovsky, D. A., Wipf, P., Kochanek, P. M., Greenberger, J. S., Pitt, B., Shvedova, A. A., & Borisenko, G.

(2009). Cytochrome c/cardiolipin relations in mitochondria: A kiss of death. *Free Radical Biology & Medicine*, *46*(11), 1439–1453. https://doi.org/10.1016/j.freeradbiomed.2009.03.004

Kampinga, H. H., Andreasson, C., Barducci, A., Cheetham, M. E., Cyr, D., Emanuelsson, C., Genevaux, P., Gestwicki, J. E., Goloubinoff, P., Huerta-Cepas, J., Kirstein, J., Liberek, K., Mayer, M. P., Nagata, K., Nillegoda, N. B., Pulido, P., Ramos, C., De los Rios, P., Rospert, S., … Marszalek, J. (2019). Function, evolution, and structure of J-domain proteins. *Cell Stress & Chaperones*, *24*(1), 7–15. https://doi.org/10.1007/s12192-018-0948-4

Kampinga, H. H., & Craig, E. A. (2010). The HSP70 chaperone machinery: J proteins as drivers of functional specificity. *Nature Reviews. Molecular Cell Biology*, *11*(8), 579–592. https://doi.org/10.1038/nrm2941

Kang, F., Xie, L., Qin, T., Miao, Y., Kang, Y., Takahashi, T., Liang, T., Xie, H., & Gaisano, H. Y. (2022). Plasma membrane flipping of Syntaxin-2 regulates its inhibitory action on insulin granule exocytosis. *Nature Communications*, *13*(1), Article 1. https://doi.org/10.1038/s41467-022-33986-3

Karaa, A., Haas, R., Goldstein, A., Vockley, J., Weaver, W. D., & Cohen, B. H. (2018). Randomized dose-escalation trial of elamipretide in adults with primary mitochondrial myopathy. *Neurology*, *90*(14), e1212–e1221. https://doi.org/10.1212/WNL.0000000000005255

Karbowski, M., & Youle, R. J. (2003). Dynamics of mitochondrial morphology in healthy cells and during apoptosis. *Cell Death & Differentiation*, *10*(8), Article 8. https://doi.org/10.1038/sj.cdd.4401260

Kaspar, S., Oertlin, C., Szczepanowska, K., Kukat, A., Senft, K., Lucas, C., Brodesser, S., Hatzoglou, M., Larsson, O., Topisirovic, I., & Trifunovic, A. (2021). Adaptation to mitochondrial stress requires CHOP-directed tuning of ISR. *Science Advances*, *7*(22), eabf0971. https://doi.org/10.1126/sciadv.abf0971

King, M. A., Heger, K., Khan, A., Sinasac, D., Huttlin, E. L., Greenway, S. C., & Lewis, I. A. (2020). *Altered glutamine metabolism of cultured fibroblasts predicts severity of cardiac dysfunction in the*

dilated cardiomyopathy with ataxia syndrome (DCMA), a mitochondrial cardiomyopathy (p. 2020.10.11.334938). bioRxiv. https://doi.org/10.1101/2020.10.11.334938

Kinnally, K. W., Peixoto, P. M., Ryu, S.-Y., & Dejean, L. M. (2011). Is mPTP the gatekeeper for necrosis, apoptosis, or both? *Biochimica et Biophysica Acta*, *1813*(4), 616–622. https://doi.org/10.1016/j.bbamcr.2010.09.013

Korennykh, A. V., Egea, P. F., Korostelev, A. A., Finer-Moore, J., Zhang, C., Shokat, K. M., Stroud, R. M., & Walter, P. (2009). The unfolded protein response signals through high-order assembly of Ire1. *Nature*, *457*(7230), 687–693. https://doi.org/10.1038/nature07661

Kostidis, S., Addie, R. D., Morreau, H., Mayboroda, O. A., & Giera, M. (2017). Quantitative NMR analysis of intra- and extracellular metabolism of mammalian cells: A tutorial. *Analytica Chimica Acta*, *980*, 1–24. https://doi.org/10.1016/j.aca.2017.05.011

Kumar, D., & Tandon, R. K. (2001). Use of ursodeoxycholic acid in liver diseases. *Journal of Gastroenterology and Hepatology*, *16*(1), 3–14. https://doi.org/10.1046/j.1440-1746.2001.02376.x

Kuo, C.-Y., Chiu, Y.-C., Lee, A. Y.-L., & Hwang, T.-L. (2015). Mitochondrial Lon protease controls ROS-dependent apoptosis in cardiomyocyte under hypoxia. *Mitochondrion*, *23*, 7–16. https://doi.org/10.1016/j.mito.2015.04.004

Lake, N. J., Compton, A. G., Rahman, S., & Thorburn, D. R. (2016). Leigh syndrome: One disorder, more than 75 monogenic causes. *Annals of Neurology*, *79*(2), 190–203. https://doi.org/10.1002/ana.24551

Lesage, S., Drouet, V., Majounie, E., Deramecourt, V., Jacoupy, M., Nicolas, A., Cormier-Dequaire, F., Hassoun, S. M., Pujol, C., Ciura, S., Erpapazoglou, Z., Usenko, T., Maurage, C.-A., Sahbatou, M., Liebau, S., Ding, J., Bilgic, B., Emre, M., Erginel-Unaltuna, N., … Brice, A. (2016). Loss of VPS13C Function in Autosomal-Recessive Parkinsonism Causes Mitochondrial Dysfunction and Increases

PINK1/Parkin-Dependent Mitophagy. *American Journal of Human Genetics*, *98*(3), 500–513. https://doi.org/10.1016/j.ajhg.2016.01.014

Lévy, E., El Banna, N., Baïlle, D., Heneman-Masurel, A., Truchet, S., Rezaei, H., Huang, M.-E., Béringue, V., Martin, D., & Vernis, L. (2019). Causative Links between Protein Aggregation and Oxidative Stress: A Review. *International Journal of Molecular Sciences*, *20*(16), 3896. https://doi.org/10.3390/ijms20163896

LeWinter, M. M., & Granzier, H. (2010). Cardiac Titin. *Circulation*, *121*(19), 2137–2145. https://doi.org/10.1161/CIRCULATIONAHA.109.860171

Lightfoot, A. P., Sakellariou, G. K., Nye, G. A., McArdle, F., Jackson, M. J., Griffiths, R. D., & McArdle, A. (2015). SS-31 attenuates TNF-α induced cytokine release from C2C12 myotubes. *Redox Biology*, *6*, 253–259. https://doi.org/10.1016/j.redox.2015.08.007

Lin, L., Kim, S. C., Wang, Y., Gupta, S., Davis, B., Simon, S. I., Torre-Amione, G., & Knowlton, A. A. (2007). HSP60 in heart failure: Abnormal distribution and role in cardiac myocyte apoptosis. *American Journal of Physiology. Heart and Circulatory Physiology*, *293*(4), H2238-2247. https://doi.org/10.1152/ajpheart.00740.2007

Lin, Y.-F., & Haynes, C. M. (2016). Metabolism and the UPRmt. *Molecular Cell*, *61*(5), 677–682. https://doi.org/10.1016/j.molcel.2016.02.004

Liu, M., Lv, J., Pan, Z., Wang, D., Zhao, L., & Guo, X. (2022). Mitochondrial dysfunction in heart failure and its therapeutic implications. *Frontiers in Cardiovascular Medicine*, *9*, 945142. https://doi.org/10.3389/fcvm.2022.945142

Liu, Z., Cai, H., Zhu, H., Toque, H., Zhao, N., Qiu, C., Guan, G., Dang, Y., & Wang, J. (2014). Protein kinase RNA-like endoplasmic reticulum kinase (PERK)/calcineurin signaling is a novel pathway regulating intracellular calcium accumulation which might be involved in ventricular arrhythmias

in diabetic cardiomyopathy. *Cellular Signalling*, *26*(12), 2591–2600. https://doi.org/10.1016/j.cellsig.2014.08.015

Lo, A. C., Callaerts-Vegh, Z., Nunes, A. F., Rodrigues, C. M. P., & D'Hooge, R. (2013). Tauroursodeoxycholic acid (TUDCA) supplementation prevents cognitive impairment and amyloid deposition in APP/PS1 mice. *Neurobiology of Disease*, *50*, 21–29. https://doi.org/10.1016/j.nbd.2012.09.003

Losón, O. C., Song, Z., Chen, H., & Chan, D. C. (2013). Fis1, Mff, MiD49, and MiD51 mediate Drp1 recruitment in mitochondrial fission. *Molecular Biology of the Cell*, *24*(5), 659–667. https://doi.org/10.1091/mbc.E12-10-0721

Lu, H.-I., Lee, F.-Y., Wallace, C. G., Sung, P.-H., Chen, K.-H., Sheu, J.-J., Chua, S., Tong, M.-S., Huang, T.-H., Chen, Y.-L., Shao, P.-L., & Yip, H.-K. (2017). SS31 therapy effectively protects the heart against transverse aortic constriction-induced hypertrophic cardiomyopathy damage. *American Journal of Translational Research*, *9*(12), 5220–5237.

Lu, Y.-W., & Claypool, S. M. (2015). Disorders of phospholipid metabolism: An emerging class of mitochondrial disease due to defects in nuclear genes. *Frontiers in Genetics*, *6*. https://doi.org/10.3389/fgene.2015.00003

Ma, K., Chen, G., Li, W., Kepp, O., Zhu, Y., & Chen, Q. (2020). Mitophagy, Mitochondrial Homeostasis, and Cell Fate. *Frontiers in Cell and Developmental Biology*, *8*, 467. https://doi.org/10.3389/fcell.2020.00467

Machiraju, P., Degtiarev, V., Patel, D., Hazari, H., Lowry, R. B., Bedard, T., Sinasac, D., Brundler, M.-A., Greenway, S. C., & Khan, A. (2022). Phenotype and pathology of the dilated cardiomyopathy with ataxia syndrome in children. *Journal of Inherited Metabolic Disease*, *45*(2). https://doi.org/10.1002/jimd.12441

Machiraju, P., Wang, X., Sabouny, R., Huang, J., Zhao, T., Iqbal, F., King, M., Prasher, D., Lodha, A., Jimenez-Tellez, N., Ravandi, A., Argiropoulos, B., Sinasac, D., Khan, A., Shutt, T. E., & Greenway, S. C. (2019). SS-31 Peptide Reverses the Mitochondrial Fragmentation Present in Fibroblasts From Patients With DCMA, a Mitochondrial Cardiomyopathy. *Frontiers in Cardiovascular Medicine*, *6*. https://doi.org/10.3389/fcvm.2019.00167

Maguire, J. J., Tyurina, Y. Y., Mohammadyani, D., Kapralov, A. A., Anthonymuthu, T. S., Qu, F., Amoscato, A. A., Sparvero, L. J., Tyurin, V. A., Planas-Iglesias, J., He, R.-R., Klein-Seetharaman, J., Bayır, H., & Kagan, V. E. (2017). Known unknowns of cardiolipin signaling: The best is yet to come. *Biochimica Et Biophysica Acta. Molecular and Cell Biology of Lipids*, *1862*(1), 8–24. https://doi.org/10.1016/j.bbalip.2016.08.001

Majumdar, R., Bandyopadhyay, A., & Maitra, U. (2003). Mammalian translation initiation factor eIF1 functions with eIF1A and eIF3 in the formation of a stable 40 S preinitiation complex. *The Journal of Biological Chemistry*, *278*(8), 6580–6587. https://doi.org/10.1074/jbc.M210357200

Melber, A., & Haynes, C. M. (2018). UPRmt regulation and output: A stress response mediated by mitochondrial-nuclear communication. *Cell Research*, *28*(3), 281–295. https://doi.org/10.1038/cr.2018.16

Memme, J. M., Oliveira, A. N., & Hood, D. A. (2016). Chronology of UPR activation in skeletal muscle adaptations to chronic contractile activity. *American Journal of Physiology - Cell Physiology*, *310*(11), C1024–C1036. https://doi.org/10.1152/ajpcell.00009.2016

Mick, E., Titov, D. V., Skinner, O. S., Sharma, R., Jourdain, A. A., & Mootha, V. K. (2020). Distinct mitochondrial defects trigger the integrated stress response depending on the metabolic state of the cell. *ELife*, *9*, e49178. https://doi.org/10.7554/eLife.49178

Migocka-Patrzałek, M., & Elias, M. (2021). Muscle Glycogen Phosphorylase and Its Functional Partners in Health and Disease. *Cells*, *10*(4), 883. https://doi.org/10.3390/cells10040883

Milenkovic, D., Ramming, T., Müller, J. M., Wenz, L.-S., Gebert, N., Schulze-Specking, A., Stojanovski, D., Rospert, S., & Chacinska, A. (2009). Identification of the Signal Directing Tim9 and Tim10 into the Intermembrane Space of Mitochondria. *Molecular Biology of the Cell*, *20*(10), 2530–2539. https://doi.org/10.1091/mbc.E08-11-1108

Miller, D. J., & Fort, P. E. (2018). Heat Shock Proteins Regulatory Role in Neurodevelopment. *Frontiers in Neuroscience*, *12*. https://www.frontiersin.org/articles/10.3389/fnins.2018.00821

Mishra, P., Carelli, V., Manfredi, G., & Chan, D. C. (2014). Proteolytic cleavage of Opa1 stimulates mitochondrial inner membrane fusion and couples fusion to oxidative phosphorylation. *Cell Metabolism*, *19*(4), 630–641. https://doi.org/10.1016/j.cmet.2014.03.011

Molfetta, R., Milito, N. D., Zitti, B., Lecce, M., Fionda, C., Cippitelli, M., Santoni, A., & Paolini, R. (2019). The Ubiquitin-proteasome pathway regulates Nectin2/CD112 expression and impairs NK cell recognition and killing. *European Journal of Immunology*, *49*(6), 873–883. https://doi.org/10.1002/eji.201847848

Moreira, S., Fonseca, I., Nunes, M. J., Rosa, A., Lemos, L., Rodrigues, E., Carvalho, A. N., Outeiro, T. F., Rodrigues, C. M. P., Gama, M. J., & Castro-Caldas, M. (2017). Nrf2 activation by tauroursodeoxycholic acid in experimental models of Parkinson's disease. *Experimental Neurology*, *295*, 77–87. https://doi.org/10.1016/j.expneurol.2017.05.009

Münch, C. (2018). The different axes of the mammalian mitochondrial unfolded protein response. *BMC Biology*, *16*(1), 81. https://doi.org/10.1186/s12915-018-0548-x

Murphy, E., Ardehali, H., Balaban, R. S., DiLisa, F., Dorn, G. W., Kitsis, R. N., Otsu, K., Ping, P., Rizzuto, R., Sack, M. N., Wallace, D., & Youle, R. J. (2016). Mitochondrial Function, Biology, and Role in Disease. *Circulation Research*, *118*(12), 1960–1991. https://doi.org/10.1161/RES.0000000000000104

Nargund, A. M., Fiorese, C. J., Pellegrino, M. W., Deng, P., & Haynes, C. M. (2015). Mitochondrial and nuclear accumulation of the transcription factor ATFS-1 promotes OXPHOS recovery during the UPR(mt). *Molecular Cell*, *58*(1), 123–133. https://doi.org/10.1016/j.molcel.2015.02.008

Needs, H. I., Protasoni, M., Henley, J. M., Prudent, J., Collinson, I., & Pereira, G. C. (2021). Interplay between Mitochondrial Protein Import and Respiratory Complexes Assembly in Neuronal Health and Degeneration. *Life*, *11*(5), Article 5. https://doi.org/10.3390/life11050432

Niyazov, D. M., Kahler, S. G., & Frye, R. E. (2016). Primary Mitochondrial Disease and Secondary Mitochondrial Dysfunction: Importance of Distinction for Diagnosis and Treatment. *Molecular Syndromology*, *7*(3), 122–137. https://doi.org/10.1159/000446586

Nunes, A. F., Amaral, J. D., Lo, A. C., Fonseca, M. B., Viana, R. J. S., Callaerts-Vegh, Z., D'Hooge, R., & Rodrigues, C. M. P. (2012). TUDCA, a Bile Acid, Attenuates Amyloid Precursor Protein Processing and Amyloid-β Deposition in APP/PS1 Mice. *Molecular Neurobiology*, *45*(3), 440–454. https://doi.org/10.1007/s12035-012-8256-y

Ojala, T., Polinati, P., Manninen, T., Hiippala, A., Rajantie, J., Karikoski, R., Suomalainen, A., & Tyni, T. (2012). New mutation of mitochondrial DNAJC19 causing dilated and noncompaction cardiomyopathy, anemia, ataxia, and male genital anomalies. *Pediatric Research*, *72*(4), Article 4. https://doi.org/10.1038/pr.2012.92

Okada, K., Minamino, T., Tsukamoto, Y., Liao, Y., Tsukamoto, O., Takashima, S., Hirata, A., Fujita, M., Nagamachi, Y., Nakatani, T., Yutani, C., Ozawa, K., Ogawa, S., Tomoike, H., Hori, M., & Kitakaze, M. (2004). Prolonged endoplasmic reticulum stress in hypertrophic and failing heart after aortic constriction: Possible contribution of endoplasmic reticulum stress to cardiac myocyte apoptosis. *Circulation*, *110*(6), 705–712. https://doi.org/10.1161/01.CIR.0000137836.95625.D4

Oliveira, A. N., & Hood, D. A. (2018). Effect of Tim23 knockdown in vivo on mitochondrial protein import and retrograde signaling to the UPRmt in muscle. *American Journal of Physiology. Cell Physiology*, *315*(4), Article 4. https://doi.org/10.1152/ajpcell.00275.2017

Omura, T., Asari, M., Yamamoto, J., Oka, K., Hoshina, C., Maseda, C., Awaya, T., Tasaki, Y., Shiono, H., Yonezawa, A., Masuda, S., Matsubara, K., & Shimizu, K. (2013). Sodium tauroursodeoxycholate prevents paraquat-induced cell death by suppressing endoplasmic reticulum stress responses in human lung epithelial A549 cells. *Biochemical and Biophysical Research Communications*, *432*(4), 689–694. https://doi.org/10.1016/j.bbrc.2013.01.131

Pakos-Zebrucka, K., Koryga, I., Mnich, K., Ljujic, M., Samali, A., & Gorman, A. M. (2016). The integrated stress response. *EMBO Reports*, *17*(10), 1374–1395. https://doi.org/10.15252/embr.201642195

Papadopoulos, C. E., Pitsiou, G., Karamitsos, T. D., Karvounis, H. I., Kontakiotis, T., Giannakoulas, G., Efthimiadis, G. K., Argyropoulou, P., Parharidis, G. E., & Bouros, D. (2008). Left ventricular diastolic dysfunction in idiopathic pulmonary fibrosis: A tissue Doppler echocardiographic study. *European Respiratory Journal*, *31*(4), 701–706. https://doi.org/10.1183/09031936.00102107

Paradies, G., Paradies, V., Ruggiero, F. M., & Petrosillo, G. (2019). Role of Cardiolipin in Mitochondrial Function and Dynamics in Health and Disease: Molecular and Pharmacological Aspects. *Cells*, *8*(7), 728. https://doi.org/10.3390/cells8070728

Paridaens, A., Raevens, S., Devisscher, L., Bogaerts, E., Verhelst, X., Hoorens, A., van Vlierberghe, H., Van Grunsven, L. A., Geerts, A., & Colle, I. (2017). Modulation of the Unfolded Protein Response by Tauroursodeoxycholic Acid Counteracts Apoptotic Cell Death and Fibrosis in a Mouse Model for Secondary Biliary Liver Fibrosis. *International Journal of Molecular Sciences*, *18*(1), 214. https://doi.org/10.3390/ijms18010214

Park, S., Lim, Y., Lee, D., Elvira, R., Lee, J.-M., Lee, M. R., & Han, J. (2018). Modulation of Protein Synthesis by eIF2α Phosphorylation Protects Cell from Heat Stress-Mediated Apoptosis. *Cells*, *7*(12), 254. https://doi.org/10.3390/cells7120254

Park, S.-M., Kang, T.-I., & So, J.-S. (2021). Roles of XBP1s in Transcriptional Regulation of Target Genes. *Biomedicines*, *9*(7), 791. https://doi.org/10.3390/biomedicines9070791

Pfanner, N., Wiedemann, N., Meisinger, C., & Lithgow, T. (2004). Assembling the mitochondrial outer membrane. *Nature Structural & Molecular Biology*, *11*(11), 1044–1048. https://doi.org/10.1038/nsmb852

Prasai, K. (2017). Regulation of mitochondrial structure and function by protein import: A current review. *Pathophysiology*, *24*(3), 107–122. https://doi.org/10.1016/j.pathophys.2017.03.001

Punzi, G., Porcelli, V., Ruggiu, M., Hossain, M. F., Menga, A., Scarcia, P., Castegna, A., Gorgoglione, R., Pierri, C. L., Laera, L., Lasorsa, F. M., Paradies, E., Pisano, I., Marobbio, C. M. T., Lamantea, E., Ghezzi, D., Tiranti, V., Giannattasio, S., Donati, M. A., … De Grassi, A. (2018). SLC25A10 biallelic mutations in intractable epileptic encephalopathy with complex I deficiency. *Human Molecular Genetics*, *27*(3), 499–504. https://doi.org/10.1093/hmg/ddx419

Qureshi, M. A., Haynes, C. M., & Pellegrino, M. W. (2017). The mitochondrial unfolded protein response: Signaling from the powerhouse. *The Journal of Biological Chemistry*, *292*(33), Article 33. https://doi.org/10.1074/jbc.R117.791061

Reddy, P. H., Manczak, M., & Kandimalla, R. (2017). Mitochondria-targeted small molecule SS31: A potential candidate for the treatment of Alzheimer's disease. *Human Molecular Genetics*, *26*(8), 1483–1496. https://doi.org/10.1093/hmg/ddx052

Reid Thompson, W., Hornby, B., Manuel, R., Bradley, E., Laux, J., Carr, J., & Vernon, H. J. (2021). A phase 2/3 randomized clinical trial followed by an open-label extension to evaluate the effectiveness of elamipretide in Barth syndrome, a genetic disorder of mitochondrial cardiolipin metabolism.

Genetics in Medicine: Official Journal of the American College of Medical Genetics, *23*(3), 471–478. https://doi.org/10.1038/s41436-020-01006-8

Richter, K., Haslbeck, M., & Buchner, J. (2010). The heat shock response: Life on the verge of death. *Molecular Cell*, *40*(2), 253–266. https://doi.org/10.1016/j.molcel.2010.10.006

Richter-Dennerlein, R., Korwitz, A., Haag, M., Tatsuta, T., Dargazanli, S., Baker, M., Decker, T., Lamkemeyer, T., Rugarli, E. I., & Langer, T. (2014). DNAJC19, a mitochondrial cochaperone associated with cardiomyopathy, forms a complex with prohibitins to regulate cardiolipin remodeling. *Cell Metabolism*, *20*(1), Article 1. https://doi.org/10.1016/j.cmet.2014.04.016

Rodrigues, C. M. P., Stieers, C. L.-, Keene, C. D., Ma, X., Kren, B. T., Low, W. C., & Steer, C. J. (2000). Tauroursodeoxycholic Acid Partially Prevents Apoptosis Induced by 3-Nitropropionic Acid. *Journal of Neurochemistry*, *75*(6), 2368–2379. https://doi.org/10.1046/j.1471-4159.2000.0752368.x

Rohani, L., Machiraju, P., Sabouny, R., Meng, G., Liu, S., Zhao, T., Iqbal, F., Wang, X., Ravandi, A., Wu, J. C., Khan, A., Shutt, T., Rancourt, D., & Greenway, S. C. (2020). Reversible Mitochondrial Fragmentation in iPSC-Derived Cardiomyocytes From Children With DCMA, a Mitochondrial Cardiomyopathy. *Canadian Journal of Cardiology*, *36*(4), Article 4. https://doi.org/10.1016/j.cjca.2019.09.021

Rolland, S. G., Schneid, S., Schwarz, M., Rackles, E., Fischer, C., Haeussler, S., Regmi, S. G., Yeroslaviz, A., Habermann, B., Mokranjac, D., Lambie, E., & Conradt, B. (2019). Compromised Mitochondrial Protein Import Acts as a Signal for UPRmt. *Cell Reports*, *28*(7), 1659-1669.e5. https://doi.org/10.1016/j.celrep.2019.07.049

Rosa, A. I., Fonseca, I., Nunes, M. J., Moreira, S., Rodrigues, E., Carvalho, A. N., Rodrigues, C. M. P., Gama, M. J., & Castro-Caldas, M. (2017). Novel insights into the antioxidant role of tauroursodeoxycholic acid in experimental models of Parkinson's disease. *Biochimica et*

Biophysica Acta (BBA) - Molecular Basis of Disease, *1863*(9), 2171–2181. https://doi.org/10.1016/j.bbadis.2017.06.004

Ruhoy, I. S., & Saneto, R. P. (2014). The genetics of Leigh syndrome and its implications for clinical practice and risk management. *The Application of Clinical Genetics*, *7*, 221–234. https://doi.org/10.2147/TACG.S46176

Russo, S., De Rasmo, D., Signorile, A., Corcelli, A., & Lobasso, S. (2022). Beneficial effects of SS-31 peptide on cardiac mitochondrial dysfunction in tafazzin knockdown mice. *Scientific Reports*, *12*(1), Article 1. https://doi.org/10.1038/s41598-022-24231-4

Sabbah, H. N. (2022). Elamipretide for Barth syndrome cardiomyopathy: Gradual rebuilding of a failed power grid. *Heart Failure Reviews*, *27*(5), 1911–1923. https://doi.org/10.1007/s10741-021-10177-8

Sabbah, H. N., Gupta, R. C., Kohli, S., Wang, M., Hachem, S., & Zhang, K. (2016). Chronic Therapy With Elamipretide (MTP-131), a Novel Mitochondria-Targeting Peptide, Improves Left Ventricular and Mitochondrial Function in Dogs With Advanced Heart Failure. *Circulation. Heart Failure*, *9*(2), e002206. https://doi.org/10.1161/CIRCHEARTFAILURE.115.002206

Santos-Ribeiro, D., Godinas, L., Pilette, C., & Perros, F. (2018). The integrated stress response system in cardiovascular disease. *Drug Discovery Today*, *23*(4), 920–929. https://doi.org/10.1016/j.drudis.2018.02.008

Schmidt, O., Pfanner, N., & Meisinger, C. (2010). Mitochondrial protein import: From proteomics to functional mechanisms. *Nature Reviews Molecular Cell Biology*, *11*(9), 655–667. https://doi.org/10.1038/nrm2959

Schneider, C. A., Rasband, W. S., & Eliceiri, K. W. (2012). NIH Image to ImageJ: 25 years of image analysis. *Nature Methods*, *9*(7), Article 7. https://doi.org/10.1038/nmeth.2089

Seiferling, D., Szczepanowska, K., Becker, C., Senft, K., Hermans, S., Maiti, P., König, T., Kukat, A., & Trifunovic, A. (2016). Loss of CLPP alleviates mitochondrial cardiomyopathy without affecting the mammalian UPRmt. *EMBO Reports*, *17*(7), 953–964. https://doi.org/10.15252/embr.201642077

Shrestha, N., Bahnan, W., Wiley, D. J., Barber, G., Fields, K. A., & Schesser, K. (2012). Eukaryotic Initiation Factor 2 (eIF2) Signaling Regulates Proinflammatory Cytokine Expression and Bacterial Invasion. *The Journal of Biological Chemistry*, *287*(34), 28738–28744. https://doi.org/10.1074/jbc.M112.375915

Signorile, A., Sgaramella, G., Bellomo, F., & De Rasmo, D. (2019). Prohibitins: A Critical Role in Mitochondrial Functions and Implication in Diseases. *Cells*, *8*(1), 71. https://doi.org/10.3390/cells8010071

Singh, R., Jamdar, S. N., Goyal, V. D., Kumar, A., Ghosh, B., & Makde, R. D. (2017). Structure of the human aminopeptidase XPNPEP3 and comparison of its in vitro activity with Icp55 orthologs: Insights into diverse cellular processes. *The Journal of Biological Chemistry*, *292*(24), 10035–10047. https://doi.org/10.1074/jbc.M117.783357

Sinha, D., Joshi, N., Chittoor, B., Samji, P., & D'Silva, P. (2010). Role of Magmas in protein transport and human mitochondria biogenesis. *Human Molecular Genetics*, *19*(7), Article 7. https://doi.org/10.1093/hmg/ddq002

Sinha, D., Srivastava, S., & D'Silva, P. (2016). Functional Diversity of Human Mitochondrial J-proteins Is Independent of Their Association with the Inner Membrane Presequence Translocase. *The Journal of Biological Chemistry*, *291*(33), Article 33. https://doi.org/10.1074/jbc.M116.738146

Smirnova, E., Griparic, L., Shurland, D.-L., & van der Bliek, A. M. (2001). Dynamin-related Protein Drp1 Is Required for Mitochondrial Division in Mammalian Cells. *Molecular Biology of the Cell*, *12*(8), 2245–2256.

Smyrnias, I., Gray, S. P., Okonko, D. O., Sawyer, G., Zoccarato, A., Catibog, N., L, ópez B., Gonz, ález A., Ravassa, S., D, íez J., & Shah, A. M. (2019). Cardioprotective Effect of the Mitochondrial Unfolded Protein Response During Chronic Pressure Overload. *Journal of the American College of Cardiology*, *73*(14), 1795–1806. https://doi.org/10.1016/j.jacc.2018.12.087

Soares, R., Ribeiro, F. F., Xapelli, S., Genebra, T., Ribeiro, M. F., Sebastião, A. M., Rodrigues, C. M. P., & Solá, S. (2018). Tauroursodeoxycholic Acid Enhances Mitochondrial Biogenesis, Neural Stem Cell Pool, and Early Neurogenesis in Adult Rats. *Molecular Neurobiology*, *55*(5), 3725–3738. https://doi.org/10.1007/s12035-017-0592-5

Sohn, J., Milosevic, J., Brouse, T., Aziz, N., Elkhoury, J., Wang, S., Hauschild, A., van Gastel, N., Cetinbas, M., Tufa, S. F., Keene, D. R., Sadreyev, R. I., Pu, W. T., & Sykes, D. B. (2022). A new murine model of Barth syndrome neutropenia links TAFAZZIN deficiency to increased ER stress-induced apoptosis. *Blood Advances*, *6*(8), 2557–2577. https://doi.org/10.1182/bloodadvances.2021005720

Sokol, A. M., Sztolsztener, M. E., Wasilewski, M., Heinz, E., & Chacinska, A. (2014). Mitochondrial protein translocases for survival and wellbeing. *FEBS Letters*, *588*(15), 2484–2495. https://doi.org/10.1016/j.febslet.2014.05.028

Song, Z., Chen, H., Fiket, M., Alexander, C., & Chan, D. C. (2007). OPA1 processing controls mitochondrial fusion and is regulated by mRNA splicing, membrane potential, and Yme1L. *The Journal of Cell Biology*, *178*(5), 749–755. https://doi.org/10.1083/jcb.200704110

Sparkes, R., Patton, D., & Bernier, F. (2007). Cardiac features of a novel autosomal recessive dilated cardiomyopathic syndrome due to defective importation of mitochondrial protein. *Cardiology in the Young*, *17*(2), Article 2. https://doi.org/10.1017/S1047951107000042

Stiburek, L., Cesnekova, J., Kostkova, O., Fornuskova, D., Vinsova, K., Wenchich, L., Houstek, J., & Zeman, J. (2012). YME1L controls the accumulation of respiratory chain subunits and is required for

apoptotic resistance, cristae morphogenesis, and cell proliferation. *Molecular Biology of the Cell*, *23*(6), 1010–1023. https://doi.org/10.1091/mbc.E11-08-0674

Stojanovski, D., Bragoszewski, P., & Chacinska, A. (2012). The MIA pathway: A tight bond between protein transport and oxidative folding in mitochondria. *Biochimica et Biophysica Acta (BBA) - Molecular Cell Research*, *1823*(7), 1142–1150. https://doi.org/10.1016/j.bbamcr.2012.04.014

Suo, M., Qi, Y., Liu, L., Zhang, C., Li, J., Yan, X., Zhang, C., Ti, Y., Chen, T., & Bu, P. (2022). SS31 Alleviates Pressure Overload-Induced Heart Failure Caused by Sirt3-Mediated Mitochondrial Fusion. *Frontiers in Cardiovascular Medicine*, *9*. https://www.frontiersin.org/articles/10.3389/fcvm.2022.858594

Sutanto, H., Lyon, A., Lumens, J., Schotten, U., Dobrev, D., & Heijman, J. (2020). Cardiomyocyte calcium handling in health and disease: Insights from in vitro and in silico studies. *Progress in Biophysics and Molecular Biology*, *157*, 54–75. https://doi.org/10.1016/j.pbiomolbio.2020.02.008

Svaguša, T., Martinić, M., Martinić, M., Kovačević, L., Šepac, A., Miličić, D., Bulum, J., Starčević, B., Sirotković-Skerlev, M., Seiwerth, F., Kulić, A., & Sedlić, F. (2020). Mitochondrial unfolded protein response, mitophagy and other mitochondrial quality control mechanisms in heart disease and aged heart. *Croatian Medical Journal*, *61*(2), 126–138. https://doi.org/10.3325/cmj.2020.61.126

Szeto, H. H. (2014). First-in-class cardiolipin-protective compound as a therapeutic agent to restore mitochondrial bioenergetics. *British Journal of Pharmacology*, *171*(8), 2029–2050. https://doi.org/10.1111/bph.12461

Szeto, H. H., & Birk, A. V. (2014). Serendipity and the Discovery of Novel Compounds That Restore Mitochondrial Plasticity. *Clinical Pharmacology & Therapeutics*, *96*(6), 672–683. https://doi.org/10.1038/clpt.2014.174

Szeto, H. H., & Schiller, P. W. (2011). Novel Therapies Targeting Inner Mitochondrial Membrane—From Discovery to Clinical Development. *Pharmaceutical Research*, *28*(11), Article 11. https://doi.org/10.1007/s11095-011-0476-8

Tarasov, A. I., Griffiths, E. J., & Rutter, G. A. (2012). Regulation of ATP production by mitochondrial Ca2+. *Cell Calcium*, *52*(1), 28–35. https://doi.org/10.1016/j.ceca.2012.03.003

Tharp, C. A., Haywood, M. E., Sbaizero, O., Taylor, M. R. G., & Mestroni, L. (2019). The Giant Protein Titin's Role in Cardiomyopathy: Genetic, Transcriptional, and Post-translational Modifications of TTN and Their Contribution to Cardiac Disease. *Frontiers in Physiology*, *10*, 1436. https://doi.org/10.3389/fphys.2019.01436

Tocchi, A., Quarles, E. K., Basisty, N., Gitari, L., & Rabinovitch, P. S. (2015). Mitochondrial dysfunction in cardiac aging. *Biochimica et Biophysica Acta (BBA) - Bioenergetics*, *1847*(11), 1424–1433. https://doi.org/10.1016/j.bbabio.2015.07.009

Ucar, S. K., Mayr, J. A., Feichtinger, R. G., Canda, E., Çoker, M., & Wortmann, S. B. (2017). Previously Unreported Biallelic Mutation in DNAJC19: Are Sensorineural Hearing Loss and Basal Ganglia Lesions Additional Features of Dilated Cardiomyopathy and Ataxia (DCMA) Syndrome? *JIMD Reports*, *35*, 39–45. https://doi.org/10.1007/8904_2016_23

Uppala, J. K., Gani, A. R., & Ramaiah, K. V. A. (2017). Chemical chaperone, TUDCA unlike PBA, mitigates protein aggregation efficiently and resists ER and non-ER stress induced HepG2 cell death. *Scientific Reports*, *7*(1), Article 1. https://doi.org/10.1038/s41598-017-03940-1

van Huizen, R., Martindale, J. L., Gorospe, M., & Holbrook, N. J. (2003). P58IPK, a novel endoplasmic reticulum stress-inducible protein and potential negative regulator of eIF2alpha signaling. *The Journal of Biological Chemistry*, *278*(18), 15558–15564. https://doi.org/10.1074/jbc.M212074200

Vang, S., Longley, K., Steer, C. J., & Low, W. C. (2014). The Unexpected Uses of Urso- and Tauroursodeoxycholic Acid in the Treatment of Non-liver Diseases. *Global Advances in Health and Medicine*, *3*(3), 58–69. https://doi.org/10.7453/gahmj.2014.017

Veereshwarayya, V., Kumar, P., Rosen, K. M., Mestril, R., & Querfurth, H. W. (2006). Differential Effects of Mitochondrial Heat Shock Protein 60 and Related Molecular Chaperones to Prevent Intracellular β-Amyloid-induced Inhibition of Complex IV and Limit Apoptosis. *Journal of Biological Chemistry*, *281*(40), 29468–29478. https://doi.org/10.1074/jbc.M602533200

Venkatesh, S., Li, M., Saito, T., Tong, M., Rashed, E., Mareedu, S., Zhai, P., Bárcena, C., López-Otín, C., Yehia, G., Sadoshima, J., & Suzuki, C. K. (2019). Mitochondrial LonP1 protects cardiomyocytes from ischemia/reperfusion injury in vivo. *Journal of Molecular and Cellular Cardiology*, *128*, 38–50. https://doi.org/10.1016/j.yjmcc.2018.12.017

Wachoski-Dark, E., Zhao, T., Khan, A., Shutt, T. E., & Greenway, S. C. (2022). Mitochondrial Protein Homeostasis and Cardiomyopathy. *International Journal of Molecular Sciences*, *23*(6), 3353. https://doi.org/10.3390/ijms23063353

Wai, T., García-Prieto, J., Baker, M. J., Merkwirth, C., Benit, P., Rustin, P., Rupérez, F. J., Barbas, C., Ibañez, B., & Langer, T. (2015). Imbalanced OPA1 processing and mitochondrial fragmentation cause heart failure in mice. *Science (New York, N.Y.)*, *350*(6265), Article 6265. https://doi.org/10.1126/science.aad0116

Waingankar, T. P., & D'Silva, P. (2021). Multiple variants of the human presequence translocase motor subunit Magmas govern the mitochondrial import. *Journal of Biological Chemistry*, *297*(6), 101349. https://doi.org/10.1016/j.jbc.2021.101349

Walsh, P., Bursać, D., Law, Y. C., Cyr, D., & Lithgow, T. (2004). The J-protein family: Modulating protein assembly, disassembly and translocation. *EMBO Reports*, *5*(6), 567–571. https://doi.org/10.1038/sj.embor.7400172

Wang, H., Xu, X., Fassett, J., Kwak, D., Liu, X., Hu, X., Falls, T. J., Bell, J. C., Li, H., Bitterman, P., Bache, R. J., & Chen, Y. (2014). Double-stranded RNA-dependent protein kinase deficiency protects the heart from systolic overload-induced congestive heart failure. *Circulation*, *129*(13), 1397–1406. https://doi.org/10.1161/CIRCULATIONAHA.113.002209

Wang, S., Binder, P., Fang, Q., Wang, Z., Xiao, W., Liu, W., & Wang, X. (2018). Endoplasmic reticulum stress in the heart: Insights into mechanisms and drug targets. *British Journal of Pharmacology*, *175*(8), 1293–1304. https://doi.org/10.1111/bph.13888

Wang, S., Yazawa, E., Keating, E., Mazumdar, N., Hauschild, A., Ma, Q., Wu, H., Xu, Y., Shi, X., Strathdee, D., Gerszten, R. E., Schlame, M., & Pu, W. T. (2023). Genetic modifiers modulate phenotypic expression of tafazzin deficiency in a mouse model of Barth syndrome. *Human Molecular Genetics*, ddad041. https://doi.org/10.1093/hmg/ddad041

Wang, Y. T., Lim, Y., McCall, M. N., Huang, K.-T., Haynes, C. M., Nehrke, K., & Brookes, P. S. (2019). Cardioprotection by the mitochondrial unfolded protein response requires ATF5. *American Journal of Physiology-Heart and Circulatory Physiology*, *317*(2), Article 2. https://doi.org/10.1152/ajpheart.00244.2019

Weitzel, G., Pilatus, U., & Rensing, L. (1985). Similar dose response of heat shock protein synthesis and intracellular pH change in yeast. *Experimental Cell Research*, *159*(1), 252–256. https://doi.org/10.1016/s0014-4827(85)80054-9

Wheeler, D. S., & Wong, H. R. (2007). The Heat Shock Response and Acute Lung Injury. *Free Radical Biology & Medicine*, *42*(1), 1–14. https://doi.org/10.1016/j.freeradbiomed.2006.08.028

Wiedemann, N., & Pfanner, N. (2017). Mitochondrial Machineries for Protein Import and Assembly. *Annual Review of Biochemistry*, *86*, 685–714. https://doi.org/10.1146/annurev-biochem-060815-014352

Wortmann, S. B., Duran, M., Anikster, Y., Barth, P. G., Sperl, W., Zschocke, J., Morava, E., & Wevers, R. A. (2013). Inborn errors of metabolism with 3-methylglutaconic aciduria as discriminative feature: Proper classification and nomenclature. *Journal of Inherited Metabolic Disease*, *36*(6), 923–928. https://doi.org/10.1007/s10545-012-9580-0

Wortmann, S. B., Kluijtmans, L. A., Engelke, U. F. H., Wevers, R. A., & Morava, E. (2012). The 3-methylglutaconic acidurias: What's new? *Journal of Inherited Metabolic Disease*, *35*(1), 13–22. https://doi.org/10.1007/s10545-010-9210-7

Wortmann, S. B., Vaz, F. M., Gardeitchik, T., Vissers, L. E. L. M., Renkema, G. H., Schuurs-Hoeijmakers, J. H. M., Kulik, W., Lammens, M., Christin, C., Kluijtmans, L. A. J., Rodenburg, R. J., Nijtmans, L. G. J., Grünewald, A., Klein, C., Gerhold, J. M., Kozicz, T., van Hasselt, P. M., Harakalova, M., Kloosterman, W., … de Brouwer, A. P. M. (2012). Mutations in the phospholipid remodeling gene SERAC1 impair mitochondrial function and intracellular cholesterol trafficking and cause dystonia and deafness. *Nature Genetics*, *44*(7), 797–802. https://doi.org/10.1038/ng.2325

Xu, Y., Malhotra, A., Ren, M., & Schlame, M. (2006). The Enzymatic Function of Tafazzin *. *Journal of Biological Chemistry*, *281*(51), 39217–39224. https://doi.org/10.1074/jbc.M606100200

Yachie, A. (2021). Heme Oxygenase-1 Deficiency and Oxidative Stress: A Review of 9 Independent Human Cases and Animal Models. *International Journal of Molecular Sciences*, *22*(4), 1514. https://doi.org/10.3390/ijms22041514

Yoneda, T., Benedetti, C., Urano, F., Clark, S. G., Harding, H. P., & Ron, D. (2004). Compartment-specific perturbation of protein handling activates genes encoding mitochondrial chaperones. *Journal of Cell Science*, *117*(18), 4055–4066. https://doi.org/10.1242/jcs.01275

Youle, R. J., & van der Bliek, A. M. (2012). Mitochondrial Fission, Fusion, and Stress. *Science (New York, N.Y.)*, *337*(6098), 1062–1065. https://doi.org/10.1126/science.1219855

Zangerolamo, L., Vettorazzi, J. F., Rosa, L. R. O., Carneiro, E. M., & Barbosa, H. C. L. (2021). The bile acid TUDCA and neurodegenerative disorders: An overview. *Life Sciences*, *272*, 119252. https://doi.org/10.1016/j.lfs.2021.119252

Zhao, H., Li, H., Hao, S., Chen, J., Wu, J., Song, C., Zhang, M., Qiao, T., & Li, K. (2017). Peptide SS-31 upregulates frataxin expression and improves the quality of mitochondria: Implications in the treatment of Friedreich ataxia. *Scientific Reports*, *7*, 9840. https://doi.org/10.1038/s41598-017-10320-2

Zhao, Q., Wang, J., Levichkin, I., Stasinopoulos, S., Ryan, M., & Hoogenraad, N. (2002). A mitochondrial specific stress response in mammalian cells. *The EMBO Journal*, *21*(17), 4411–4419. https://doi.org/10.1093/emboj/cdf445

Zhao, W., Xu, Z., Cao, J., Fu, Q., Wu, Y., Zhang, X., Long, Y., Zhang, X., Yang, Y., Li, Y., & Mi, W. (2019). Elamipretide (SS-31) improves mitochondrial dysfunction, synaptic and memory impairment induced by lipopolysaccharide in mice. *Journal of Neuroinflammation*, *16*(1), 230. https://doi.org/10.1186/s12974-019-1627-9

Zhou, B., & Tian, R. (2018). Mitochondrial dysfunction in pathophysiology of heart failure. *The Journal of Clinical Investigation*, *128*(9), 3716–3726. https://doi.org/10.1172/JCI120849

Zhou, D., Palam, L. R., Jiang, L., Narasimhan, J., Staschke, K. A., & Wek, R. C. (2008). Phosphorylation of eIF2 directs ATF5 translational control in response to diverse stress conditions. *The Journal of Biological Chemistry*, *283*(11), 7064–7073. https://doi.org/10.1074/jbc.M708530200

Zhou, Y., Zhou, B., Pache, L., Chang, M., Khodabakhshi, A. H., Tanaseichuk, O., Benner, C., & Chanda, S. K. (2019). Metascape provides a biologist-oriented resource for the analysis of systems-level datasets. *Nature Communications*, *10*(1), 1523. https://doi.org/10.1038/s41467-019-09234-6

Zuo, Y., Yin, L., Cheng, X., Li, J., Wu, H., Liu, X., Gu, E., & Wu, J. (2020). Elamipretide Attenuates Pyroptosis and Perioperative Neurocognitive Disorders in Aged Mice. *Frontiers in Cellular Neuroscience*, *14*, 251. https://doi.org/10.3389/fncel.2020.00251

Zurita Rendón, O., & Shoubridge, E. A. (2018). LONP1 Is Required for Maturation of a Subset of Mitochondrial Proteins, and Its Loss Elicits an Integrated Stress Response. *Molecular and Cellular Biology*, *38*(20), e00412-17. https://doi.org/10.1128/MCB.00412-17